ROTAXANES AND POLYROTAXANES BASED ON CUCURBIT[6]URIL AND PORPHYRIN

A THESIS
SUBMITTED TO THE DEPARTMENT OF CHEMISTRY
AND THE INSTITUTE OF ENGINEERING AND SCIENCES
OF BILKENT UNIVERSITY
IN PARTIAL FULFILLMENT OF THE REQUIREMENTS
FOR THE DEGREE OF
MASTER OF SCIENCE

By
NESİBE CINDIR
AUGUST 2005

I certify that I have read this thesis and in my opinion it is fully adequate, in scope and in quality, as a thesis of the degree of Master of Science

_____

Asst. Prof. Dr. Dönüş TUNCEL

I certify that I have read this thesis and in my opinion it is fully adequate, in scope and in quality, as a thesis of the degree of Master of Science

_____

Prof. Dr. Engin AKKAYA

I certify that I have read this thesis and in my opinion it is fully adequate, in scope and in quality, as a thesis of the degree of Master of Science

_____

Assoc. Prof. Dr. Ulrike SALZNER

Approved for the Institute of Engineering and Sciences

_____

Prof. Dr. Mehmet Baray

Director of Institute of Engineering and Sciences

ABSTRACT

ROTAXANES AND POLYROTAXANES BASED ON CUCURBIT[6]URIL AND PORPHYRIN

NESİBE CINDIR

M.S. in Chemistry

Supervisor: Asst. Prof. Dr. Donus Tuncel

August 2005

In this study, the ability of CB[6] to catalyze 1,3-dipolar cycloaddition reaction between diazido and dialkyne functionalized trans substituted porphyrin monomers has been investigated. The main objective of this work is to synthesize a novel polyrotaxane containing porphyrin and CB[6] as stopper and macrocycle respectively by the self-threading method.

In the first part of the thesis, porphyrin containing monomers with diazido and dialkyne functional groups have been synthesized. These monomers have been characterized by FT-IR, UV-Vis, ^{1}H NMR and ^{13}C NMR. After they have been protonated, there have been changes in solubility and red shifts in the UV spectra. Although free base monomers are soluble in organic solvents, they are soluble in neither organic solvents nor water at high pH. However, they are soluble in acidic solutions at low pHs.

In the second part, before synthesis of polyrotaxanes, [3] rotaxane and [5] rotaxanes have been synthesized to model the properties and characterization of polyrotaxanes. Although [3] rotaxane has better solubility than monomers, its water solubility was not good enough. However, [5] rotaxane is well soluble in water.

Finally, after characterization of the rotaxanes with the same methods, polyrotaxanes have been synthesized and characterized. Although better water solubility with polymerization is expected, the water solubility has not improved. Additionally, it is expected to have better solubility by replacement of one of the porphyrin containing monomer to long aliphatic chain. However, there is also no improvement in solubility by this technique.

Keywords; Polyrotaxanes, rotaxanes, cucurbit[6]uril, 1,3-dipolar cycloaddition, porphyrin.

ÖZET

KUKURBİT[6]YURİL VE PORFİRİNE DAYALI ROTAKSAN VE POLYROTAXANLAR

NESiBE CINDIR

Kimya Bölümü Yüksek Lisans Tezi

Tez Yöneticisi: Asst. Prof. Dr. Dönüş Tuncel

Ağustos 2005

Bu çalışmada, çift azido ve çift alkinle karşılıklı dallanarak fonksiyonellenmiş porfirin monomerleri arasındaki, CB[6]nın kataliz ettiği 1,3-dipolar siklo katılma tepkimesi araştırıldı. Bu çalışmanın ana amacı, porfirin ve CB[6]yı sırasıyla durdurucu ve makrodaire olarak içeren yeni bir polyrotaksanı kendi kendine dikilme yöntemi ile sentezlemektir.

Bu tezin ilk bölümünde, çift azido ve çift alkin fonksiyonel gruplarını ihtiva eden porfirin monomerleri sentezlendi. Bu monomerler FT-IR, UV-Vis, ^{1}H NMR and ^{13}C NMR ile karakterize edildi. Monomerler protonlandıktan sonra, çözünürlüklerinde değişiklikler ve UV spektrumlarında kızıla doğru kaymalar vardı. Serbest baz haldeki monomerler organik çözücülerde çözünür olmalarına rağmen, yüksek pHda ne organik çözücülerde ne de suda çözünür değildirler. Mamafih, düşük pHlardaki asidik solusyonlarda çözünür haldedirler.

İkinci bölümde, polyrotaksanların sentezinden önce, [3] rotaksan ve [5] rotaksan polyrotaksanların özelliklerini ve karakterize edilişini örneklemek için sentezlendiler. [3] rotaksanın monomerlerden daha iyi çözünürlüğe sahip olmasına rağmen, sudaki çözünürlüğü yeterince iyi değildi. Fakat, [5] rotaksan suda iyi çözünürdür.

Son olarak, rotaksanların aynı yöntemlerle karakterize edilişinden sonra polyrotaksanlar sentezlendi ve karakterize edildi. Polymerizasyon ile daha iyi çözünürlük umulmasına rağmen, sudaki çözünürlük gelişmedi. Buna ek olarak, porfirin ihtiva eden monomerlerden birinin uzun alifatik zincir ile değiştirilmesiyle daha iyi çözünürlük umulur. Buna rağmen bu teknikle de çözünürlükte bir gelişme olmadı.

Anahtar kelimeler; polyrotaksan, rotaksan, kükürbit[6]yuril, 1,3-dipolar siklo katılma, porfirin.

ACKNOWLEDGEMENT

I would like to express my deep gratitude to Asst. Prof. Dr. Dönüş TUNCEL for her supervision throughout my studies.

I am very thankful to Ahmet Faik DEMİRÖRS, Mehtap KÜYÜKOĞLU, İlknur TUNÇ, Olga SAMARSKAYA, Oğuzhan ÇELEBİ, Yaşar AKDOĞAN, Anıl AĞIRAL, Ünsal KOLDEMİR, Hasan Burak TİFTİK and all present and former members of Bilkent University Chemistry Department for their kind helps and supports during all my study.

A special thanks to all of my family members who have supported me with encouragement.

TABLE OF CONTENTS

ABREVATIONS

CD Cyclodextrin

CB Cucurbituril

DTA Differential Thermal Analysis

THF Tetrahydrofuran

GPC Gel Permeation Chromatography

MALDI-TOF Matrix-Assisted Laser Desorption/Ionization Time-Of-Flight

DSC Differential Scanning Calorimetry

TGA Thermogravimetric Analysis

DPP Diphenylporphyrin

TLC Thin Layer Chromatography

TFA Trifluoroacetic acid

DCM Dichloromethane

DIBAL Diisobutylaluminium

TCBQ Tetrachloro-p-benzoquinone

MeOH Methanol

EtOH Ethanol

DPM Dipyrromethane

DSS 2,2-Dimethyl-2-silapentane- 5-sulfonate sodium salt

LIST OF FIGURES

LIST OF SCHEMES

LIST OF TABLES

CHAPTER 1. INTRODUCTION

1.1. Literature Review

1.1.1. Rotaxanes and Polyrotaxanes

By the recognition of the importance of specific noncovalent interactions in chemical processes and in biological systems, supramolecular science has been of great interest in recent years.[1-3] The association of two or more chemical species held together by intermolecular forces yields the organized noncovalent assembly with high complexity. Supramolecular science investigates the chemistry of these assemblies. Much more attention has been focused on the design of nanoscale molecular or supramolecular architectures that have specific structures, properties and functions.[4,5]

Supramolecular chemistry covers two main categories, host-guest chemistry and self assembly. Synthesis of mechanically interlocked molecules such as rotaxanes and polyrotaxanes is one of the most significant developments in host-guest chemistry.[6] Rotaxanes, from the Latin *rota* meaning wheel, and *axis* meaning axle, are composed of a ring threaded on a linear chain terminated by bulky stoppers.[7] Pseudorotaxanes are compounds in which a chain threads rings but both ends of the chain are not blocked by bulky substituents. A rotaxane containing n rings is named [n]rotaxane. A macrocyclic compound is threaded onto a segment of a polymer main chain or side chain to form a supramolecular entity that is called polyrotaxane, the polymeric analog of rotaxane (Figure 1.1).[8]

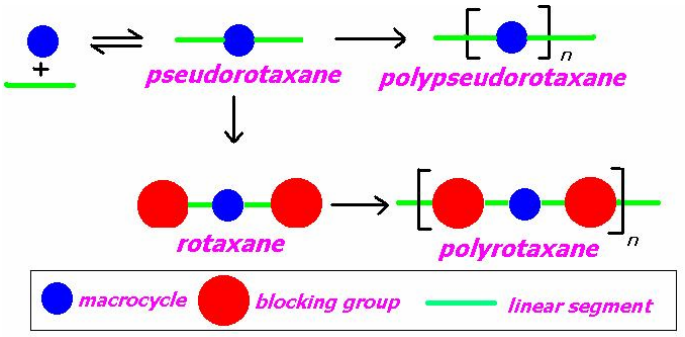

Figure 1.1. Schematic representation for a pseudorotaxane, pseudopolyrotaxane, rotaxane and polyrotaxane.

In 1967, Harrison and Harrison[6] reported the synthesis of first [2]rotaxane. In this rotaxane, the linear segment was decane- 1,10-diol bis(triphenylmethyl) ether and the macrocycle was 2-hydroxy-cyclotriacontanone. Structural investigation was done by IR spectroscopy. Recently, polyrotaxanes have attracted considerable attention because of not only their aesthetic structure but also their potential applications such as molecular switches and machines. For example, biodegradable polyrotaxanes can be used as drug delivery vehicles in biomedical applications.[7-12] Polyrotaxanes are used to prepare triggerable macromolecular switching devices that may be thermo-responsive, [13-15] photo-responsive, [16] and pH-responsive.[17,18] Another potential application area is polymer electronics. Since threading changes the electronic properties of polymers, protection and insulation of conducting polymer backbones by high levels of threading is crucial to the exploitation of molecular semiconductors for polymer electronics.[19] Threading changes not only electronic properties but also increases thermostability of polymer backbones and changes the solubility, solution viscosity, phase and melt characteristics of polymers. Additionally, threading leads to changes in photochemical properties of polymers such as fluorescence and luminescence.

1.1.2. Classification of Rotaxanes and Polyrotaxanes

Polyrotaxanes can be classified into different groups depending on how cyclic and linear units are connected, how they are synthesized, what their cyclic units are.

1.1.2.1. According to the location of rotaxane units

According to the location of the rotaxane unit, polyrotaxanes can be divided into two main groups as main chain and side chain polyrotaxanes.[20-24] In the main chain polyrotaxanes, rotaxane unit is located on the main chain (Figure 1.2), while in side chain polyrotaxanes, on the side chain (Figure 1.3). A [2] rotaxane polymer and many macrocycle-threaded polymers are main chain polyrotaxanes. Many different combinations of macrocycle and polymer were used to synthesize main-chain

polyrotaxanes. Ritter et al.[25] reported the first side chain polyrotaxane resulted from the reaction of preformed poly(methyl methacrylate) with β-cyclodextrin threaded blocking groups.

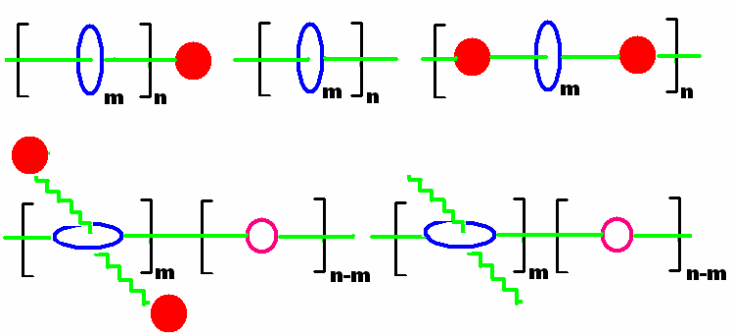

Figure 1.2. Schematic representation of various types of main chain polyrotaxanes

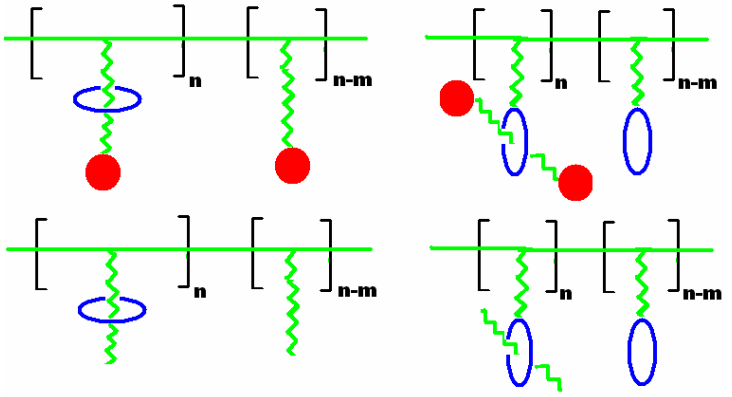

Figure 1.3. Schematic representation of various types of side chain polyrotaxanes

1.1.2.2. According to the synthetic route

Polyrotaxanes can be grouped in respect to the synthetic methods which are statistical and templated or direct methods. The synthetic method of the first reported rotaxane by Harrison[6] was a purely statistical threading. In this threading process there is no attractive force between the linear segment and cyclic moieties of the rotaxane. The same group also found the dependence of the rotaxane yield on macrocycle size in statistical threading. It was observed that as the size of the macrocycle increases up to optimum size the yield of rotaxane increases. The slippage of macrocycle over blocking

groups was also introduced first time in this work. Since ΔS^6 is always negative in threading and ΔH is almost zero with the statistical method, according to $\Delta G=\Delta H-T\Delta S$ equation statistical approach is not as smart as other methods.

In 1964 Schill et al.[26,27] synthesized rotaxanes by chemical conversion method. As it can be seen from the Scheme 1.1, linear segment with reactive end groups was chemically bonded to the cyclic moieties. Then blocking groups were added to prevent dethreading of cyclic species. Finally, the chemical bond between the linear segment and the macrocycle underwent a cleavage to yield rotaxane. This method is both time consuming and gives low yields overall.

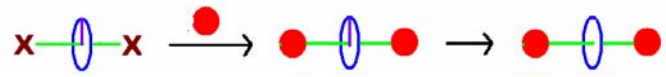

Scheme1.1. Chemical conversion method

Alternatively, the macrocycle may be threaded onto the pre-synthesized polymer backbone. If the macrocycle forms from the linear segments in the presence of polymer, then the process is called as clipping. In the entering route, disassembling of the polymer chain that reassembles by incorporation with macrocycle is observed.

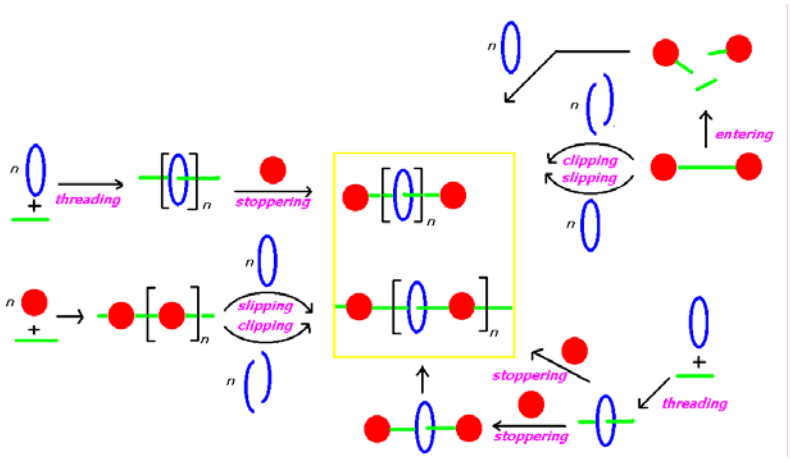

Scheme 1.2. Schematic representation of the methods for the synthesis of rotaxanes and polyrotaxanes

In the direct or template method, threading is driven by enthalpy. The intermolecular attractive force between the linear segment and the macrocycle, is a driving force leading to negative ΔH for threading. Because of the existence of attractive forces, this method is more effective and gives higher yields than the statistical threading method. There are different types of driving forces used in rotaxane synthesis such as hydrogen bonding, hydrophobic effect, ion-dipole interaction, metal-ligand complexation, and π-π interactions.

Stoddart's research group reported[23] that the self-assembly threading method resulted from the pair rule between an electron-rich and an electron-poor species, between macrocycle and linear segment. As a combined result of hydrogen bonding, dipole-dipole interaction and π-π stacking/charge transfer, there was a strong association. This method became highly popular in supramolecular architecture.

Recently, Steinke et al.[28] introduced the catalytic self threading method in which the macrocycle has catalytic ability to catalyze the 1,3-dipolar cycloaddition reaction between functionalized monomers to produce polymer threaded by macrocycles. The most important characteristics of this method is to control the number of macrocycles per repeating units and as a result the preparation of the well-defined structures.

1.1.2.3. According to the type of macrocycle

One of the classification criteria of polyrotaxanes is the type of cyclic moieties that are named as macrocycle or host of the polyrotaxane system. There are a number of different rotaxane and polyrotaxane systems that are designed by using cyclodextrins,[29-43] crown ethers,[44-54] cyclophanes[55-60] and cucurbituril[69-84] as macrocycle. Choosing suitable macrocycle and polymer are important for the design of polyrotaxanes with well defined functions and applications.

1.1.2.3.1. Cyclodextrins as a macrocycle

Cyclic oligosaccharides consisting of glucose units linked through α-1,4-glycosidic linkages form a series of cyclic compounds that are called cyclodextrins whose

derivatives are the most widely used macrocycles in the synthesis of rotaxanes and polyrotaxanes. α-, β-, and γ- cyclodextrins (CD) consist of 6, 7, and 8 glucose units, respectively (Figure 1.4). Because of their ability to be threaded onto a long axle and to slide along a chain or to rotate around an axle and because of their solubility in water, CDs have become some of the most common macrocycles used in rotaxanes and polyrotaxanes.[29-43]

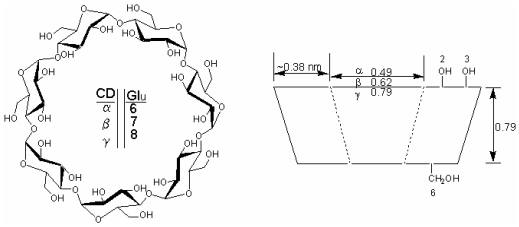

Figure 1.4. α-, β-, and γ- cyclodextrins (CD)

The first pseudopolyrotaxanes incorporating CDs were reported by Otaga in 1975.[29] In this work β-CD was threaded onto the four structurally different polyamides to obtain pseudopolyrotaxanes by interfacial or solution polymerization in the presence of diacid chlorides. But there was no direct evidence of threading and the molecular weights of the poly(amide rotaxane)s were low. Ogino et al.[30] reported CD-based [2]rotaxanes and polyrotaxanes containing cobalt complexes as stopper groups that increase the thermostability of inclusion complexes.[30,31] The necessity of having certain length of a linear molecule for threading was concluded.

Lawrence.[32-34] used biphenyls or porphyrins and Kaifer[35] used ferrocenes and naphthalene sulfonate as stoppers. Wenz et al. prepared bipyridinium containing [2]rotaxane[36] while Nakashima et al. prepared a rotaxane consisting of 4,4'-diaminostilbene and β-CD.[37] Harada and coworkers indicated that poly(ethyleneoxide) ,[38,39] poly(propylene oxide)[40,41] and polyisobutylene[42] can be used as polymeric backbones of CD based polyrotaxanes. It was observed that the cavity sizes of CDs determine the structures of polyrotaxane and whether threading can occur or not.

1.1.2.3.2. Crown Ethers as macrocycle

One of the other attractive macrocycles for polyrotaxane synthesis are crown ethers (Figure 1.5). Crown ethers can form inclusion complexes with different linear molecules. The ability of crown ethers to form hydrogen bonds with acidic protons i.e. –OH and –NH is the main driving force for the formation of polyrotaxanes.[44] For the first time, Agam et al.[45] prepared pseudopolyrotaxanes by threading of appropriate crown ethers onto poly(ethylene glycol) followed by the treatment with 1,5-diisocyanotonaphthalene. In their following study,[46] the same polymer backbone was threated through a crown ether in a statistical manner. Then trityl blocking groups were attached covalently to prepare the polyrotaxane. It was observed that the threading efficiency depends on the molar ratios between acylic and cyclic components, the diameter and the length of the acyclic components, the size of the macrocyclic cavity, temperature of the medium and the volume of the system.

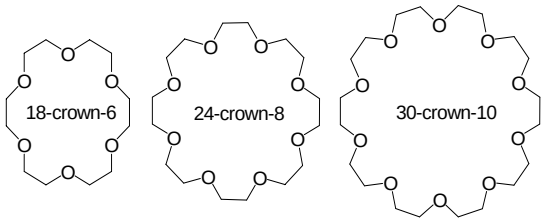

Figure 1.5. Crown ethers with various size

The solubility of crown ethers in almost all organic solvents renders easy for polymerization conditions. As a result of its good solubility, in addition to the more possibilities of synthetic methods and backbone types, purification is easier for crown ether based polyrotaxanes.[47] Numerous pseudopolyrotaxanes and polyrotaxanes formed from polyurethane, polyester, polystyrene, polyamides and poly(arylene ether)s[48-54] incorporating different crown ethers, 30-crown-10 (30C10), 42C14, 48C16 and 60C20 have also been prepared by Gibson et al. Crown ethers were used as solvent for poly(urethane crown ether rotaxane)s by solution polycondensation.[48] Although there were no bulky blocking groups at the end of chain, the macrocycles did not dethread. It was concluded that the cooling of chains and hydrogen bond formation between macrocycles and polymer backbone prevent dethreading. The authors proved that the threading efficiency (x/n) increases with increasing ring size at constant cyclic to linear unit ratio. Also the feed ratio of the cyclic to glycol monomer affected the threading

efficiency: the larger the ring, the higher the equilibrium constants. They also showed that the glass transition temperature increased as the mass fraction of crown ether increased. Additionally, it was found that the crown ether can crystallize without dethreading, when the mass fraction of crown ether is large.

Marand et al. addressed the role of intra-annular hydrogen bonding between the threaded crown ether and the in-chain NH groups.[49] By transesterification methods, poly(ester crown ether rotaxane)s were prepared with diacid chloride in the presence of crown ethers.[50] As in the case of poly(urethane rotaxane)s, the larger the ring was, the higher the threading efficiency was. In contrast to poly(urethane rotaxane)s, the poly(ester crown ether rotaxane)s have two glass transition temperatures. This was attributed due to the movement of the threaded cyclic along the polyester backbone. Therefore it was concluded that no apparent backbone-cyclic interaction exists.

1.1.2.3.3. Cyclophanes as macrocycle

Various main-chain pseudopolyrotaxanes incorporating cyclophanes, for example cyclobis(paraquat-*p*-phenylene) as shown in Figure 1.6 threaded onto a π-electron-rich polymer backbone, were prepared by Stoddart[55-60] by mixing polymers and cyclophanes in solvents such as acetonitrile.

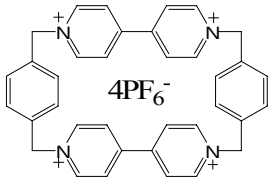

Figure 1.6. Cyclobis(paraquat-*p*-phenylene) as macrocycle

1.1.3. Cucurbituril

1.1.3.1. Synthesis and Recognition

In 1905, Behrend[61] reported the acid catalyzed condensation between an excess of formaldehyde and glycoluril (Scheme 1.3). It was observed that the initial product had an amorphous character and it was insoluble in all common solvents. As a result of these

physical properties it was assumed that the initial product was a cross-linked aminal type polymer. Dissolving the solid in hot concentrated sulfuric acid followed by dilution with cold water, then filtering out the precipitate and heating the filtrate have yielded a crystalline solid. Although the structure of the product was not identified exactly, it was characterized as $C_{10}H_{11}N_7O_4.2H_2O$ through elemental analysis. It was shown that the product was very stable towards strong acid and bases also it had ability to form crystalline complexes with several metal salts and dyes.

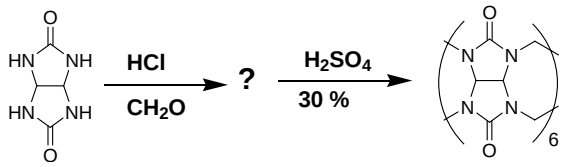

Scheme 1.3. Synthesis of CB[6]

Mock,[62] who synthesized CB[6] by modifying the procedure reported by Behrend, interpreted the steps of the reaction as the thermodynamically controlled rearrangement of an initially formed macromolecular condensation product. The structure was characterized through IR, ^1H and ^{13}C NMR. The carbonyl absorption at 1720 cm^{-1} indicated the existence of the glycoluril units, while the presence of only three signals, a doublet at about 4.5 ppm and a singlet and a doublet at about 5.5 ppm with equal intensity in the ^1H NMR spectrum proved the highly symmetric non aromatic structure. As a result of the NMR data and elemental analysis of the product in hydrate form, they introduced the stoichiometry as

$$n C_4H_6N_4O_2 + 2n CH_2O \rightarrow (C_6H_6N_4O_2)_n + 2n\ H_2O$$

In addition, X-ray crystallography was used to determine the structure of CB[6] with calcium bisulfate in the sulfuric acid solution. Octa-coordination of the metal ions with the carbonyl oxygen atoms of the substance, water and sulfate ligands and threading of the hydrogen-bonded chain of three water molecules through the interior of the structure were observed.

Consequently, the chemical structure of the substance was described[62] as a cyclic hexamer of glycoluril units linked by methylene bridges. It was also reported that it forms from 19 rings held together entirely by aminal linkages. Since it looks like a pumpkin, it was named as the cucurbituril from the 'cucurbita' in the Latin. From the crystal structure of CB[6], it was determined that it has an internal cavity of approximately 5.5Å which is a useful feature for host-guest chemistry (Figure 1.7). Six carbonyl groups of the glycolurils form the 4Å diameter portals of the CB[6]. Although the size of its cavity is similar to that of α-CD, it's highly symmetrical structure with two identical openings distinguishes it from α-CD.

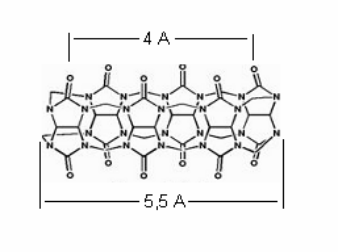

Figure 1.7. Structural characteristics of CB[6]

In 2000, Kim et al. [63] reported the synthesis and characterization of cucurbituril homologues, CB[5], CB[7], CB[8]. They carefully adjusted the reaction conditions such as temperature. Since the cyclization of the pre generated oligomers formed from glycoluril and formaldehyde yields cucurbituril, the synthesis procedure of CB homologues is the same as that of CB[6] as shown in Scheme 1.4. Instead of working at high temperature it is necessary to work at lower temperature.

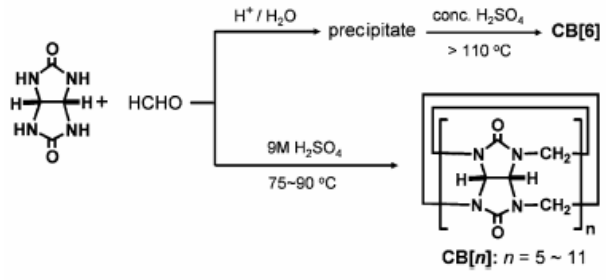

Scheme 1.4. The synthesis of cucurbituril homologues

In the same work, it was observed that although the ^{1}H NMR chemical shift values were different for CB[5], CB[7], and CB[8], their peak patterns were similar. By using XRD, structures of the derivatives (Figure 1.8) and some structural parameters such as portal diameter, cavity diameter, cavity volume, outer parameter and height of the cucurbituril derivatives were determined as shown in Table 1.1.

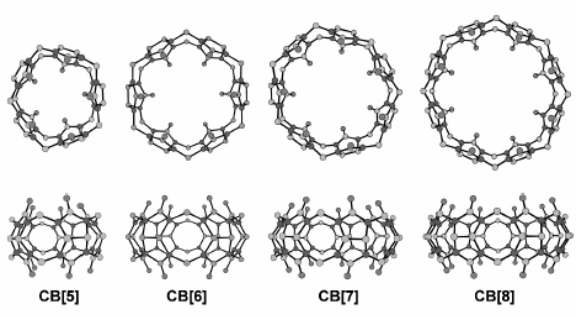

Figure 1.8. X-ray crystal structures of CB[n] (n= 5–8).

	CB[5]	CB[6]	CB[7]	CB[8]
Outer diameter(Å)	13.1	14.4	16.0	17.5
Portal Cavity(Å)	2.4	3.9	5.4	6.9
Interior Cavity(Å)	4.4.	5.8	7.3	8.8
Height(Å)	9.1	9.1	9.1	9.1
Cavity Volume ($Å^3$)	82	164	279	479

Table 1.1. Structural parameters of cucurbituril derivatives

1.1.3.2. Properties of CB[6]

In this thesis, CB[6] will be employed as a macrocycle. Therefore the properties of CB[6] will be discussed in more details. After synthesizing and characterizing CB[6], Mock et al.[64] also investigated its binding behavior with sterically unhindered aliphatic amines in acidic solution through ^{1}H NMR and UV-Vis. According to this study, the methylene protons of alkanediammonium ions which encapsulated by CB[6] shielded from the magnetic field by showing upfield shifts around 0.6-1.0 ppm as shown in Figure 1.9. Moreover, having no averaging of signals in the presence of excess guest alkylammonium ions was attributed to slow exchange between external and internal environments on the NMR time scale, which enabled to determine the relative binding

constants of various alkylammonium ions with CB[6]. Formation constants for over 60 substituted alkylammonium ion ligands were reported, by using competitive NMR experiments. According to this method, two different alkylammonium ions competed for a limited amount of CB[6]. By accurate NMR integration the relative affinities of the alkylammonium ions were determined. Then the 4-methylbenzylammonium ion was determined as the reference guest and by using UV technique all the affinities converted to an absolute scale.

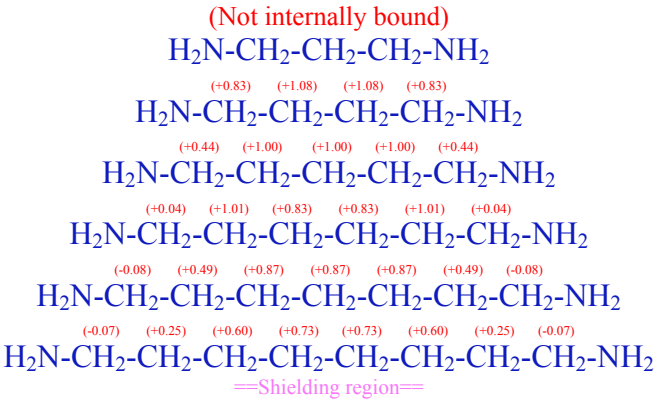

Figure 1.9. Induced shifts (ppm) of methylene groups of alkanediammonium ions upon complexation with CB[6]

It was reported[65] that n-butylammonium ion and n-hexyldiammonium ion are the most tightly bound aliphatic monoalkaneamine and dialkaneamine respectively (Figure 1.10). The distance between the two occuli of CB[6] was found to be almost equal to the distance between nitrogens extended conformation of 1,6-hexanediamine. It was observed that although the isopentylammonium ion binds as tight as the n-butyl ammonium ion, the neohexylammonium ion could not. Therefore, the existence of no characteristic NMR shift resulted from the complexation with CB[6] implies that the internal cavity of CB[6] is not big enough to encapsulate the t-butyl group.

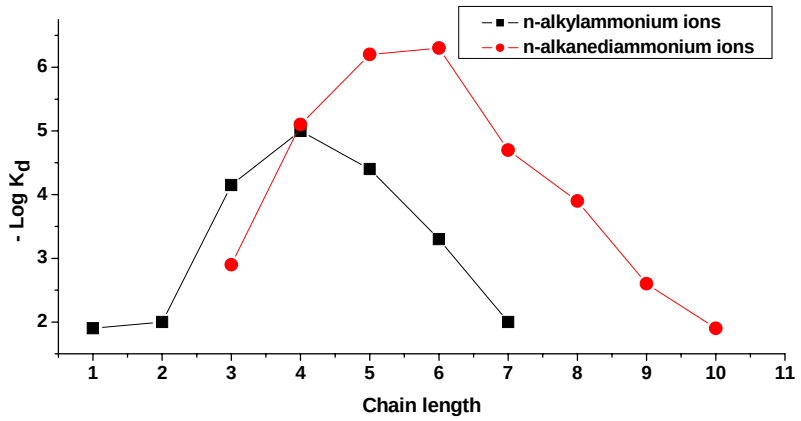

Figure 1.10. CB[6] binding strength dependence upon chain length

Moreover the encapsulation ability of CB[6] was investigated by using various cycloaliphatic ammonium ions. As a consequence it was reported that the cyclopentanemethyl ammonium ion was the most tightly bounded cycloaliphatic ammonium ion. Furthermore, it was demonstrated that except p-methylbenzyl ammonium ion, ortho and meta derivatives of methylbenzyl ammonium ion could not form an inclusion complex with CB[6]. The larger the dissociation constant (K_d), the stronger the binding. Crystallographic determination of the structure of the thiophenemethyl ammonium ion indicated that some distortion is necessary to be encapsulated by CB[6] for the larger six-membered aromatics. From all these studies it can be concluded that the interior of CB[6] is hydrophobic, whilst the carbonyl fringed portals are polar and hydrophilic, hence resembling the cross-sectional properties of a lipid bilayer. Therefore CB[6] has the ability to selectively bind to n-alkylammonium salts. As a result of the binding, the lipophilic n-alkyl chain extends into the interior by freeing the water molecule while the positively charged ammonium ions bind via ion-dipole forces to the carbonyl-fringed portal. The complexation selectivity depends on the length of the organic n-alkyl chains. It was stated that the free energy of interaction between the hydrophobic interior of CB[6] and the alkyl group of guest molecules was not low enough to confer sufficient thermodynamic stability for guest molecules shorter than four methylene units. On the other hand, if the chain is too long there would be a

part of the chain extending beyond the interior towards the opposite portal where the intermolecular forces would be unfavorable.

Although a tripodal H-bonding scheme between the oxygen atoms of alternate carbonyls of CB[6] occuli and hydrogens of RNH_3^+ seems possible, it was observed that the binding capacities of n-$C_4H_9NH_3^+$ and n-$C_4H_9NH_2CH_3^+$ are 1000-fold greater than that of n-$C_4H_9NH(CH_3)_2^+$. The same result was also observed for hexanediamine. As a result, it was concluded that one of the three protons on nitrogen projects away from the occuli while the other two contact carbonyl oxygens.

Kim et al. [66] reported the inclusion complex formation abilities of cucurbituril homologues by using different guest molecules. Some results of these studies were reported as shown in Figure 1.11.

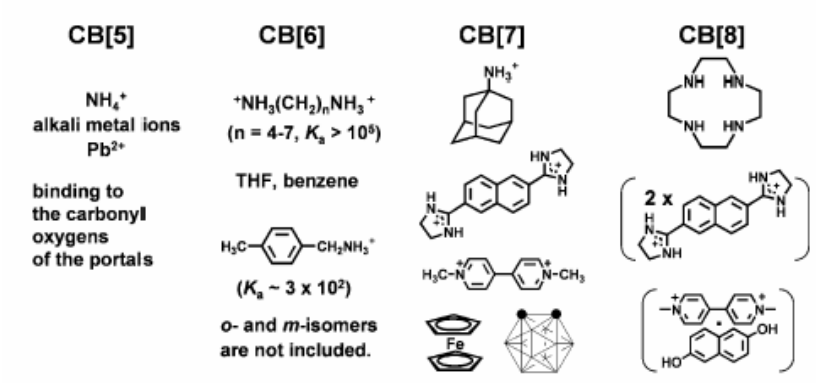

Figure 1.11. Inclusion complex formation abilities of cucurbituril homologues

1.1.3.3. 1,3-Dipolar Cycloaddition

Although CB[6] has all of these attractive properties, the most important property of CB[6] that differs from the other macrocycles is its ability to catalyze 1,3-dipolar cycloaddition reactions. Mock[65] et al. demonstrated that CB[6] was able to enhance the rate of 1,3-dipolar cycloadditions between alkylazidoammonium and alkynylammonium species to yield a regioselective 1,4-disubstituted triazole ring. During this process (Scheme 1.5), the reactants are bound to opposite carbonyl portals of CB[6] via their ammonium function by extending their alkylazido and alkynyl segments through the

interior of CB[6]. Therefore a ternary complex forms by azide-substituted and alkyne-derived ammonium ions and CB. In this ternary complex azido and alkynyl groups of the guest molecules come into closer proximity for cycloaddition to occur. These steps were inscribed as that in 1,3-dipolar cycloaddition reaction, strong ion-dipole interaction between portals of CB and each ammonium ions leads to steric crowding which results in the pressure inside the cavity. A triazole is the product of the release of the steric strain.

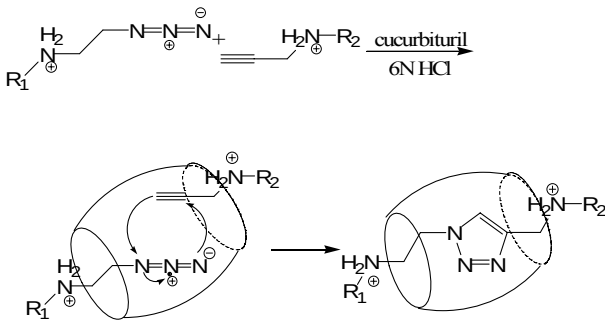

Scheme 1.5. 1, 3-Dipolar cycloadditions of alkylazidoammonium and alkynylammonium catalyzed by CB[6]

1.1.3.4. Switching Processes of CB[6]

As a result of having quantitative guest affinity data for CB[6], Mock[67] constructed the first molecular switch based on it. The movement of CB[6] through a protonated triamine ligand, $C_6H_5NH(CH_2)_6NH(CH_2)_4NH_2$, was investigated. It was observed that when pH is <6.7, CB[6] locates at the hexanediamine portion while by increasing the pH to >6.7 moves through the butanediamine portion as shown in Figure 1.12.

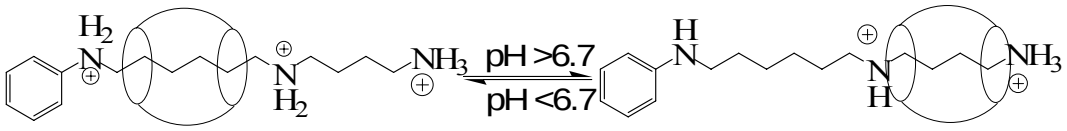

Figure 1.12. The first molecular switch based on CB[6].

In 2000 Kim's group reported[68] the first fluorescent reversible rotaxane-based molecular switch (Scheme 1.6). Characterization was done by ^{1}H and ^{13}C NMR

spectroscopy, mass spectrometry and elemental analysis.[1]H NMR spectra indicated that at low pH CB[6] locates at the protonated diaminohexane site while at high pH it moves through the protonated diaminobutane site. Moreover at intermediate pH separate resonances due to the location either at protonated diaminohexane or at protonated diaminobutane site revealed that the movement of CB[6] between two sites was slow on the NMR time scale. Switching of CB[6] from one site to the other was also observed through UV-Vis and Fluorescent spectroscopy by change in color and fluorescence. For an example, the intensity of absorption band at 265 nm decreases and the band at 300 nm increases when the pH increases.

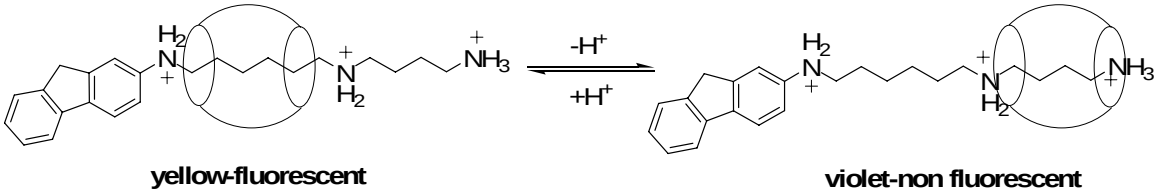

Scheme 1.6. The movement of CB[6] by pH change

Kim et al. also introduced[69] a kinetically controlled molecular switch that is a novel bistable [2]rotaxane in solution state consisting of CB[6], one protonated diaminobutane unit as a station (**A**), two pyridinium groups as linkers, two hexamethylene units as further stations (**B**), and two terminal viologen groups as shown in the Figure 1.13. The station (**A**) was determined as the exclusive position of CB[6] from [1]H NMR data and the movement of CB[6] from (A) to (B) is possible by deprotonation of protonated diaminobutane unit fast in the NMR time scale. In contrast, only 50 % of CB[6] shuttles back from station B to station A at the end of two weeks at room temperature. In summary, the switching of CB[6] from one state to the another was driven upon changing the pH but for the reverse process thermal activation plus pH change was necessary.

Faster rate by applying higher temperature alludes such a conclusion the pH change is enough to swith the molecular bead from one site to the other whereas thermal activation plus to the pH change is necessary for the reverse process.

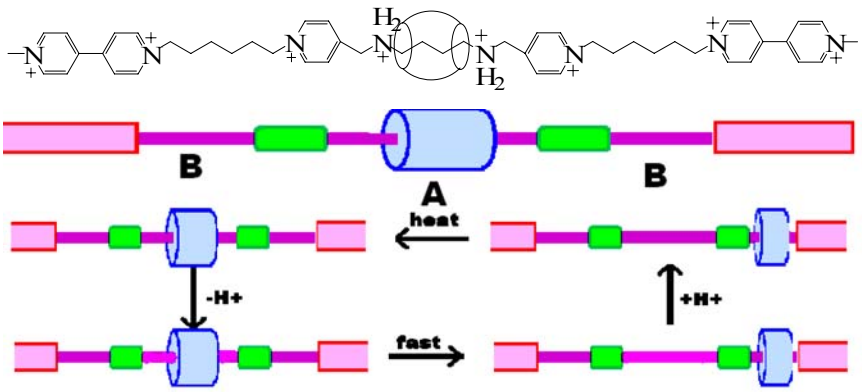

Figure 1.13. Switching properties of Bistable [2]rotaxane

1.1.4. Cucurbituril Based Polyrotaxanes and Polypseudorotaxanes

1.1.4.1. Solid State Coordination Polyrotaxanes

In 1996 Kim et al.[70] reported a first example to CB containing polyrotaxanes, which contained a macrocycle in every repeating unit. In their strategy as shown in Scheme 1.7, first the building block *N, N'*-bis(4-pyridylmethyl)-1,4-diaminobutane dihydrochloride with suitable functional groups at both ends was synthesized. Then macrocycles, CB[6]s were threaded to form a pseudorotaxane. After the treatment of pseudorotaxane with $Cu(NO_3)_2$, due to the coordination of Cu^{2+} with the nitrogen of pyridine, a pseudorotaxane was formed with high structural regularity. Furthermore this polypseudorotaxane with strong coordinative bonds was the first that was structurally characterized by single-crystal X-ray crystallography, although X-ray crystal structure of polypseudorotaxanes in which H bonding is the linkages between pseudorotaxanes was reported earlier.[71,72]

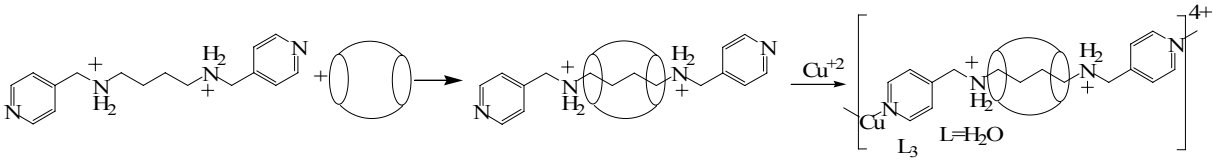

Scheme 1.7. Synthesis of one dimensional coordination polyrotaxane

The X-ray crystal structure demonstrated that a copper ion, two independent halves of a CB[6] molecule, two independent halves of the polymer chain, and three

water molecules that bind to the copper ion coordinated to form the asymmetric repeating unit of the polyrotaxane. It was observed that the charge balance of each repeating unit was obtained by four nitrate ions. In addition to indicating the existence of hydrogen bonding between the CB[6] and the protonated amine nitrogen atoms of the polymer chain, X-ray data revealed that the copper ion has a square pyramidal coordination geometry. The zigzag shape of the polyrotaxane was attributed to the cis coordination of two pyridine units to the metal center that leads to a change of direction of the polymer chain. Moreover it was stated that the attempts to synthesize the corresponding polyrotaxane with other divalent first-row transition metal salts are unsuccessful. This observation proved the importance of proper metal choice to synthesize a polyrotaxane coordination polymer.

By changing the structure of the polymer string and adding sodium oxalate to the reaction mixture of the pseudorotaxane with $Cu(NO_3)_2$, a 2D polyrotaxane (Scheme 1.8) with large cavities and channels was synthesized by Kim's group.[73] The X-ray data revealed that the coordination geometry of the copper ion is distorted octahedral and is formed by coordination with two pyridyl units of the two pseudorotaxanes, a bidentate oxalate anion, and two water molecules. Two types of cavities surrounded by six or three CB[6]s were observed. X-ray diffraction patterns indicated that by removing the water molecules occupying the channels under vacuum destroys the crystal structure of the polyrotaxane. However, it was possible to restore crystallinity by adding water molecules. Furthermore the crystallinity of the structure preserves upon changing the type of anions and there was a size selectivity of anions for the channels of the polyrotaxane. Moreover, it was demonstrated that the replacement of water molecules coordinated to the copper by NH_3 responds with color change of the crystals from blue to deep blue while retaining its crystal structure.

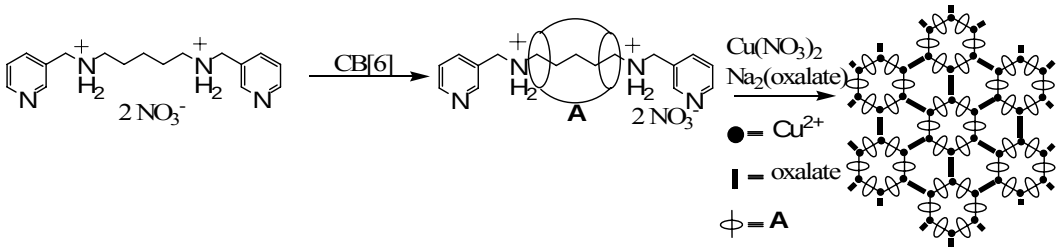

Scheme 1.8. Synthesis of two dimensional coordination polyrotaxane

Kim et al [74] reported the construction of polyrotaxane, in which CB[6] was threaded on 2D coordination polymer networks. Since the networks are fully interlocked, this polyrotaxane was a first example to polycatenated polyrotaxane networks. Their strategy was the same as the previously reported procedure[70] up to the formation of pseudorotaxane. Then the reaction between the pseudorotaxane and $AgNO_3$ yields the polycatenated two dimensional polyrotaxane net. It was declared that the solid state structure of the polyrotaxane coordination polymers depends on the counteranions of the coordination metal. It was observed that although the structure of the polyrotaxane containing $AgNO_3$ was interlocked two dimensional polycatenated polyrotaxane nets, the structure of the polyrotaxane formed from the reaction of same pseudorotaxane with silver tosylate was a one dimensional polyrotaxane coordination polymer

Replacement of the string *N*,*N*'-bis(4-pyridylmethyl)-1,4-diaminobutane by the longer and more flexible string *N*,*N*'-bis(3-pyridylmethyl)-1,5-diaminopentane yielded the first example of helical polyrotaxanes, in which cyclic beads are threaded on helical one-dimensional coordination polymers.[75] The reaction of the pseudorotaxane with $AgNO_3$ yielded the helical 1D polyrotaxane that its one turn in helix constructed from two pseudorotaxane and two silver ions. Each asymmetric unit contains a pseudorotaxane, a silver ion, one of the pyridine units coordinated with the silver ion and nitrate counter ions. In this study, the reason of having a helical structure was attributed to the sharp change in the direction of the polymer chain due to the parallel conformation of the 3-pyridyl unit attached to the 27^{th} nitrogen atom in the string with the six-oxygen plane in spite of the fact that the 3-pyridyl unit connected to the 26^{th} nitrogen atom make a dihedral angle of 61°.

In a more recent study, Kim[76] introduced 3D polyrotaxanes formed by coordination of pseudorotaxane, synthesized from CB[6] and *N, N'*-bis(3-cyonobenzyl)-1,4-diammoniabutane dinitrate, $Tb(NO_3)_3$, lanthanide metal with larger ionic radii and higher coordination number than the transition metals. The investigations proved that six pseudorotaxanes with 3-phenylcarboxylate at the terminal coordinate with a binuclear Tb^{3+} ion at the center to produce one structural unit of a three dimensional polymer network threaded by CB[6]. Also it was stated that any change in building block leads to a change in the solid state structure of the network.

1.1.4.2. Solution State Polyrotaxanes

The polyrotaxanes which were discussed so far were not soluble in any solvent. Therefore they could not be characterized well. Buschmann et al.[77] reported the synthesis of polyrotaxanes and pseudopolyrotaxanes containing CB[6] threaded on organic polymers by interfacial polymerization of CB[6]-1,6-diaminohexane complex and acid chlorides such as adipyl chloride, 1,4-or 2,6-naphthalene dicarboxylic acid chlorides. These polyamide polyrotaxanes were not soluble in common organic solvents, they were partly soluble in acidic solution. The threading by CB was proved by ^{1}H NMR spectroscopy. Upfield shift of the methylene protons of amine parts in the ^{1}H NMR spectrum proved threading by CB. Having no averaged NMR signal was ascribed as the slowness of CB motion on the NMR time scale. The existence of diamine units both complexed and uncomplexed with CB was demonstrated by ^{1}H NMR and elemental analysis. IR spectroscopy also confirmed the presence of polyamide rotaxanes.

Formation of polyrotaxane was also proved by comparing the DTA curves of the physical mixture and the polyrotaxane with different ratio of CB[6]. It was obvious that by increasing the number of threaded amide part compared to the free amides, the peaks at lower temperatures disappeared whereas the peaks at higher temperatures increased. This effect was not observable for physical mixtures. From the shift of the melting peak in DTA through lower temperatures, it was deduced that the crystallinity of the polymer decreased by increasing the threaded CB[6] ratio. Consequently it was proved that the presence of CB[6] in polyamide changed the thermal behavior of the polymer.

Furthermore, dying the pulled polymer films from the liquid interface of CB free polyamide and polyamide-CB[6] polyrotaxane with an acid dye indicated that the dyeability of polyrotaxane was less than that of the polyamide chain, since the amino groups of the polymer chain were shielded by CB[6].

The first polyrotaxane containing CB[6] which is well-soluble in water was prepared by Steinke et al.[28] through catalytic-self threading. Firstly, azide and alkyne functionalized 1,6-hexanediammonium ions were synthesized as monomers. By treatment with CB[6], instead of synthesizing expected polyrotaxane, [2]-pseudorotaxanes were obtained. ^{1}H NMR data for various reaction conditions indicated that polyrotaxane formation was not possible for the system. Polymer formation was possible only in the case of elevated temperature and prolonged times but not due to the catalytic effect of CB[6]. To investigate the reasons, a pseudopolyrotaxane was synthesized[78] by post-threading of CB[6] through poly(iminohexamethylene) which was synthesized by reduction of Nylon 6/6 with $BH_3.Me_2S$ in THF. The alternate sequence of threaded and unthreaded hexamethylene units, because of energetically unfavorability of complex formation of secondary ammonium ion with two CB[6] at the same time, was determined by ^{1}H NMR. High activation energy necessity for the translocation of CB[6] from one repeat unit to the other was ascribed as resulted from strong binding ability between CB[6] and the protonated hexamethylene repeat units, the existence of queuing of CB[6]s, and side-on complexation of CB[6] to the ammonium groups along the polymer chain (Scheme 1.9). As a consequence, this study introduced a new class of pseudorotaxanes with controllable number of CB[6] proceeding through the post threading route.

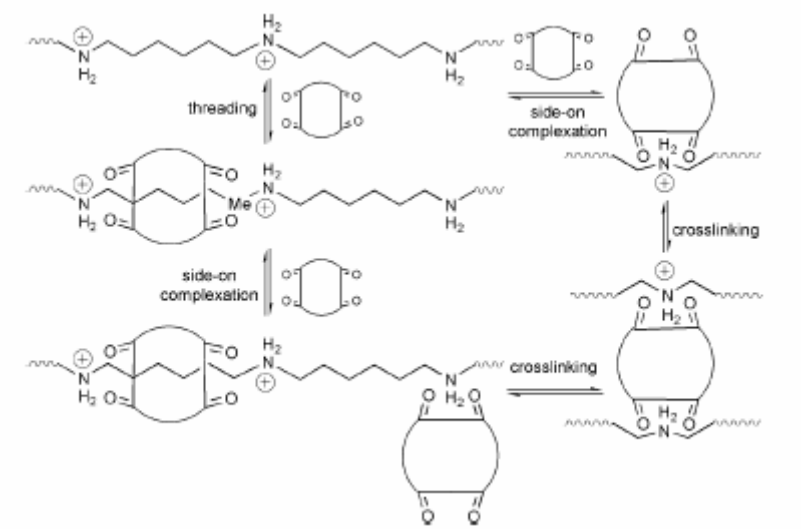

Scheme 1.9. Dynamic equilibria that are part of the complex threading process of cucurbituril onto linear poly(iminiumoligoalkylene)s.

Secondly, they introduced stopper groups containing polyrotaxanes[79,80] synthesized through 1,3-dipolar cycloaddition catalyzed by CB[6]. Catalytic self threading of equimolar amounts of diazide and dialkyne monomers in the presence of two equivalents of CB[6] yielded a well defined water soluble polyrotaxane. The structure of the polyrotaxane was confirmed by ^{1}H NMR and ^{13}C NMR spectra. Furthermore, GPC and MALDI-TOF were used to determine the molecular weight of the polymer and molar masses of repeat units.

Later on, Kim et al. reported[81] an example of solution state pseudopolyrotaxane synthesized by mixing a polyviologen polymer with slight excess of CB[6] . The polymer backbone that resulted from reaction between 4,4`-bipyridine and dibromodecane in methanol/*N*-methylformamide consists of approximately 10 bipyridinium units linked by decamethylene units in between. According to ^{1}H NMR data threaded CB[6] are localized on the internal *decamethylene* units, not on the internal *bipyridyl* units as shown in Scheme 1.10. The hydrophobic interaction between the decamethylene unit and the interior of the macrocycle cavity and the charge-dipole interaction between the bipyridinium unit and the portal oxygen atoms were the driving force for the threading. ^{1}H NMR spectra of the pseudopolyrotaxane with different molar ratios of backbone to

CB[6] indicated that although the "hopping" of CB[6] from one decamethylene site to the neighboring site is slow on NMR time scale the shuttling of CB[6] back and forth within a decamethylene unit was quite fast. By comparing the intensity of the signal of the CB[6] methylene proton and the terminal methylene proton of the polymer, it was suggested that all of the decamethylene units in the backbone can be threaded and the number of threaded CB[6] can be controlled by the addition of necessary amount of CB[6].

By examining the spin-lattice relaxation time the formation of pseudopolyrotaxane was also confirmed. The greater hydrodynamic volume and higher intrinsic viscosity of pseudopolyrotaxane were results of being more expanded compared to the free polymer. DSC traces implied that the polymer backbone that decomposes at 300 °C was a crystalline. TGA results indicated the increment of polymer stability by protecting the aliphatic chain with threading process. Finally, it was reported that the intensity of the UV visible band increased with increasing threaded CB[6] on the backbone.

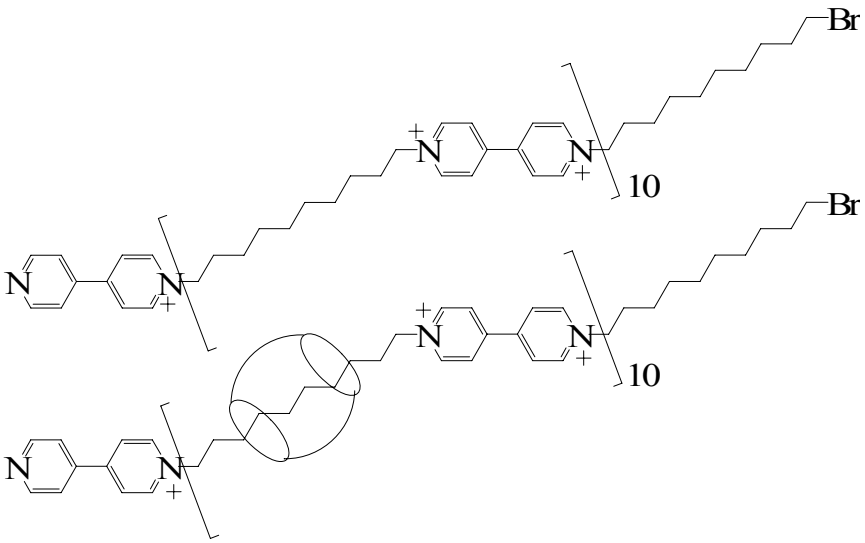

Scheme 1.10. Polyrotaxane containing polyviologen and CB[6] in solution state

Kim et al. reported[82] solution state side-chain polypseudorotaxanes whose characterizations were done by ^{1}H NMR and TGA in a similar fashion as in the previous study. The treatment of pre-synthesized side chain polymers with CB[6] yielded side-

chain polypseudorotaxanes (Figure 1.14) that exhibit higher conformational rigidity and thermal stability than their parent polymers. Furthermore for these polypseudorotaxanes, it was observed that threading and dethreading of the CB[6] macrocycles can be reversibly controlled by changing the pH of the solution.

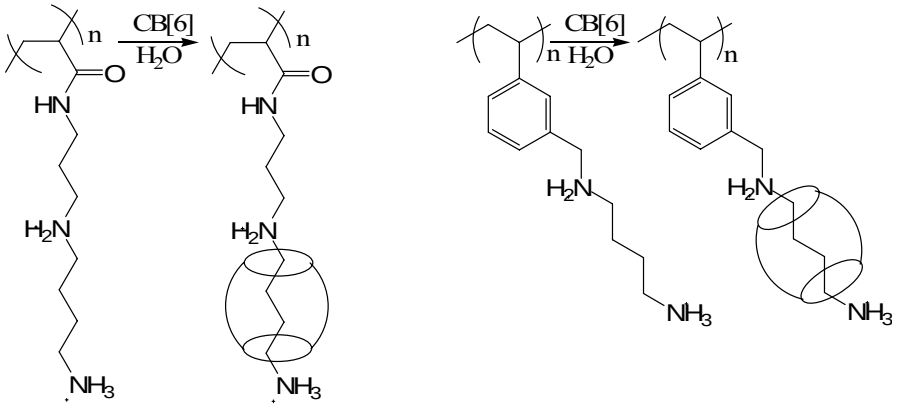

Figure 1.14. Side-chain polypseudorotaxanes in solution states

1.1.5. Porphyrin containing rotaxanes and polyrotaxanes

To design a rotaxane with various application areas in daily life is strongly dependent on choosing proper stopper group. Rich electro- and photo-physical properties of porphyrin make them attractive as stoppers. Porphyrins can be used to investigate the synthetic energy and electron transfer systems as models of natural photosynthetic systems[83, 84] and enzyme mimics.[85] In photodynamic therapy[86] and in various biological areas, especially water soluble porphyrins which may be cationic or anionic are widely used.

Although there are various potential application areas of porphyrins, self aggregate formation and solubility are two main problems to explore them. J- and H-aggregates are mainly two types of porphyrin aggregates due to π-π stacking and Van Der Walls interaction. There are many studies to explore the aggregate and interaction types of porphyrin containing molecular systems. Schneider et al.[87] reported about the stacking and ionic contributions of interaction between 23 different ligands and 3 porphyrins. It was reported that both water solubility and constant salt-bridges to substrates can be obtained by introducing ionegenic groups into meso positioned aryls of porphyrins. The

same group also reported[88] the interaction between 11 new porphyrins with meso positioned tertiary amines or ammonium groups and DNA. It was observed that the DNA viscosity decreases whereas the melting point of DNA increases in the presence of porphyrins and their copper and zinc derivatives. It was also stated that both red and blue shifts of the Soret bands are possible in the presence of DNA. Self-aggregation of cationic porphyrins in aqueous solution and factors affecting it were reported by Kano.[89] It was proved that peripheral meso substituents affect the self-aggregation of porphyrins.

There are many groups study to prevent the aggregation of porphyrin with encapsulation by a macrocycle as cyclodextrin. After reporting about the self-aggregation of cationic porphyrin, Kano et al.[90] also introduced static and dynamic behaviour of 2:1 complexes of cyclodextrin and charged porphyrins quantitatively. In this study, trans type 2:1 complex formation was observed by dissociation of high self-aggregates of porphyrins in the presence of cyclodextrin. In another study of the group,[91] it was indicated that selective anion coordination to the Fe(III)porphyrin occurs and that there is no porphyrin dimer formation in the presence of cyclodextrin. Wang et al.[92] investigated porphyrins and cyclodextrins spectroscopically. LKarge deviation from Beer's law in the absence of cyclodextrin was ascribed to aggregation of porphyrin. In 2002[93] Wamser's group investigated 1:1 and 1:2 complex formation between anionic free base porphyrin and the methyl violegen dication. Induced porphyrin dimerization was proved with blue shift of the Soret band at high propyl viologen sulfonate concentration.

1.1.6. Synthesis and the spectroscopic properties of porphyrin

In 1968 Haberle and Treibs[94] first introduced 5,15-diphenylporphyrins (DPP). One unsubstituted and one phenyl bearing carbons are two types of meso-carbons that diphenyl porphyrins contain. In a retrosynthetic manner, two dipyrrolic compounds can be used to synthesize these porphyrins through (2+2) type condensation route. The precursor dipyrrolic compounds are formed by fusion of two pyrroles through one type of meso-carbon bridge either unsubstituted or phenyl bearing. By condensation of these dipyrrolic precursors the other type of meso-carbon bridge is formed. As a result of (2+2) type condensation the primary product is obtained. Although the classic Mac Donald type

synthesis (pathway A, Figure 1.15) is advantageous to create asymmetric DPPs, to synthesize two different dipyrrolic precursors is time consuming to hold symmetric DPPs. Disadvantages of pathway B are extra synthetic steps for addition of a formyl group to the dipyrrolic compounds. Pathways C and D involve the condensation of precursors including the linkage carbon unit in the form of a hydroxymethyl group. Although to synthesize symmetric DPPs is possible by using only one type of dipyrrolic compounds, pathways C and D require additional synthetic steps. In addition to this disadvantage, the sensitivity of the hydroxymethyl compound is another problem. Pathways E and F are more profitable because there is no need for extra steps for carbon linkage in precursors. Since the yield percentage of the method through pathway F is higher, it was decided to follow it for this project.

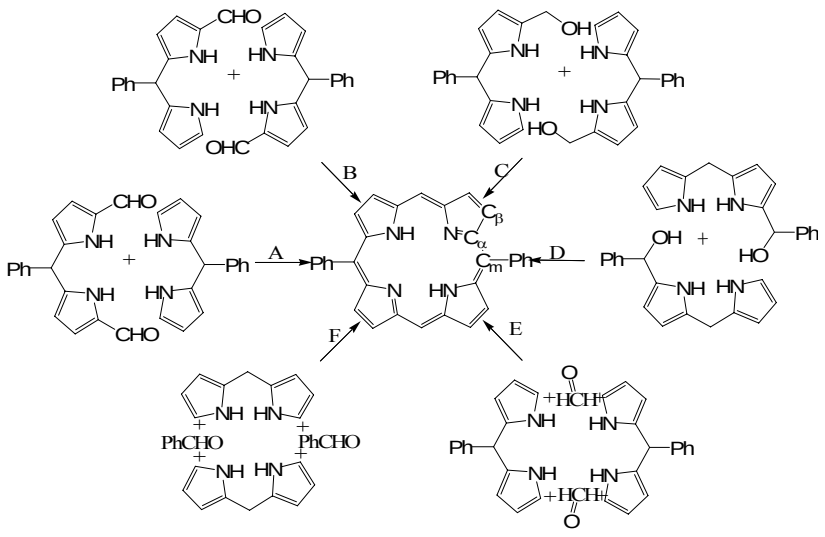

Figure 1.15. Principal pathways for the formation of 5, 15-diphenylporphyrin (DPP)

It is known that the central substituent leads to considerable variety in electronic and optical properties of porphyrin and there are mainly two different types of absorption spectra of porphyrin containing molecules. Porphyrin rings with two hydrogens in the center, free-base, have a characteristic absorption spectrum with four bands. In contrast, two bands appear in the absorption spectrum of most porphyrin metal complexes and acid dications with two hydrogens in the center. It is obvious that by going from an acid dication type of porphyrin to a free-base type, the conjugated ring symmetry changes from square planar that is D_{4h} to rectangular, D_{2h}. As a consequence of this reduction of

symmetry and the change in the electronic structure of the system, there is an observable change in the absorption spectrum.

Additionally porphyrins are divided into irregular and regular ones. Regular group contains metalloporphyrins with closed shells metals, free base porphyrins and their acid dications. In the absorption spectrum of regular porphyrins, there are characteristic bands named as Q, B, N, L and M originating from $\pi - \pi^*$ interactions. According to the Gouterman four orbital theory (Figure 1.16), B or the Soret band results from the strong transition from ground state to the second excited state ($S_0 \rightarrow S_2$) while the Q band originates from a weak transition to the first excited state ($S_0 \rightarrow S_1$). The spectrum of the free base contains four Q bands that arise from splitting of Q (0, 0) to Q_x (0, 0) and Q_y (0, 0) and additionally Q_x (1, 0) and Q_y (1, 0) which are the vibronic overtones of the previous two.

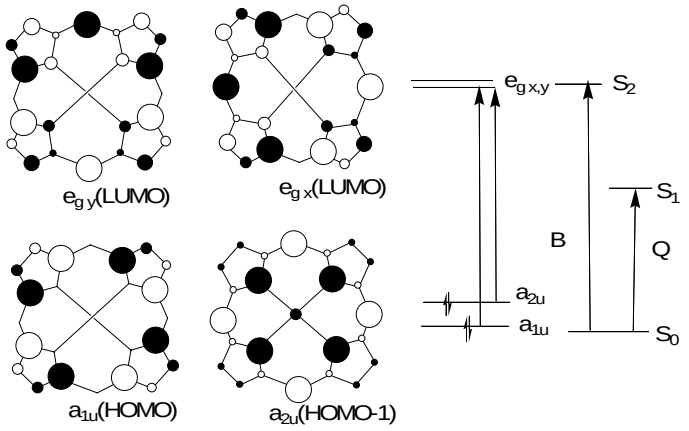

Figure 1.16. The four Gouterman molecular orbitals

1.2. Aim of the Study

As mentioned in the Literature Review part, by the time interlocked structures such as polyrotaxane became attractive because of their potential application areas that range from pharmacy to electronics. Especially the usage of polyrotaxanes to design molecular switches and machines that respond to external stimulus have prompted many research groups to synthesize new polyrotaxanes. Different types of macrocycles such as cyclodextrins, and crown ethers have been used. Characterization of newly synthesized

polyrotaxane with valuable physical and chemical characteristics is important in development of host-guest chemistry and its potential application areas.

There are many studies investigate synthesis and characterization of polyrotaxanes by using different macrocycles. Although each macrocycle has its smart properties, cucurbituril has attracted our attention because of its catalytic ability for 1,3-dipolar cycloaddition reaction between azide and alkyne functional groups. This ability is important in the self threading of polyrotaxane. Instead of other methods, we have followed the self threading method which provides the complete control over the number of macrocycle threaded.

The introduction of catalytic ability of CB[6] led some research groups to use this ability to synthesize self threading polyrotaxanes. There are some solid state polyrotaxanes based on CB[6]. But since they are not soluble in organic solvents or water, their application areas are limited. Synthesizing polyrotaxanes in solution states is very important especially to use in biological applications. Therefore, we synthesize and characterize rotaxanes and polyrotaxanes based on CB[6] in solution states.

Because of their rich electronic and photochemical properties and their ability to model photosynthetic systems and enzymes, porphyrins are attractive macromolecules. Since choosing the proper stopper group is important to design new polyrotaxanes with various application areas, using porphyrin as stopper groups may be smart for same purpose. Additionally, formation of self-aggregates of porphyrins may be overcome by synthesis of porphyrin containing rotaxanes and polyrotaxanes. There are some groups investigate the solution state polyrotaxanes based on CB[6] and different stopper groups but there is no study that introduces the polyrotaxane based on CB[6] and porphyrin. We have used porphyrin ring as stopper group. To the best of our knowledge, this is the first study that introduces rotaxanes and polyrotaxanes containing porphyrin as stopper group and CB[6] as macrocycle.

In this thesis, using the ability of CB[6] to catalyze 1,3-dipolar cycloaddition, novel rotaxanes and polyrotaxanes containing an electro- and photoactive porphyrin core are aimed to design, synthesize and characterize. Accordingly, after literature review and

introduction parts, detailed procedures of syntheses and FT-IR, UV-Vis, ^{1}H NMR, ^{13}C NMR and elemental analysis data are reported in experimental part. After discussing the results and characterizing the compounds in results and discussions part, conclusions take place.

CHAPTER 2. EXPERIMENTAL

2.1. Materials

All reagents and solvents were of the commercial reagents grade and used without further purification where noted. Column chromatography was carried out using silica gel (Kieselgel 60, 0.063-0.200 mm). Thin layer chromatography(TLC) was performed on silica gel plates (Kieselgel 60 F254, 1mm)

2.2. Instrumentation

2.2.1. FT-IR Spectroscopy

Absorption FT-IR spectra were recorded with a Bomem Hartman MB-102 model FT-IR spectrometer. A standard DTGS detector was used with a resolution of 4 cm^{-1} and 64 scans for all samples. All the samples were grinded very well to a fine powder before further grinding with KBr powder. Then these samples were dried under reduced pressure. IR spectra of them were recorded as KBr pellets. FT-IR spectra of all of the samples were recorded in 500-4000 cm^{-1} range.

2.2.2. UV-VIS Spectroscopy

UV-Vis spectra were recorded using a Varian Cary 5 double beam spectrophotometer with 60 nm/min speed with a resolution of 2 nm over the wavelength range from 800 to 200 nm. The UV-Vis absorption measurements were recorded using quartz cuvettes with 1 cm length.

2.2.3. ^{1}H-NMR and ^{13}C-NMR Spectroscopy

Nuclear Magnetic Resonance (NMR) spectra were recorded on Bruker Avance DPX -400 MHz nuclear magnetic resonance spectrometer. (HACETTEPE CHEM. DEPT. and TUBITAK ANALYSIS CENTER)

2.2.4. Elemental Analysis

Elemental analyse were carried out at the TUBITAK test and analysis center.

2.3. Synthesis

2.3.1. Synthesis of Dipyrromethane (5)[97]

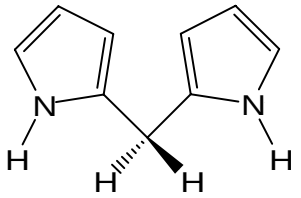

5

Paraformaldehyde **2** (1.64g, 54.7 mmol) and freshly distilled pyrrole **4** (95.0 ml; 1.37 mol) were placed in a 250ml three necked round bottom flask under N_2. The mixture was heated to 50 ^oC. After removing the heat source, TFA (421 μL, 5.47 mmol) was added immediately. The solution became clear and dark. After 10 min the solution was quenched with 0.1 M aq. NaOH solution. Then ethyl acetate was added and the organic phase was washed with water; dried with Na_2SO_4. By vacuum distillation, unreacted pyrrole was removed and an orange oil was obtained. The product was purified with column chromatography by using the DCM: Cyclohexane: Et_3N (20:5:0.1) solvent system and the solvent was removed under vacuum. The product recrystallized from ethanol: water (1:1) giving **5** as colorless crystals.

Yield=3.39g (42.5%)

mp= 75 ^oC (Lit: 75 ^oC)[97]

2.3.2. Synthesis of α-Bromo-p-tolualdehyde(8)[97]

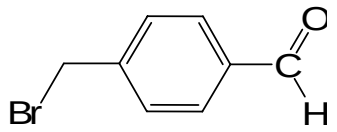

8

α-Bromo-p-tolunitrile **6** (6.00g, 30.6 mmol) was dissolved in toluene (80 ml) and cooled to 0 ^oC. DIBAL-H **7** (55 ml, 59.4 mmol) in hexane was added dropwise under

nitrogen. The solution was stirred for an hour at 0 ^{o}C. Chloroform (80 ml) and then 10% HCl (200 ml) were added. After stirring for 1 hour at room temperature, the organic layer was separated. It was washed with distilled water and dried over Na_2SO_4. Upon cooling the remaining mixture at 0 ^{o}C, precipitates formed, which were filtered and washed with cold hexane. The product (**8**), colorless crystals, was dried under vacuum.

Yield= 4.71g (77%);

mp= 97-99 ^{o}C (Lit: 97-99 ^{o}C)[97]

IR (KBr, υ_{max}/ cm^{-1}) : 601 (C-Br), 832(p-Ph), 1577 and 1604 (C=C), 1706 (C=O), 2752 and 2843 (CHO), 3080 (C-H)

2.3.3. Synthesis of 5, 15- Bis-(4-bromomethyl-phenyl)-porphyrin (12)

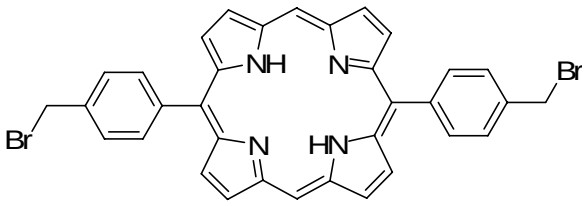

12

Compound **5** (1.2g, 8.2 mmol) and **8** (1.65g, 8.2 mmol) were dissolved in chloroform (1.5 lt) and stirred under nitrogen by keeping the solution away from light. Then $Et_2O.BF_3$ **9** (348µl, 2.74 mmol) was added. It was stirred for 1 hour under nitrogen. The color became pink and reddish over the time. Then Et_3N **10** (465µl, 3.28 mmol) and TCBQ **11** (1.53 g, 6.18 mmol) were added. After stirring approximately 30 min at rt, the mixture was refluxed for 1 hour. After cooling to rt, the mixture was eluted through silica. The solvent was removed under reduced pressure. The resultant purple sediments were purified with column chromatography using toluene as an eluent and then the solvent was removed. After washing the solid residue with methanol, shiny purple crystals **12** were obtained and dried under vacuum.

Yield= 0.47 g (18%)

mp> 300 ^{o}C (decomp.)

IR (KBr, υ_{max}/ cm^{-1}) : 596 (CBr), 1227(CH_2Br), 2924(CH_2), 2962(CH_2), 3271 (NH)

UV-Vis ($CHCl_3$): λ_{max} nm (ε); 409 (2.828 x 10^5), 504 (1.316 x 10^4), 539 (5.551 x 10^3), 576 (4.835 x 10^3), 631 (2.054 x 10^3)

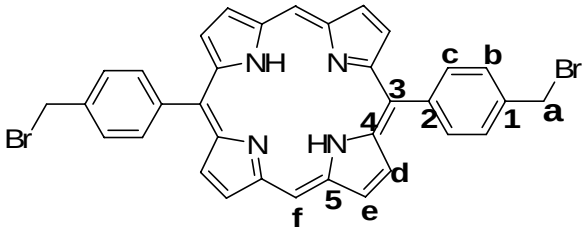

^{1}H NMR (250 MHz, $CDCl_3$): δ -3.10 (s, 2, g), 4.87 (s, 4, a), 7.83 (d, 4, J=2.01 Hz, b), 8.24 (d, 4, J=1.91 Hz, c), 9.06 (d, 4, J=1.21 Hz, d), 9.39 (d, 4, J=1.21 Hz, e), 10.31 (s, 2, f).

2.3.4. Synthesis of Prop-2-ynyl-{4-[15-(4-prop-2-ynylaminomethyl-phenyl)-porphyrin-5-yl]-benzyl}-amine (14)

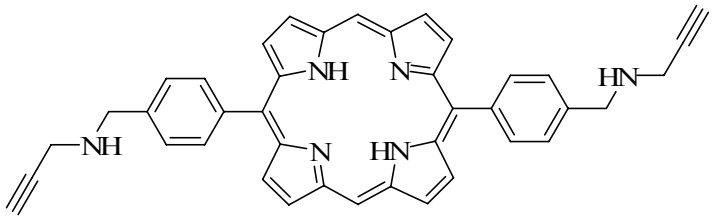

14

12 (200 mg, 0.31 mmol) was dissolved in $CHCl_3$ at rt. Propargylamine **13** (2 ml, 29 mmol) was placed in a round bottom flask. The solution of **12** was added dropwise into the propargylamine **13** containing flask under stirring at rt. The mixture was left stirring for 72 hrs, until the reaction completed by controlling with TLC. The solution of 0.1 N NaOH (5 ml) was added to the reaction mixture and stirred for 1 hour. The organic phase was extracted with 30 ml portions of $CHCl_3$ three times. The organic layer was dried with $CaCl_2$. The solvent was removed under vacuum. Column chromatography was carried out to purify the resultant purple solid by using MeOH-DCM solvent system (1:9, v:v). **14** was obtained after removing the solvent under reduced pressure and drying in vacuum.

Yield= 176.7 mg (88.35%).

mp >300 °C (decomp).

IR (KBr, υ_{max}/ cm^{-1}) : 667 and 692 (≡C-H), 956(≡C-C), 974(≡C-C), 2127(C≡C), 3281(NH and ≡C-H)

UV-Vis ($CHCl_3$): λ_{max} nm (ε); 409 (3.433 x 10^5), 504 (2.124 x 10^4), 539 (1.172 x 10^3), 575 (8.900 x 10^3), 631 (4.485 x 10^3)

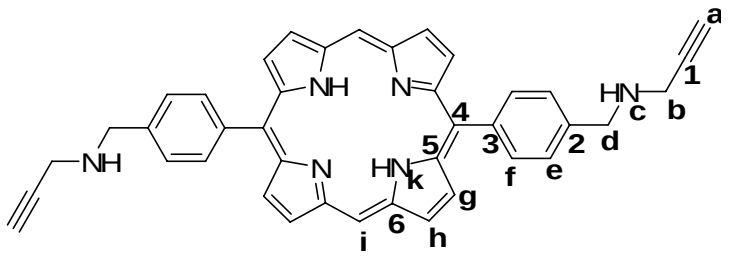

^{1}H NMR (250 MHz, $CDCl_3$): δ -3.07 (s, 2, k), 2.45 (s, 2, a), 3.75(d, 4, J= 1.83 Hz, b), 4.30(s, 4, d), 7.82 (d, 4, J= 7.60 Hz, e), 8.27 (d, 4, J=7.60 Hz, f), 9.12 (d, 4, J=4.44, g), 9.42(d, 4, J=4.46, h), 10.33(s, 2, i).

^{13}C NMR (100 MHz, $CDCl_3$): δ 37.75(b), 52.36(d), 71.88(a), 82.22(1), 105.29(i), 118.91(4), 127.06(f), 131.04(h), 131.64(g), 135.02(e), 138.96(3), 140.30(2), 145.17(5), 147.22(6).

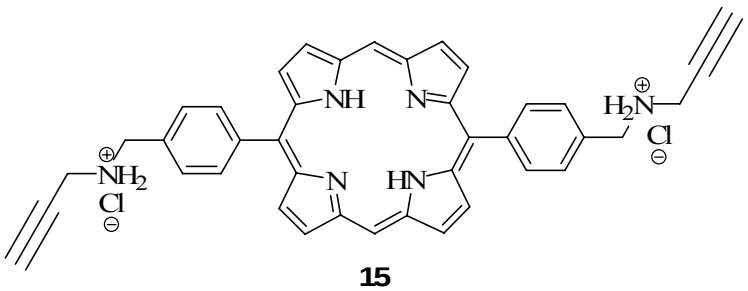

15

Compound **14**(100 mg) was added into the aqueous solution of 0.1 N HCl (5 ml) and the mixture was stirred at rt. After 24 hours stirring, a green colored solution was obtained and the volume of the mixture was concentrated under reduced pressure. The remaining solution was precipitated into excess of acetone.**15** was obtained.

Yield=95 mg (95 %)

IR (KBr, υ_{max}/ cm^{-1}) : 667 and 692 (≡C-H), 972 and 980 (≡C-C), 2125 (C≡C), 3246(NH and ≡CH)

UV-Vis (2 N HCl): λ_{max} nm (ε); 418 (8.532×10^4), 565 (3.324×10^3), 613 (5.054×10^3)

2.3.5. Synthesis of 2-Azido-ethylamine (18)

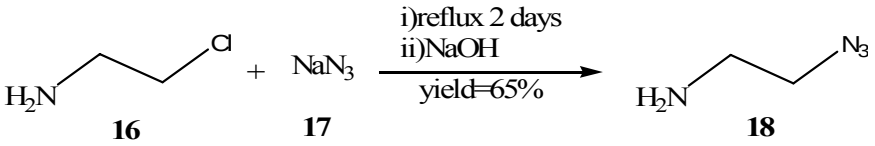

16 **17** **18**

16 (5 g, 0.115 mol) and **17** (3.35g, 0.052 mol) were refluxed in water (50 ml) approximately 2 days. Then the mixture was cooled down to room temperature. NaOH was added until the pH was 12. The organic phase was extracted with DCM (50 ml) three times. After removing the solvent, a yellowish oil (**18**) was obtained.

Yield=2.88g (65%)

IR (KBr, υ_{max}/ cm^{-1}): 2099 (N=N=N), 3255 and 3263 (NH)

2.3.6. Synthesis of (2-Azido-ethyl)-[4-(15-{4-[(2-azido-ethylamino)-methyl]-phenyl}-porphyrin-5-yl)-benzyl]-amine(19)

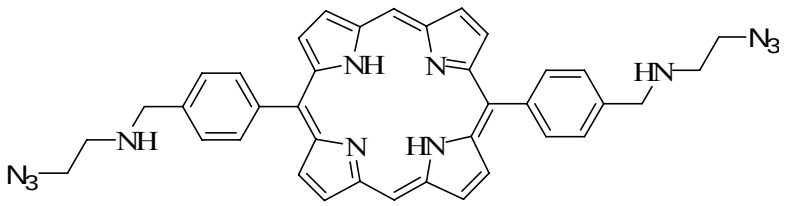

19

12 (200 mg, 0.31 mmol) was dissolved in $CHCl_3$ at rt. **18** (1.29g, 14.98 mmol) was placed in a round bottom flask. The solution of **12** was added dropwise into the 2-azidoethylamine containing flask while stirring at rt. The mixture was left stirring until the reaction completed by checking with TLC. 0.1 N NaOH (5 ml) was added to the

reaction mixture and stirred for 1 hour. The mixture was extracted three times with 30 ml portions of DCM. The organic layer was dried with $CaCl_2$. The solvent was removed under vacuum. For purification, the product was eluted through silica gel with MeOH-DCM mixture. **19** was obtained.

Yield= 106.8 mg(52.3%).

mp >300 °C (decomp).

IR (KBr, υ_{max}/ cm^{-1}) : 2096 (N=N=N), 2854 (CH_2), 2924 (CH_2), 3267 (NH)

UV-Vis ($CHCl_3$): λ_{max} nm (ε); 410 ($2.090x10^5$), 504 ($1.088x10^4$), 541 ($6.198x10^3$), 577 ($4.076x10^3$), 632($1.939x10^3$)

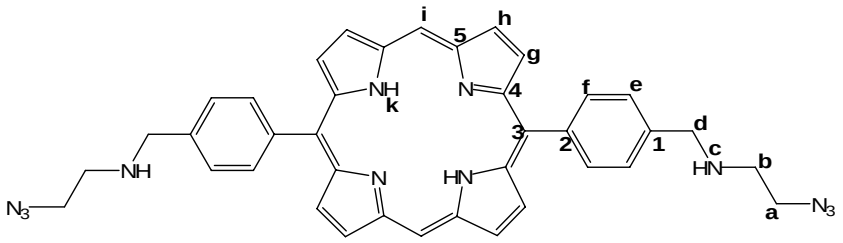

^{1}H NMR (250 MHz, $CDCl_3$): δ -3.07 (s, 2, k), 3.12 (t, 4, J=5.67 Hz a), 3.66(t, 4, J=5.65 Hz, b), 4.22(s, 4, d), 7.79 (d, 4, J=7.80 Hz, e), 8.27 (d, 4, J=7.85 Hz, f), 9.12 (d, 4, J=4.58, g), 9.42(d, 4, J=4.58, h), 10.34(s, 2, i).

^{13}C NMR (100 MHz, $CDCl_3$): δ 48.33(b), 51.67(a), 53.66(d), 105.29(i), 118.90(3), 126.72(f), 131.05(g), 131.64(h), 135.05(e), 139.45(2), 140.23(1), 145.19(4), 147.24(5).

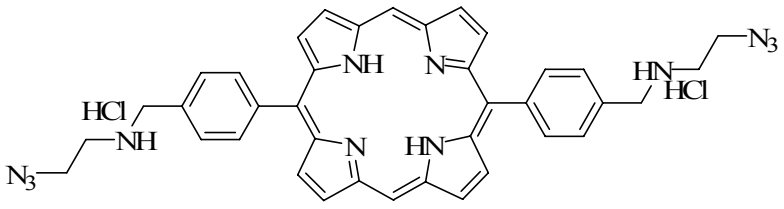

20

To protonate **19,** it was stirred with 2N HCl for 1 day at room temperature. The solvent was removed under reduced pressure. **20** was obtained. For recrystallization the product was dissolved in minimum amount of hydrochloric acid and precipitated into large amount of acetone.

IR (KBr, υ_{max}/ cm^{-1}) : 2116 (N=N=N), 3245 (N-H)

UV-Vis (2N HCl): λ_{max} nm (ε); 417.8 (6.049 x 10^4), 566.8 (3.045 x 10^3), 612.5(4.577 x 10^3)

2.3.7. Synthesis of Prop-2-ynyl-{4-[10,15,20-tris-(4-prop-2-ynylaminomethyl-phenyl)-porphyrin-5-yl]-benzyl}-amine(22)

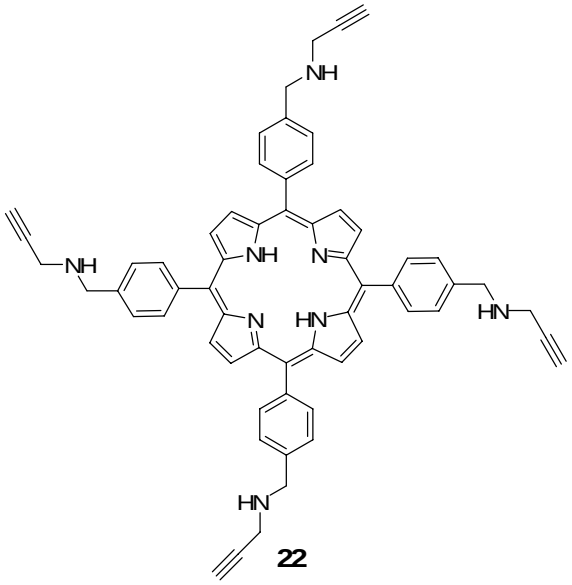

22

21 (mg, mmol) was dissolved in DCM at rt. Propargylamine **13** (ml, mmol) was placed in a round bottom flask. The solution of **21** was added dropwise into the propargylamine **13** containing flask by stirring at rt. The mixture was left stirring 72 hours until the reaction completed by checking with TLC. 0.1 N NaOH (ml) was added to the reaction mixture and stirred for 1 hour. The mixture was extracted three times with 30 ml portions of DCM. The organic layer was dried with $CaCl_2$. The solvent was removed under vacuum. Then column chromatography was prepared to purify the product by using MeOH-DCM as eluent. The obtained purple solid was **22**. To salt out

22, the solution was stirred with 0.1 N HCl (ml). After recrystallization with water/acetone solvent system, **23** was obtained.

Yield= mg (80%).

mp >300 °C.

UV-vis (H_2O): λ_{max} nm (ε) = 413 nm (5.78x 10^5), 518 (1.5x10^4), 554 (8.3x10^3), 585 (5.7x10^3), 645 (4.9x10^3)

Elemental Analysis of $C_{60}H_{54}Cl_4N_8.3H_2O$

Calc.: C, 66.54; H, 5.58; N, 10.34

Found: C, 66.44; H, 5.52; N, 10.82

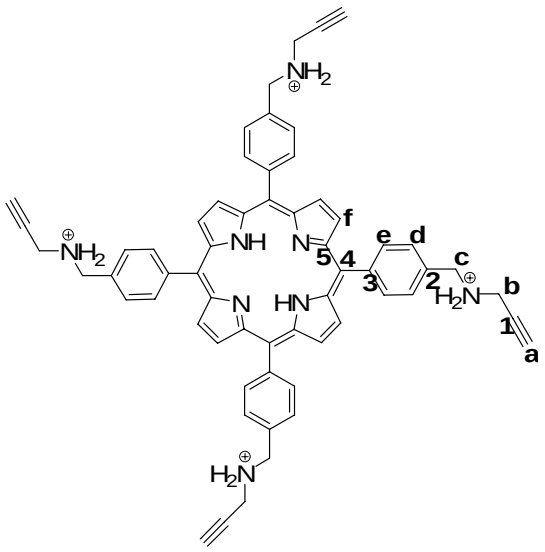

^{1}H-NMR (400 MHz, D_2O): δ 3.22 (, **a**), 4.18 (d, 8H, $^4J_{HH}$ = 3.15 Hz**, b**), 4.85 (s, 8H, **c**), 8.18 (d, 8H, $^3J_{HH}$ = 10.05 Hz, **d**), 8.71 (d, 8H, $^3J_{HH}$ = 10.05 Hz, **e**), 9.09 (s, 8H, **f**).

^{13}C-NMR (100 MHz, D_2O, DSS): δ 36.3 (**b**), 50.0 (**c**), 73.5 (**a**), 79.2 (**1**), 122.9 (**2**), 130.6 (**d**), 130.8 (**4**), 133.3 (**3**), 140.0 (**e**), 141.0 (**5**), 145.9 (**f**).

2.3.8. Synthesis of [3]-Rotaxane(25)

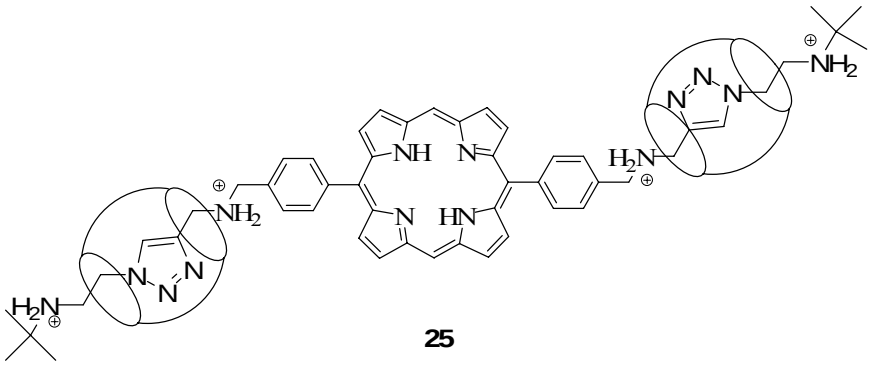

25

One equivalent of **15** (30.535 mg, 0.0456 mmol) was dissolved in minimum amount of 6N HCl at 50 ^{o}C while 2.5 equivalents of (2-Azido-ethyl)-tert-butyl-amine hydrochloride **24** (24,440 mg, 0.1368 mmol) were dissolved in minimum amount of water at the same temperature. After mixing these two solutions, the solution of 2.5 equivalents of **3** (100 mg, 0,1003 mmol), dissolved in minimum amount of 6N HCl, was added dropwise. The mixture was heated at 70 ^{o}C for 48 hrs. The solvent was removed under reduced pressure. To remove excess monomers, the residue was washed with MeOH followed by dissolving in hot water and filtering through a 0.45 μm membrane to remove excess CB[6]. The filtrate was concentrated under reduced pressure and precipitated into the EtOH-acetone mixture. After filtration and drying under vacuum green powder, **25** was obtained.

Yield= 97.96 mg (73.8%)

IR (KBr, υ_{max}/ cm^{-1}) : 1700 (-C≡N and C=O), 3426 (NH)

UV-Vis (H_2O): λ_{max} nm (ε); 402 (5.20 x 10^5), 505 (6.47 x 10^4), 541 (5.24 x 10^4), 566 (5.23 x 10^4), 621 (4.78 x10^4).

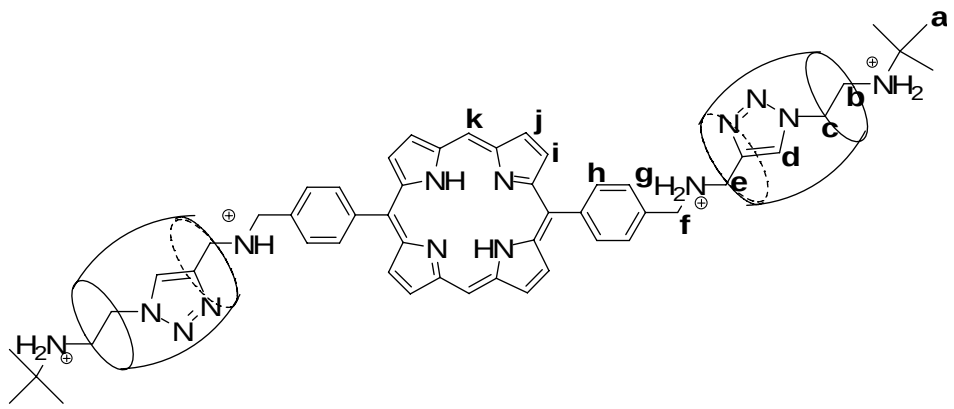

^{1}H-NMR (400 MHz, D_2O): δ 1.6(s, 18, a), 3.8 (4, b), 4.2(4,c), 4.25(24, CB[6]), 4.4(s, 4, e), 4.85(s, 4, f), 5.45(24, CB[6]), 5.68(24, CB[6]), 6.58(s, 2, d), 7.9(d, 4, g), 8.0(d, 4, h), 8.4(4,i), 9.2(4, j), 9.4(2, k).

2.3.9.Synthesis of [5]Rotaxane (26)

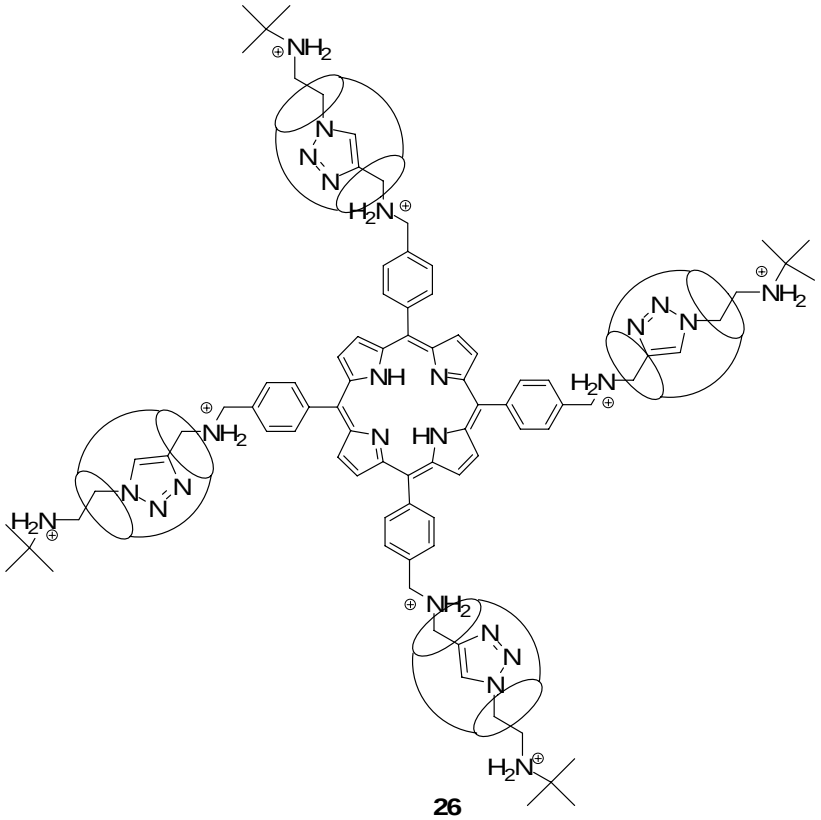

26

1 equivalent of **23** (35.121 mg, 0.0342 mmol) was dissolved in minimum amount of 6N HCl at rt while 4 equivalents of (2-Azido-ethyl)-tert-butyl-amine hydrochloride **24**

(24,440 mg, 0.1368 mmol) were dissolved in minimum amount of water at same temperature. After mixing these two solutions, the solution of 4 equivalents of **3** (100 mg, 0,1003 mmol), dissolved in minimum amount of 6N HCl, was added dropwise. Then the resulting mixture was stirred for two days at rt. The solvent was removed under reduced pressure. To remove excess CB[6], it was dissolved in hot water and filtered through a 0.45 μm membrane. The filtrate was concentrated under reduced pressure and precipitated into EtOH-acetone mixture. After filtration and drying under vacuum, **26** was obtained.

Yield= 145.82 mg (85%)

mp >300 °C (decomp).

UV-vis (H_2O): λ_{max} 415 nm ($3.66x10^5$), 518 ($1.36x10^4$), 555 ($8.3x10^3$), 583 ($6.2x10^3$), 637 ($4.2x10^3$)

Elemental Analysis of $C_{228}H_{258}Cl_8N_{120}O_{48}$ x $30H_2O$

Calc.: C, 43.41; H, 5.19; N, 26.64

Found: C, 43.52; H, 5.41; N, 26.71

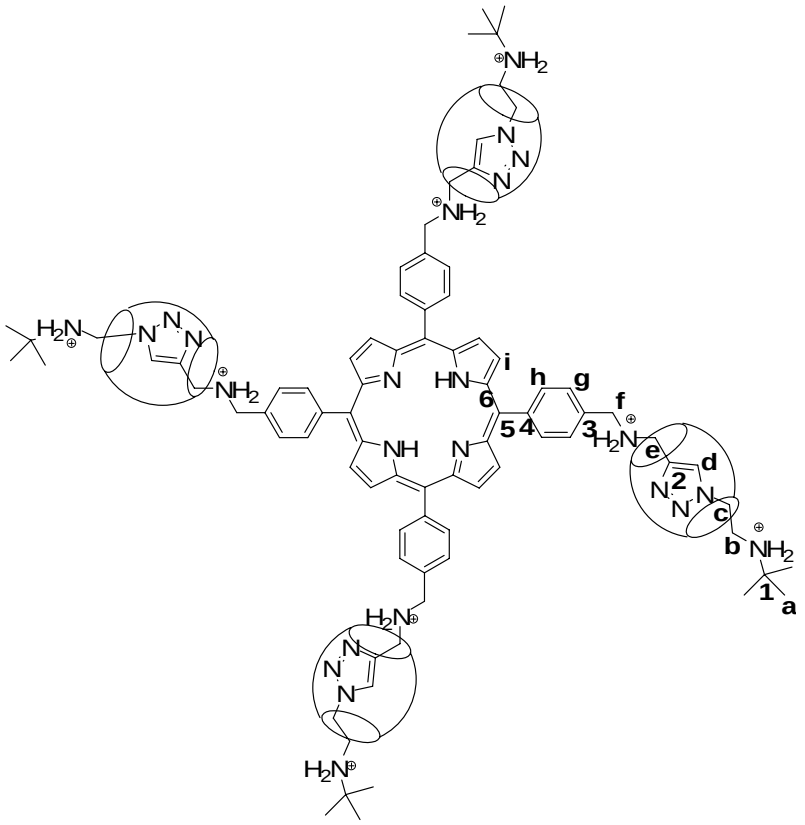

^{1}H-NMR (500 MHz, D_2O): δ 1.61 (s, 36H, **a**), 3.81 (t, 8H, $^{3}J_{HH}$ = 7.95 Hz, **b**), 4.13 (t, 8H, $^{3}J_{HH}$ = 8.15 Hz**, c**), 4.25 (48 H, **CB[6]**), 4.39 (s, 8H, **e**), 4.86 (s, 8H, **f**), 5.52 (48H, **CB[6]**), 5.75 (48H, **CB[6]**), 6.62 (s, 4H, **d**), 8.52 (d, 8H, $^{3}J_{HH}$ = 9.9 Hz, **g**), 8.79 (d, 8H, $^{3}J_{HH}$ = 10.1 Hz, **h**), 9.09 (s, 8H, **i**).

^{13}C-NMR (125 MHz, D_2O, DSS): δ 25.2 (**a**), 40.0 (**b**), 42.5 (**c**), 47.5 (**f**), 51.3 (**CB[6]**), 51.5(**CB[6]**), 52.5 (**1**), 70.2 (**CB[6]**), 120.9 (**d**), 122.5 (**3**), 129.9 (**g**), 130.8 (**5**), 132.7 (**4**), 138.8 (**h**), 138.9 (**2**), 140.1 (**6**), 145.1 (**i**), 156.3 (**CB[6]**), 156.7 (**CB[6]**).

2.3.10. Synthesis of Polyrotaxane (27)

20 (21.855 mg, 0.0299 mmol) was dissolved in 6N HCl solution (10 ml) while **15** (20 mg, 0.02987 mmol) was dissolved in same solvent (8 ml). Then these two solutions were mixed in a 50 ml round bottom flask. Into this mixture a solution of CB[6] prepared by dissolving 59.501 mg (0.0597 mmol) of **3** in 5 ml 6N HCl was added dropwise. Then the mixture was heated at 70 ^{o}C. After two days of heating the solvent was concentrated its 0.5 initial volume. Then it was precipitated into EtOH/acetone mixture.

UV-vis (H_2O): λ_{max} nm; 420, 567, 614.

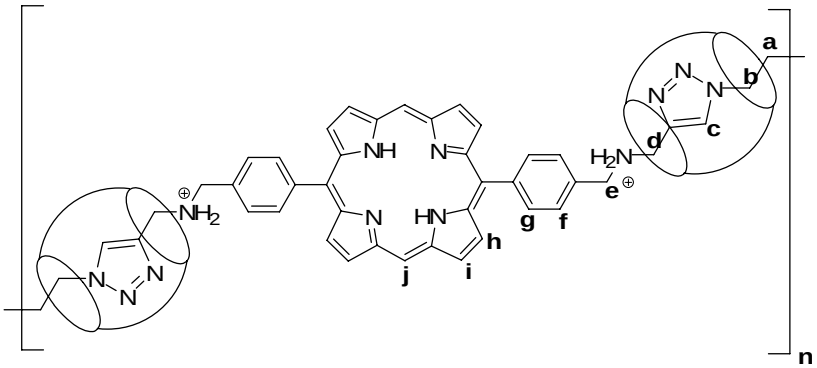

^{1}H-NMR (500 MHz, D_2O-CH_3COOH): δ 3.4(**a**), 4(**b**), 4.2(CB[6]), 5.3(CB[6]), 5.6(CB[6]), 6.6(encaps. **c**), 7.9(non-encaps. **c**), 8.3(**f**), 8.5(**g**), 9.1(**h**), 9.2(**i**), 9.7(**j**).

2.3.11. Synthesis of Copolyrotaxane (28)

29 (41.272 mg, 0.1003 mmol) was dissolved in water (6 ml) while **15** (67.176 mg, 0.1003 mmol) was dissolved in 6N HCl (15 ml). Then these two solutions were mixed in a 50 ml round bottom flask. Into this mixture a solution of CB[6] prepared by dissolving 200 mg (0.2006 mmol) of **3** in 9 ml 6N HCl was added dropwise. Then the mixture was heated at 70 ^oC. After two days of heating the solvent was removed and the concentrated solution was precipitated into a MeOH/acetone mixture to recrystallize it. The resultant copolyrotaxane **28** was dried under reduced pressure.

UV-vis (H_2O): λ_{max} nm; 420, 568, 613.

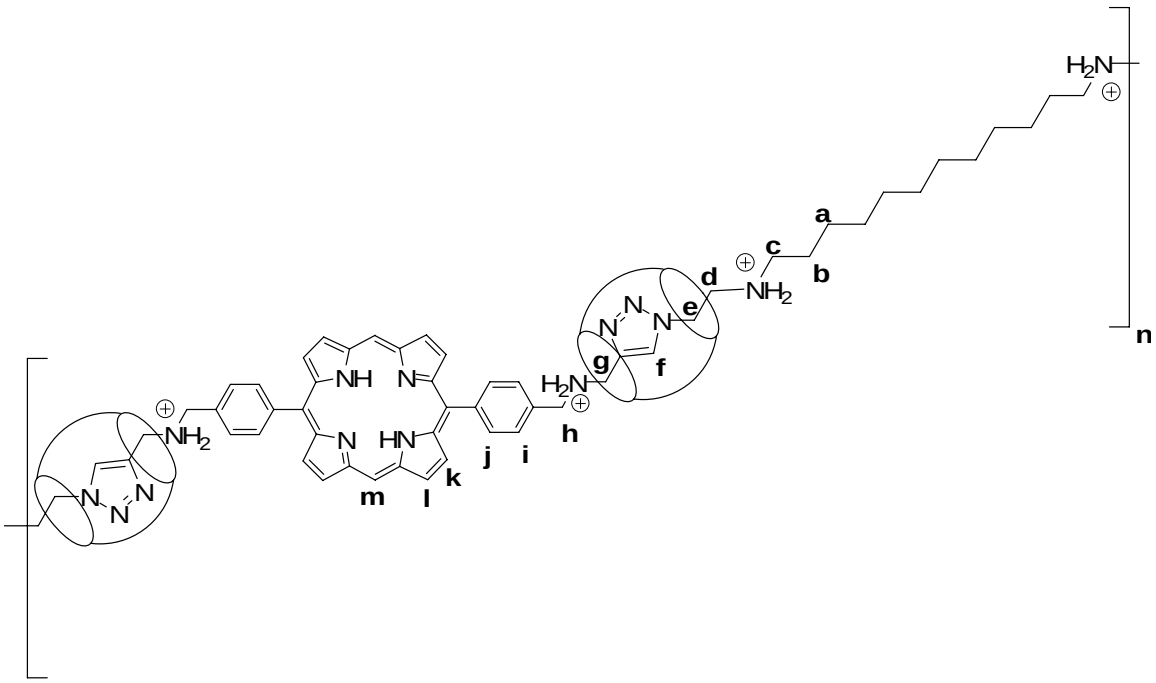

^{1}H-NMR (500 MHz, D_2O-CH_3COOH): δ 1.6(**a**), 1.8 (**b**), 3.1(**c**), 3.7(**d**), 4.3(CB[6]), 5.5(CB[6]), 5.7(CB[6]), 6.6(encaps. **f**), 8.1(non-encaps. **f**), 8.4(**i**), 8.7(**j**), 9.3(**k**), 9.4(**l**), 9.8(**m**).

CHAPTER 3. RESULTS AND DISCUSSIONS

3.1. Introduction

The results and discussions part will consist of three sections: in the first section the synthesis and characterization of monomers and their precursors required for the preparation of rotaxanes and polyrotaxanes will be discussed. Section 2 will cover the synthesis and characterization of rotaxanes and finally the section 3 will present the synthesis and the attempted characterization of polyrotaxanes.

3.2. Synthesis and Characterization of Macrocycle (3)

CB[6], the macrocycle of this project, was synthesized according to literature[62] by the condensation of glycoluril **1** with excess formaldehyde **2** in strongly acidic medium.

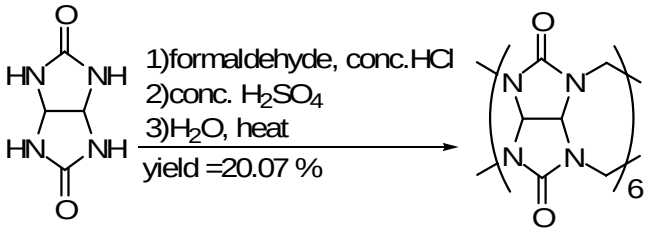

1 **3**

It was characterized by IR, ^{1}H NMR, ^{13}C NMR and elemental analysis. In its IR spectrum (Figure 3.1), there is a strong carbonyl peak at 1745 cm^{-1} while antisymmetric and symmetric stretching vibrations of C-H bonds gave peaks at 2854 and 2924 cm^{-1} respectively. The broad peak observed at about 3450 cm^{-1} belongs to NH stretching.

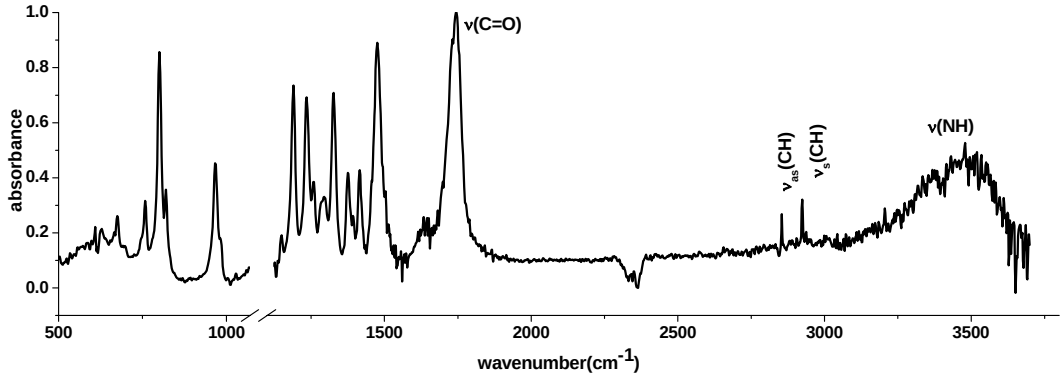

Figure 3.1. Infrared spectrum of CB[6].

The characterization was also carried out by ^{1}H NMR (Figure 3.2). The ^{1}H NMR spectrum revealed three types of protons as expected. The aminal protons gave a singlet resonance at 5.64 ppm. Magnetically non-equivalent methylene protons assigned as H_a and H_b coupled with each other to yield two doublets with a J-J coupling constant of 15.6 Hz at 5.73 and 4.36 ppm respectively. Elemental analysis result has shown that CB[6] contained 3 moles of water molecules.

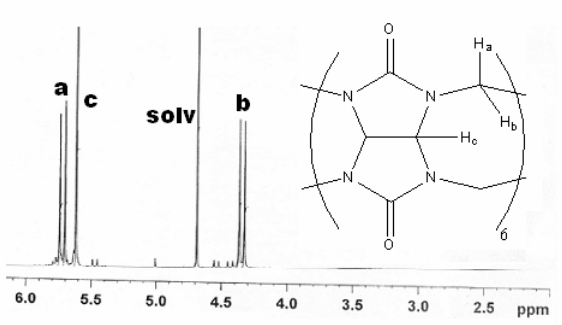

Figure 3.2. ^{1}H NMR spectrum of CB[6].

3.3. Synthesis and Characterization of Monomers

To synthesize rotaxanes and polyrotaxanes, firstly the necessary monomers should be synthesized. But to synthesize monomers it is needed to synthesize precursors such as porphyrin.

3.3.1. Synthesis and Characterization of Precursors

3.3.1.1. Dipyrromethane (5)

To synthesize 5,15-bis-(4-bromomethyl-phenyl)-porphyrin **12**, one of the key precursors is dipyrromethane which can be synthesized in high yield through a (2+2) condensation reaction. Many research groups[95-97] improved one pot syntheses of dipyrromethanes in terms of the purification and isolation. The condensation of an aldehyde with pyrrole in the presence of catalytic amounts of an acid is the main synthetic route. However, one of the main problems of this method is the formation of oligomers and polymers as well as the formation of N-confused dipyrromethane and tripyrromethanes. This problem can be minimized by using large excess of pyrrole, which suppresses the polymerization.

Lee et al.[98] addressed that the product composition, the ratio of amount of dipyrromethane to that of higher pyrrolic oligomers, depends on the sequence of addition of reagents. It was reported that dipyrromethane was the major product when pyrrole and aldehyde were stirred before addition of catalytic amounts of acid. Therefore pyrrole and paraformaldehyde were stirred before the catalyst was added as seen in the Scheme 3.1.

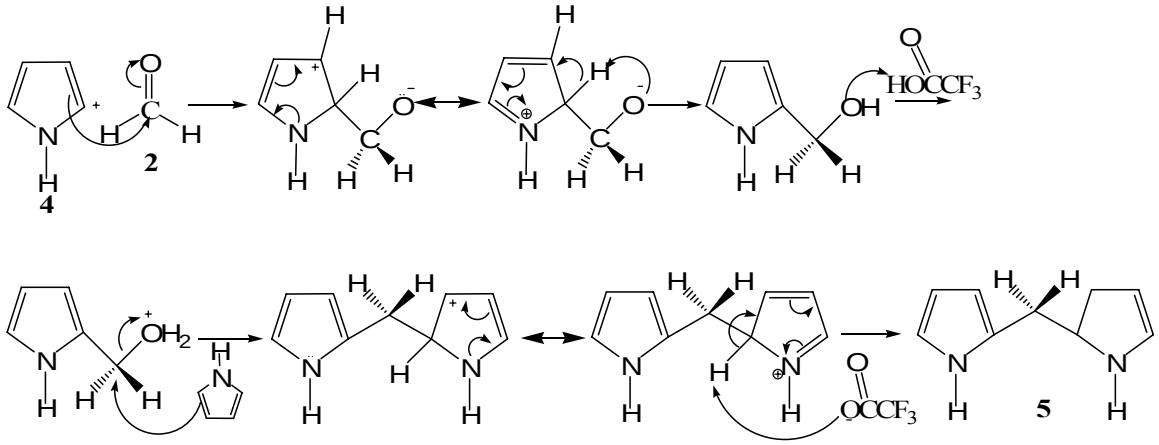

Scheme 3.1. Synthesis of dipyrromethane (**5**) and the proposed reaction mechanism

In 1999, Lindsey`s group[97] investigated the optimum conditions for the formation of the dipyrromethane. It was reported that although $BF_3.Et_2O$ is a better acid catalyst with respect to DPM yield, the amount of the side product, N-confused dipyrromethane, is much lower with TFA. Additionally, it was established that 25:1 is the best ratio of

pyrrole: aldehyde for yield of dipyrromethane, since excess pyrrole suppresses the formation of higher pyrrolic oligomers. Furthermore, it was reported that 0.1 equiv of acid relative to aldehyde is most proper amount to be used.

Therefore, for dipyrromethane synthesis, the well established Lindsey's procedure was adopted and 25 fold excess freshly distilled pyrrole with 1 equivalent paraformaldehyde was used. At room temperature, paraformaldehyde is insoluble in pyrrole. Hence the reaction was very slow and the yield of dipyrromethane was low. To increase the yield, the solubility of paraformaldehyde was increased by heating the reaction mixture to approximately 50^{o}C. The mixture was heated until all paraformaldehyde was dissolved. After removing the heat source, a catalytic amount of acid was added. It was observed that TFA addition leads to a sharp increase in the temperature from 50^{o}C to 70^{o}C and with color change from colorless to dark brown. This indicates pyrrole condensation.

From the reported procedure[97] as well as our own observations, it was found that the rate of the reaction of pyrrole with aldehyde is quite fast. Therefore, after stirring the mixture for 10 minutes, the standard work up steps were carried out. Although the work-up of the reaction was straightforward, the purification of the desired product proved to be difficult.

To isolate the desired product, the following method was employed. First TLC was run by using DCM: Cyclohexane: Et_3N (20:1:0.1) as solvent system. Since dipyrromethane can easily convert to other pyrrolic compounds on silica, a mildly basic solvent system was used as an eluent. As a result of the TLC, the presence of pyrrole was observed. After the removal of excess pyrrole under vacuum, an orange clear oil was obtained. Vacuum distillation was carried out to isolate dipyrromethane from other side products.

However, TLC showed that not all the pyrrolic oligomers were removed by vacuum distillation; therefore column chromatography was indispensable by using the same solvent system. Actually, column chromatography removed not only pyrrolic oligomers but also N-confused dipyrromethane. After running TLCs and collecting the

fractions which contained the desired product, the solvent was removed under reduced pressure and an orange oil was obtained which crystallized upon standing. Then the product was recrystallised by using an ethanol/ water mixture to collect pure dipyrromethane as a colorless crystalline solid with 42.5 % yield which is a little bit higher than the reported[97] yield. It was observed that its melting point was 75 ^{o}C as reported in the literature.[97] Furthermore, it was realized that dipyrromethane is not very stable, it decomposes under light. Therefore, it should be kept in the dark and at low temperatures. It was usually used straight after purification in the synthesis of porphyrin.

3.3.1.2. α-bromo-p-tolualdehyde(8)

To synthesize **8**, one of the procedures reported in the literature was adopted.[97] α-Bromo-p-tolunitrile that is commercially available. It was dissolved in toluene and cooled to 0 ^{o}C. DIBAL-H in hexane that reduces nitrile to aldehyde was added dropwise under nitrogen in slight excess to prevent over-reduction. The solution was stirred for an hour at 0 ^{o}C. The plausible reaction mechanism is given in the Scheme 3.2.

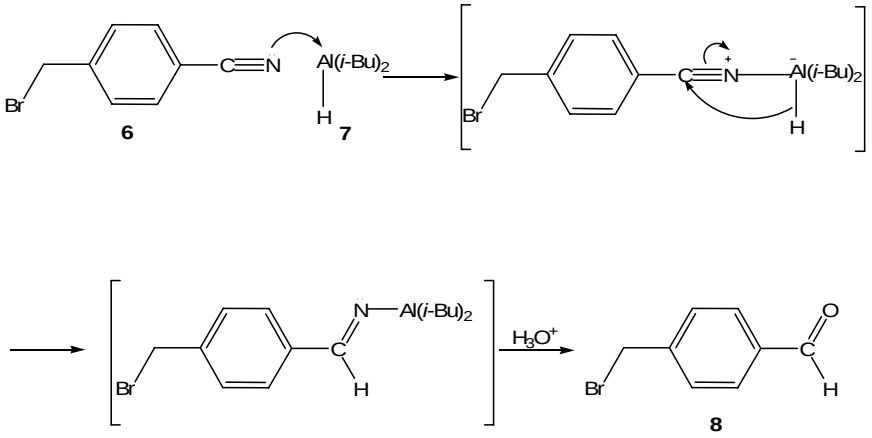

Scheme 3.2. Synthesis of α-bromo-p-tolualdehyde(**8**)

The key steps in this reaction mechanism are believed to be as follows; the electron deficient aluminum atom accepts an electron pair from the nitrile in a Lewis acid-base reaction. Then a hydride ion transfers to the nitrile carbon and leads to the formation of relatively stable intermediate. The addition of acidified water causes hydrolysis of the aluminum complex to take place, to form the target aldehyde. After

extraction, washing, filtration and drying steps, colorless crystals in 77% yield were collected. It was observed that the melting point of the product was consistent with the literature value 97-99 ^{o}C.

Characterization of the compound was performed by FT-IR. It is known that most halocompounds show strong bands in the low frequency region of their infrared spectra because of the C-X (X= F, Cl, Br, I) stretching vibrations. Generally C-Br stretching vibrations are observed in the 510-700 cm^{-1} region. When the spectrum of the aldehyde was checked, a strong peak, which may be assigned as C-Br stretching frequency was observed at 601 cm^{-1}. The strong peak observed at 832 cm^{-1} may be ascribed as para substituted benzene ring torsion. Two different bending motions of methylene wagging and rocking were observed as strong bands at 1164 cm^{-1} and 1211 cm^{-1} respectively. C=C symmetric stretching and C=C asymmetric stretching vibrations were observed at 1576 cm^{-1} and 1604 cm^{-1} as medium and strong bands respectively. As the most characteristic peak for the aldehyde, stretching vibration of carbonyl attached to an aryl group produce a strong band at 1706 cm^{-1} as expected. The two weak bands observed at 2752 cm^{-1} and 2843 cm^{-1} may be assigned as out-of-plane motion of CH of aldehyde. Additionally, there was an aromatic CH absorption at about 3080 cm^{-1}. No absorption peak due to -C≡N at around 2200 cm^{-1} was observed, indicating the complete reduction of nitrile to aldehyde.

3.3.1.3. 5, 15- bis-(4-bromomethyl-phenyl)-porphyrin (12)

As shown in the Figure 1.16 of the introduction, there are many synthetic routes to synthesize porphyrin. At the very beginning of the project, a one pot synthetic approach which yields a statistical mixture of products was used as shown in the Scheme 3.3. Product isolation required careful and tedious chromatographic separations, the yield was very poor and it was not always possible to isolate pure porphyrin. Therefore, the strategy needed to be changed.

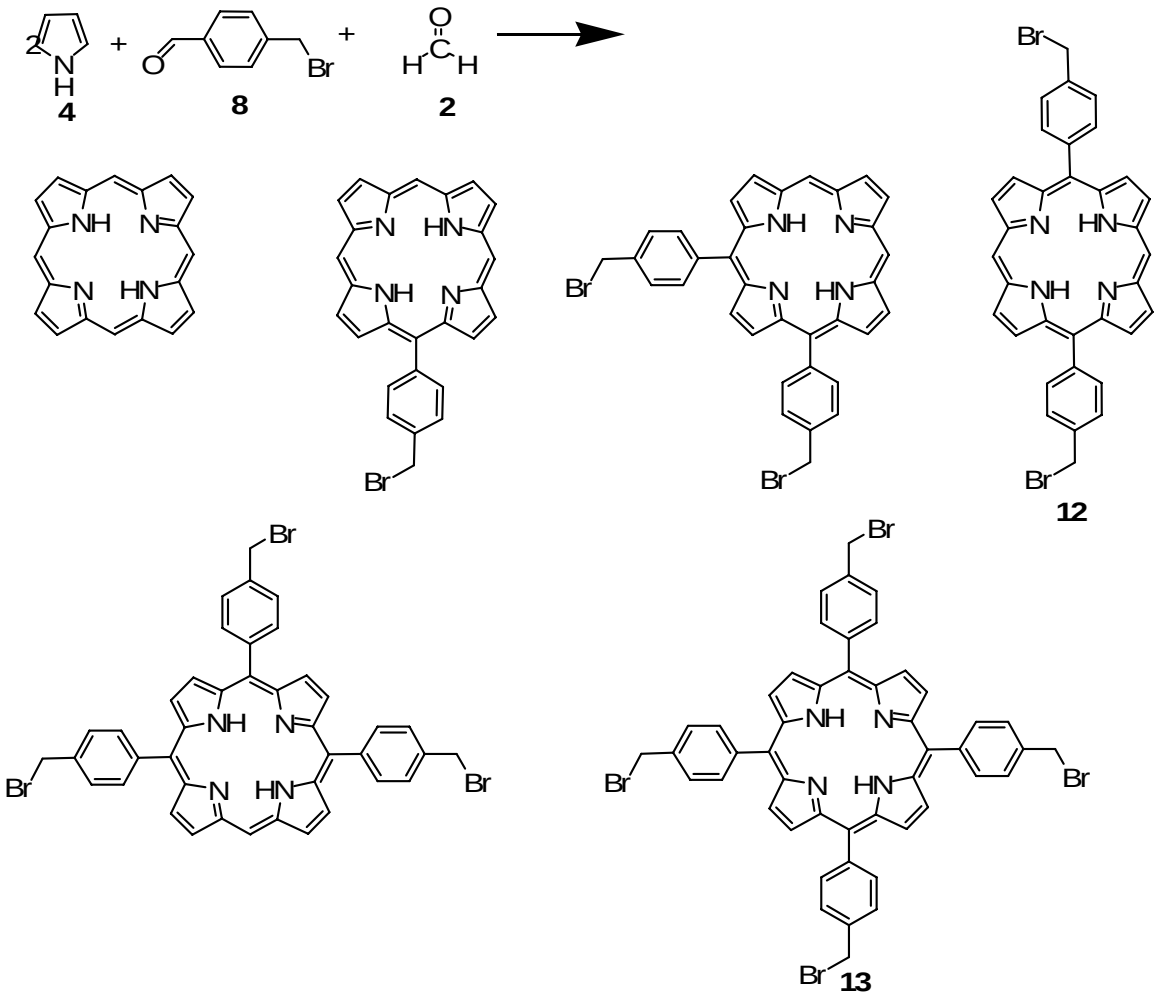

Scheme 3.3. One pot synthetic approach gives a statistical mixture.

The procedure of 5, 10, 15, 20-tetrakis (α-bromo-p-tolyl)porphyrin synthesis addressed by Wen et al.[99] was adopted to synthesize 5, 15-diphenylporphyrin. After stirring equimolar dipyrromethane and α-bromo-p-tolualdehyde, a catalytic amount of $Et_2O.BF_3$ was added. Scheme 3.4 shows the proposed reaction mechanism of porphyrin formation.

After stirring the reaction mixture for 1 hour under nitrogen at room temperature, triethylamine was added followed by the addition TCBQ to oxidize the porphyronic ring and to obtain complete aromatization. After refluxing, the reaction mixture was eluted through silica to remove porphyrinic oligomers. The filtrate was collected and the solvent was removed under reduced pressure. TLC results of the obtained purple sediments

indicated that there were some derivatives of porphyrin. Therefore the resultant purple sediments were eluted through silica gel by using toluene. The desired fractions were collected and the solvent was removed. After washing with methanol, shiny purple crystals were filtered and dried under vacuum with 18% yield.

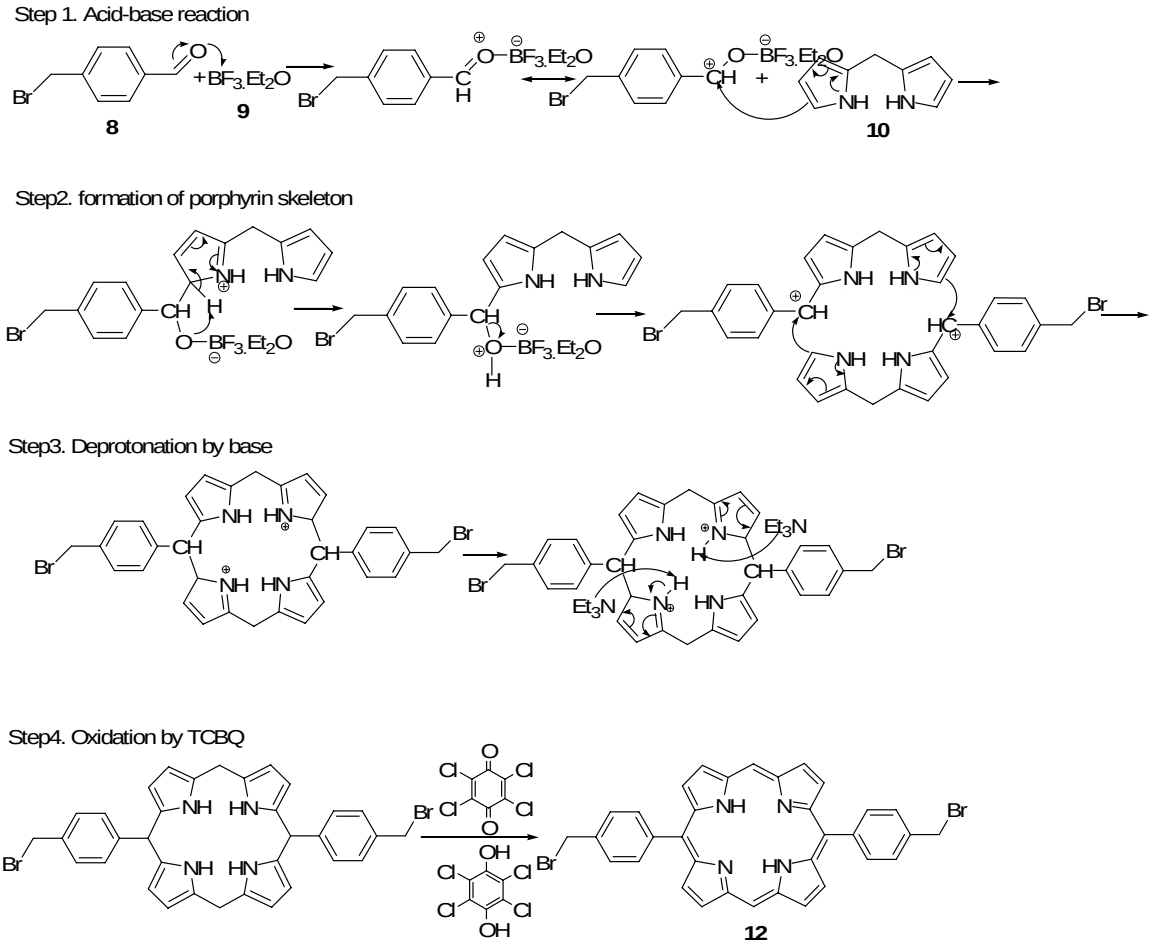

Scheme 3.4. Mechanism of porphyrin synthesis

As in the case of α-bromo-p-tolualdehyde, the infrared spectrum revealed a peak at 596 cm $^{-1}$ belonging to the C-Br stretching motion. Since two adjacent H atoms of a para substituted phenyl ring have a strong vibration around at 795-880 cm^{-1}, the strong peak at 796 cm^{-1} may be attributed to the phenyl in-phase C-H wagging vibrations for two adjacent hydrogen atoms. Both of the peaks observed at 1146 and 1180 cm^{-1} may be ascribed to the combination of vibration due to phenyl ring bending and deformation of pyrrole C-H. The asymmetric stretching vibration of meso and α carbons of the porphyrin

ring was observed at 1576 cm^{-1}. As expected for a compound with CH_2 group, symmetric and antisymmetric CH_2 stretching vibrations, both with medium intensity, were observed at 2924 and 2962 cm^{-1} respectively. Additionally, two types of C-H symmetric stretching vibrations that belong to phenyl and pyrrole were observed at 3026 and 3090 cm^{-1} respectively, whereas asymmetric C-H stretching vibrations of the same rings were observed at 3113 and 3138 cm^{-1} respectively. In the most upfield region of the spectrum, the peak due to the N-H stretching vibration was observed at 3271 cm^{-1}.

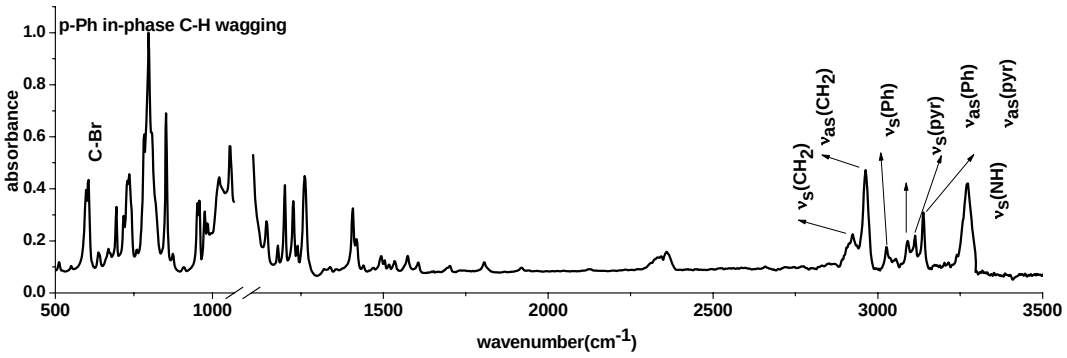

Figure 3.3. FT-IR spectrum of compound **12**.

In the UV-Vis spectrum of **12**, it is expected to see four absorption bands, in the Q band region due to D_{2h} symmetry of free base porphyrin as explained in the section 1.5. The solution of **12** in chloroform with a concentration of 3.7869 x 10^{-6} M was prepared and then by using 1 cm quartz cuvettes the UV absorption spectrum was obtained as shown in Figure 3.4. By using Beers' Law, molar absorptivities of **12** were calculated as tabulated in Table 3.1.

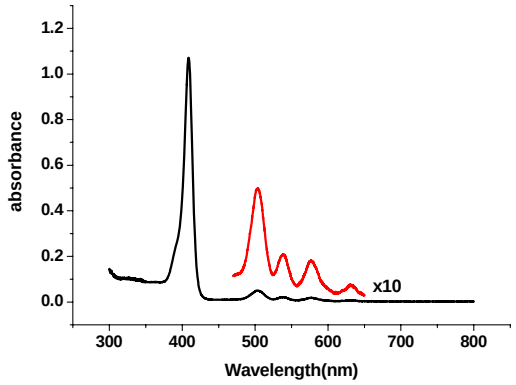

Figure 3.4.UV absorption spectra of **12** (3.7869 x 10^{-6} M, $CHCl_3$).

	Wavelength, λ (nm)	Molar Absorptivity ($mol^{-1}.L.cm^{-1}$)
B(0,0)	408.83	$2.828x10^5$
$Q_y(1,0)$	504.17	$1.316x10^4$
$Q_x(1,0)$	538.83	$5.551x10^3$
$Q_y(0,0)$	576.17	$4.835x10^3$
$Q_x(0,0)$	630.67	$2.054x10^3$

Table 3.1. UV-Vis data for **12**

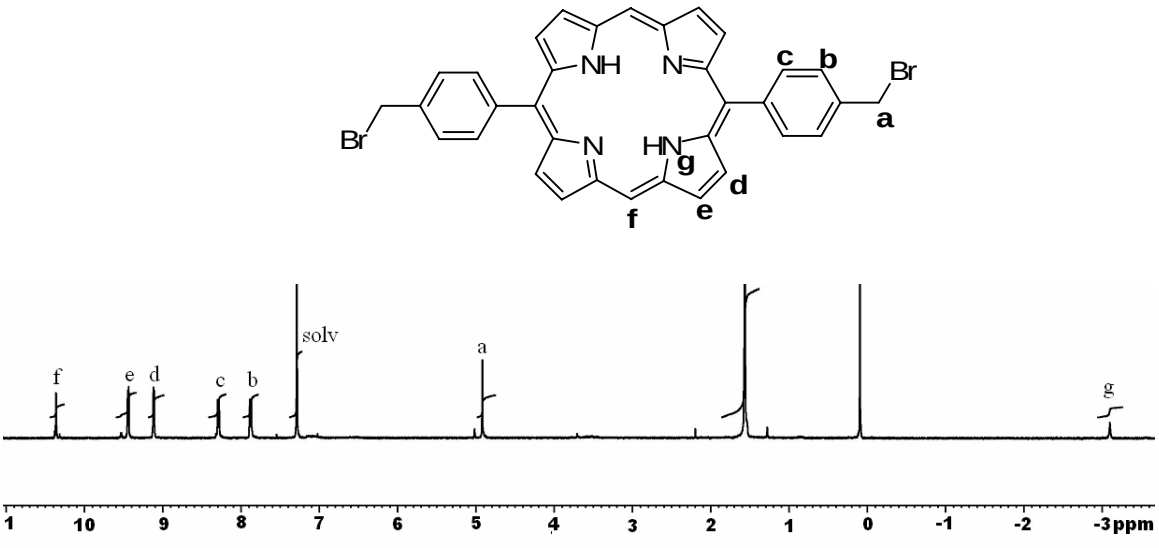

Figure 3.5. ^{1}H NMR spectrum of **12** in $CDCl_3$ at rt.

The ^{1}H-NMR spectrum of **12** (Figure 3.5) revealed seven types of hydrogen environments as expected. The aminal protons gave a singlet resonance in the upfield region at about -3.10 ppm. The integration of these protons confirms that there are two aminal protons.

The singlet at 4.87 ppm was assigned as arising from the benzylic protons **a**. Because of the existence of a benzene ring adjacent to methylene as an electron withdrawing group, the σ electron density around these methylene protons is less, therefore more deshielded, than an ordinary alkyl bromide. By checking the integration of this singlet, it was observed that there are four protons. This observation indicated that two α-bromo-p-tolualdehyde molecules were added successfully to one porphyrin molecule.

The ^{1}H NMR spectrum further shows two doublets due to the protons of the para substituted benzene ring at about 7.83 ppm and 8.24 ppm, whose $^{3}J_{Hb\text{-}Hc}$ coupling constants are 7.85 and 7.84 Hz respectively. The protons of the benzene ring assigned as **b** absorb at higher magnetic field (7.83 ppm) than the proton of carbon assigned as **c** (8.24 ppm). The reason for this assignment is that the protons **c** are closer to the electron withdrawing porphyrin ring than the protons **b**. Integration intensity also shows the presence of four hydrogens due to a benzene ring.

In the downfield region of the spectrum, there are two doublets at 9.06 and 9.39 ppm due to β-pyrrolic protons assigned as **e** and **d** respectively. Since the protons assigned as **d** are nearer to the electron donating benzene ring, the electron density around them is greater. Therefore protons due to **d** have a chemical shift to higher magnetic field strength (9.06 ppm), while the protons due to **e** absorb at lower magnetic field strength (9.39 ppm). From their integration intensities, it can be deduced that there are four hydrogens due to these doublets of β-pyrrolic protons.

In the most downfield region, there is a singlet resonating at 10.31 ppm due to meso-hydrogens of the porphyrin ring assigned as **f**. The integration intensity is also consistent with the existence of two hydrogens at the meso positions of porphyrin.

Information gathered from spectroscopic characterization and also a single spot in TLC confirmed the proposed structure.

3.3.2. Prop-2-ynyl-{4-[15-(4-prop-2-ynylaminomethyl-phenyl)-porphyrin-5-yl]-benzyl}-amine (14)

After the synthesis of the necessary precursor **12**, the monomer **14** was prepared according to reaction Scheme 3.5.

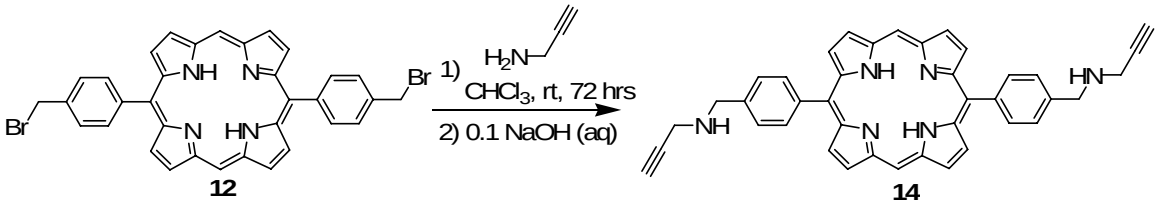

Scheme 3.5. Synthesis of **14**.

The precursor **12** was dissolved in minimum amount of chloroform and then the resulting solution was added slowly to the excess propargyl amine at rt. The mixture was left stirring until the reaction was completed as determined with TLC. Since the reaction is a nucleophilic substitution, the nonbonding electrons of nitrogen of propargylamine attack the benzylic carbon of the porphyrin **12**. Then bromide behaves as a good leaving group and probably the hydrogen bromide salt of the propargyl amine is formed. To convert the resulting ammonium salt into free base, aq. NaOH solution was added and the organic layer was extracted with chloroform.

Since the boiling point of propargyl amine is quite low, excess propargyl amine can be removed easily under reduced pressure. The resulting purple coloured solid was purified by column chromatography using a methanol-DCM mixture as an eluent. The free base monomer **14** was obtained in 88% yield.

To characterize the compound firstly its IR spectrum was taken. The peak assigned as C-Br stretching frequency at 596 cm^{-1} was not observed in the spectrum of **14**. Proper functionalization **12** was determined not only by disappearance of the C-Br peak but also by appearance of the characteristic frequencies of acetylenes arising from

vibrations involving ≡C-H stretching and bending, C≡C stretching, and ≡C-C stretching and bending modes. ≡C-C stretching band identification is comparably difficult since in the same region it is possible to observe the absorption of other types of C-C stretching modes. For monosubstituted acetylenes this motion has a characteristic peak in 940-1000 cm^{-1} region. Therefore in the spectrum of the molecule the peak at 956 cm^{-1} can be assigned to the symmetric stretching motion of C-C adjacent to the triple bond whereas the band at 974 cm^{-1} can be ascribed as the antisymmetric stretching motion of the same group of atoms.

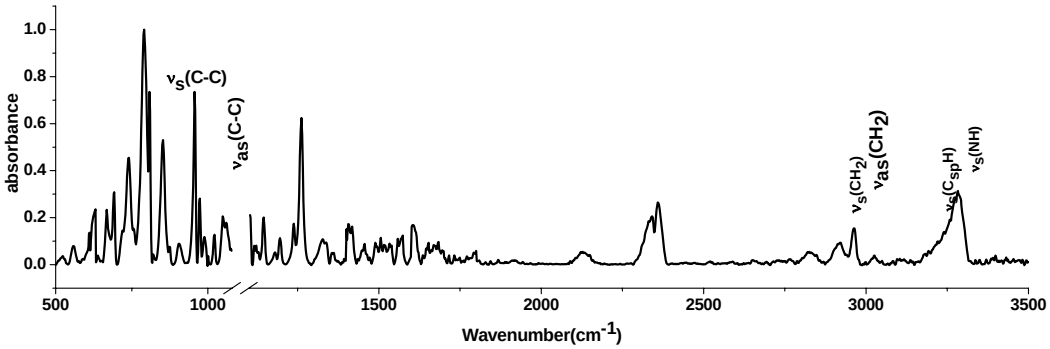

Figure 3.6. FT-IR spectrum of **14**

Another characteristic frequency of the triple bond containing compounds belongs to the ≡C-H bending mode. The characteristic IR bands in the 610-681cm^{-1} region are attributed to the ≡C-H bending modes. Additionally, it is known that the frequency of this motion tends to be increased by the decrease of the total electron density on the alkyne carbon by the help of substituents. Since the neighboring atoms are C and N, delocalization of electrons is possible. Therefore the molecule will have signs of ≡C-H bending modes at the upper part of the region. For compounds with no axial symmetry about the triple bond there is a splitting of the ≡C-H bending modes, the out-of-plane, and the in-plane bending modes. In the spectra of propargyl derivatives the splitting of these frequencies is proportional to the difference between the electronegativities of the adjacent substituents and the carbon atom. For the compounds similar in structure to **15**, the difference of splitting frequencies is approximately 25 cm^{-1}. As expected the infrared

spectrum of the compound has two bands at 667 cm^{-1} and 692 cm^{-1} due to the ≡C-H bending modes with the difference 25 cm^{-1}.

The acetylenic C-H stretching vibration is characterized by the sharp IR absorption band in the 3200-3340 cm^{-1} region. The compound with alkyne end group absorbs IR radiation at 3281 cm^{-1} due to the combination of the stretching motion of the C-H neighbor to the triple bond and the stretching motion of NH.

The UV-Vis spectrum of **14** in chloroform reveals a strong Soret band at 409 nm and four absorption peaks in the Q band region as shown in Figure 6. UV-Vis data are tabulated in Table 3.2. The molar absorptivity of **14** is higher than that of **12**. This result may be explained by better delocalization of electrons due to functionalizing of **12** with alkyne and amine containing groups.

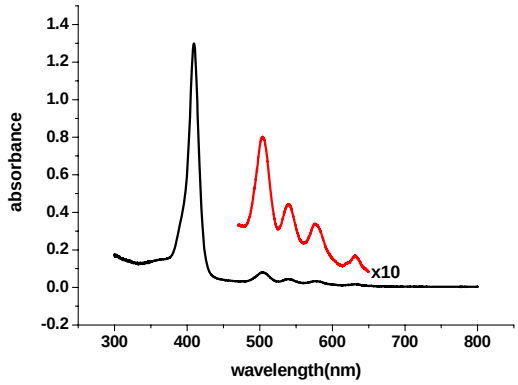

Figure 3.7. UV absorption spectrum of **14 (**3.7841 x 10^{-6} M, $CHCl_3$, rt)

	Wavelength, λ (nm)	Molar Absorptivity ($mol^{-1}.L.cm^{-1}$)
B(0,0)	409.33	$3.433x10^5$
$Q_y(1,0)$	504.17	$2.124x10^4$
$Q_x(1,0)$	539.00	$1.172x10^3$
$Q_y(0,0)$	575.33	$8.900x10^3$
$Q_x(0,0)$	630.67	$4.485x10^3$

Table 3.2. UV-Vis data of **14.**

The characterization of **14** was also carried out by ^{1}H-NMR spectroscopy. There are ten different hydrogen environments as expected. In the most upfield region of the spectrum at -3.07 ppm a singlet resonance was observed whose integration intensity indicates that there are two hydrogens involved. These hydrogens can be attributed as the aminal hydrogens assigned as **k** in the porphyrin ring of the molecule. At 1.8 ppm there is a broad signal that possibly belongs to hydrogens of the secondary amine assigned as **c** functional groups.

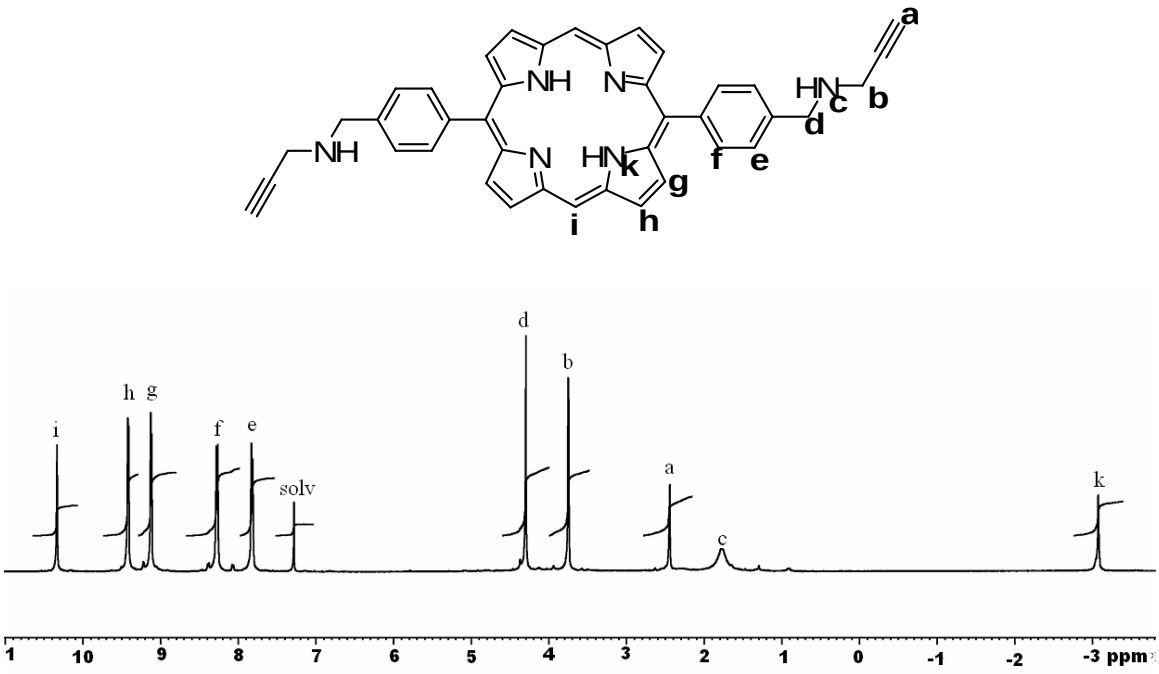

Figure 3.8. ^{1}H NMR of **14** in $CDCl_3$ at rt.

In going through downfield region, at 2.45 ppm there is a triplet whose intensity of integration indicates that there are two equivalent terminal alkyne protons, **a**. Due to ^{4}J coupling to H_b, coupling constant is quite small (2.1 Hz).

Magnetic fields created by circulating delocalized π electrons shield the protons of the terminal alkyne, causing them to absorb at higher magnetic field strengths. This is the reason of having a chemical shift at upfield region for an alkyne proton as expected. The integration implies the presence of two equivalent terminal alkyne protons. It proves

that two propargylamine molecules were added successfully to one porphyrin molecule without over-alkylation.

The methylene protons of propargylamine **b** gave a resonance as a doublet at 3.75 ppm. Their integration confirms that there are four methylene protons, **b**, whose J_b-J_a coupling constant is 1.83.

The ^{1}H NMR spectrum further reveals a resonance as a singlet due to benzylic protons, **d**, at 4.30 ppm. Since circulating π electrons of benzene ring cause deshielding of protons **d**, contrast to, the shielding effect of the circulating π electrons of alkyne on protons **b**, protons assigned as **d**, absorbs at a lower magnetic field strength (4.30 ppm) than the protons **b** (3.75 ppm).

Because of the ring current effect of benzene ring, the absorption of aromatic protons occurs downfield at about 7-7.5 ppm. The closely spaced doublets at about 7.82 ppm and 8.27 ppm elucidated as the protons **e** and **f** of a para substituted benzene ring, respectively. The coupling constants for each doublet were calculated to be 7.60 Hz.

In the more downfield region of the spectrum at 9.12 ppm and 9.42 ppm, two doublets due to non-equivalent β-pyrrolic protons of porphyrin were observed. The coupling constants for these doublets assigned as **h** and **g** were calculated to be 4.44 Hz and 4.46 Hz respectively. From the integration, the expected number of protons was calculated.

At 10.33 ppm, a singlet due to the protons of meso position of porphyrin was observed, which corresponded to 4H as expected.

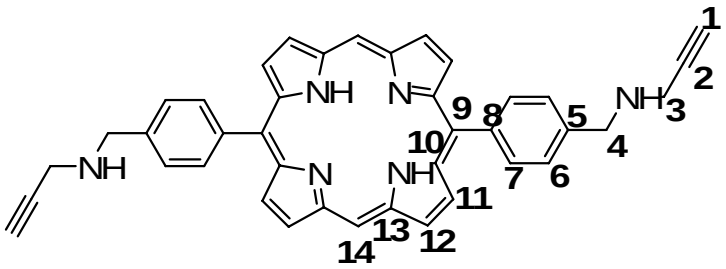

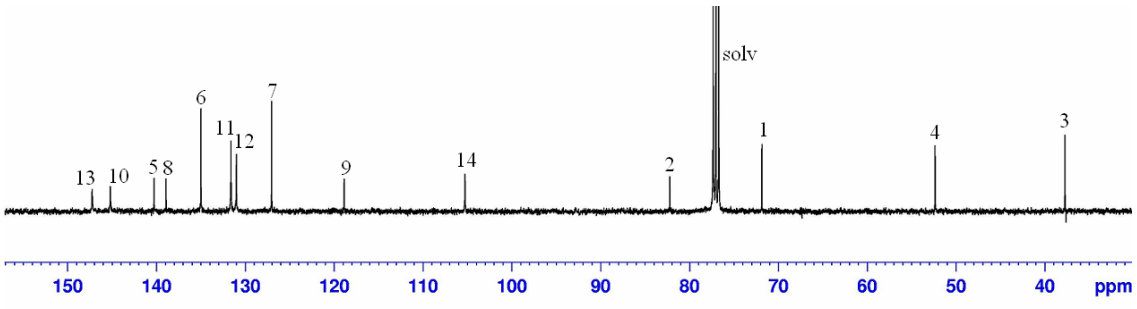

Figure 3.9. ^{13}C NMR spectrum of **14** in $CDCl_3$ at rt.

^{13}C NMR of porphyrin **14** is shown in Figure 3.9. From the spectrum it can be easily deduced that the peaks at 37.75 ppm and 52.36 ppm belong to aliphatic carbons assigned as **3** and **4**, since they are the most shielded carbons of the molecule. The carbon atom assigned as **3** is attached to alkyne while the other, **4**, is at the benzylic position. Due to inductive effect of benzene, benzylic carbon resonated further downfield than carbon **3**. Therefore the carbon near the terminal alkyne is more shielded and shifted upfield.

All the other carbons may be divided into two groups namely carbons belonging to the aromatic system (**5**-**14**) and carbons belonging to the non-aromatic system, (**1**-**4**). As a result, ^{13}C NMR data confirm the proposed structure of the desired monomer. Moreover in the ^{13}C NMR spectrum no chemical shift other than the expected ones confirms the purity of synthesized compound.

Prop-2-ynyl-{4-[15-(4-prop-2-ynylaminomethyl-phenyl)-porphyrin 5-yl]-benzyl}-amine dihydrochloride (**15**) was obtained by protonation of **14**. In the IR spectrum, the out-of-plane ≡C-H bending modes were observed at 667 cm^{-1} and 692 cm^{-1}, while the symmetric and the antisymmetric stretching vibrations were seen at 972 cm^{-1} and 980 cm^{-1} respectively. The most characteristic absorption band of the monomer, the C≡C stretching band that was observed as a weak peak at 2127 cm^{-1} in the spectrum of free base porphyrin **14,** became more intense in the spectrum of the acid dication **15** at 2125 cm^{-1}. The N-H stretching band of the free base at 3281 cm^{-1}, shifted to 3246 cm^{-1} in the acid dication **15**. The shifting of the absorption upon protonation may be attributed to

the weakening of the N-H bond due to the decrease in electron density at the pyrrole N or H atoms.

The UV-Vis spectrum of **15** reveals the Soret band at 417 nm, which is 8 nm red shifted relative to the Soret band of **14**, and two absorption peaks due to Q band indicating the D_{4h} symmetry of porphyrin dication.

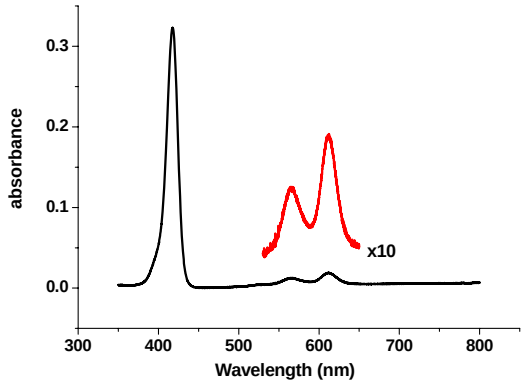

Figure 3.10. UV absorption of **15** (3.7852×10^{-6} M, 2N HCl, rt)

	Wavelength, λ (nm)	Molar Absorptivity ($mol^{-1}.L.cm^{-1}$)
B(0,0)	417.6	8.532×10^4
Q(1,0)	565.0	3.324×10^3
Q(0,0)	612.5	5.054×10^3

Table 3.3. UV-Vis data of **15**

3.3.3. (2-Azido-ethyl)-[4-(15-{4-[(2-azido-ethylamino)-methyl]-phenyl}-porphyrin-5-yl)-benzyl]-amine(19)

The second monomer which is required for the polymerization via 1,3-dipolar cycloaddition is the porphyrin functionalized with azide groups. According to the studies of Mock[64] the best spacing group between the azido substituent and the ammonium ion is ethyl. The monomer **19** was synthesized according to Scheme 3.6. First, 2-chloro ethylamine was converted via nucleophilic substitution to 2-azidoethylamine (**18**) using

sodium azide in water at 75 ^{o}C. Then dibromoporphyrin **12** was N-alkylated adding excess 2-azidoethylamine dropwise at rt.

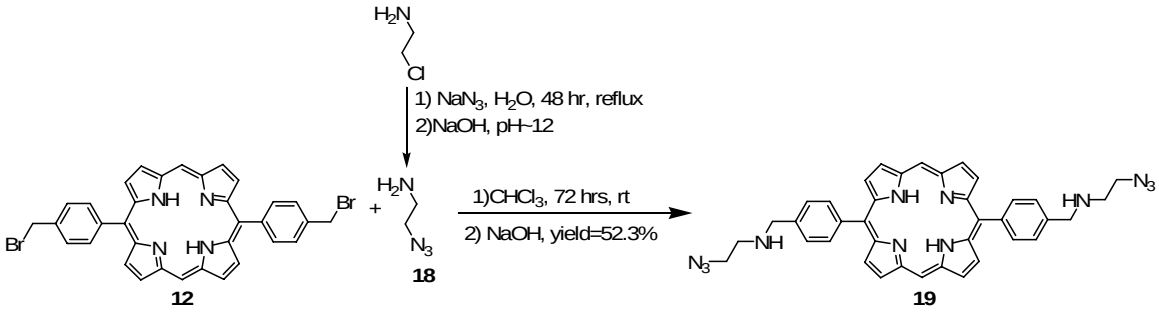

Scheme 3.6. Synthesis of **19**.

After stirring the reaction mixture for 72 hrs at rt, TLC confirmed the completion of the reaction. After the standard working-up stage, the purple colored residue was purified through column chromatography using a MeOH, DCM mixture. The yield was 52%.

The infrared spectrum of the compound revealed that the characteristic peaks belong to the motion of the porphyrin skeleton. The absence of the C-Br frequency at 596 cm^{-1} indicated that **12** was functionalized successfully by azide groups. As expected, in the spectrum, there was a very strong peak at 2096 cm^{-1} which belongs to the out-of-phase N=N=N stretching mode as shown in Figure 3.11.

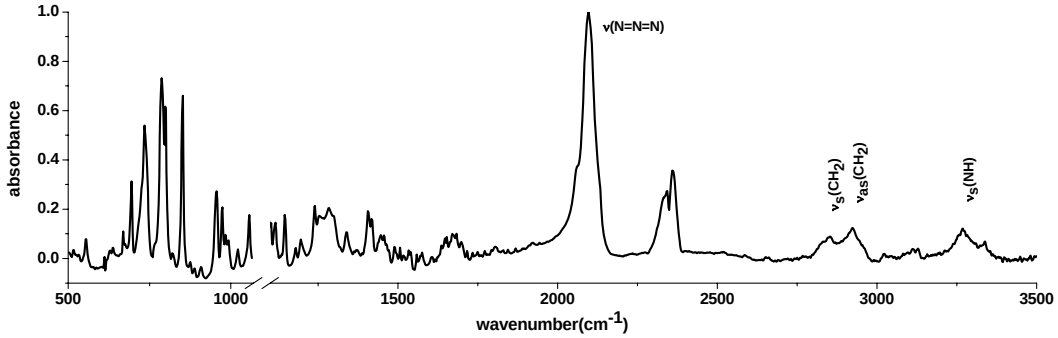

Figure 3.11. FT-IR spectrum of **19**.

The UV-Vis spectrum of **19** exhibited the Soret band at 410 nm with four absorption peaks due to the Q band indicating D_{2h} symmetry of porphyrin, which is in the free base form. The wavelength and absorptivity values obtained from the UV-Vis spectrum are tabulated in Table 3.4. Replacement of Br with azide and amine containing groups led to better delocalization of the electrons. Therefore it was observed that **19** has a higher molar absorptivity compared to precursor **12**.

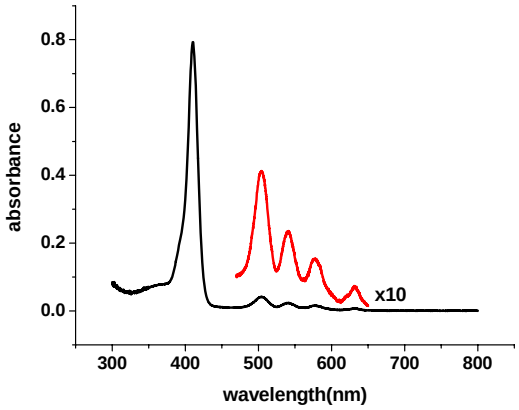

Figure 3.12. Absorption spectrum of **19**(3.7950 x 10^{-6} M, $CHCl_3$, rt)**.**

	Wavelength, λ (nm)	Molar Absorptivity ($mol^{-1}.L.cm^{-1}$)
B(0,0)	410.33	$2.090x10^5$
$Q_y(1,0)$	504.17	$1.088x10^4$
$Q_x(1,0)$	541.17	$6.198x10^3$
$Q_y(0,0)$	577.17	$4.076x10^3$
$Q_x(0,0)$	631.67	$1.939x10^3$

Table 3.4. UV-Vis data for compound **19**

The ^1H NMR spectrum of **19** shows ten different hydrogen environments, as expected. As addressed in the interpretation of the previous spectra, in the most upfield region of the spectrum at -3.07 ppm, there is a resonance as singlet due to aminal hydrogens, **k**, of the porphyrin ring. The integration of this resonance proves the

assignment. At 1.8 ppm there is a broad signal that possibly belongs to the aminal hydrogens **c**.

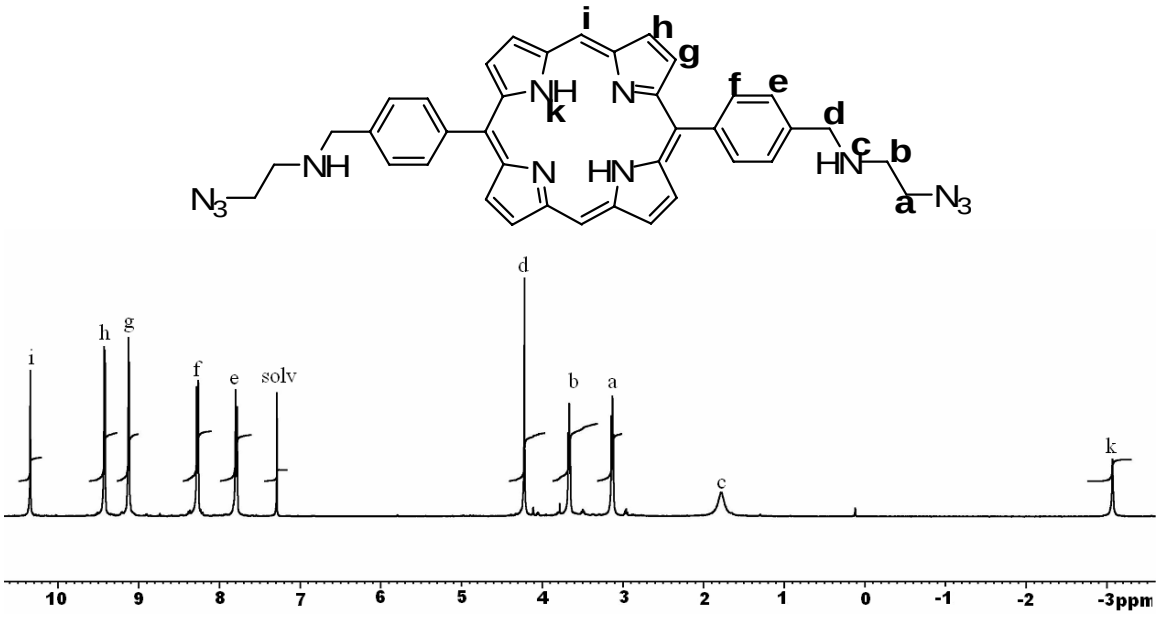

Figure 3.13. ^{1}H NMR spectrum of **19** in $CDCl_3$ at rt.

Two closely spaced triplets in the upfield region are assigned as protons **a,** and protons **b** with ^{3}J coupling constants 5.67 and 5.65 Hz respectively. This also indicates that dibromoporphyrin was substituted with ethyl group. The intensity of integration gives the expected number of hydrogens (4H) for **a** and **b.**

As in the case of the ^{1}H NMR spectrum of the previous monomer, at 4.22 ppm there is a signal as a singlet due to benzylic protons. However, the chemical shift due to the benzylic protons of dibromo porphyrin was observed at 4.95 ppm, whereas upon N-alkylation, it shifted approximately 0.7 ppm upfield. This result as well as the integration indicate that dibromo porphyrin was functionalized successfully.

The resonances as doublets at 7.79 and 8.27 ppm were assigned as protons **e** and **f,** respectively due to the para-substituted benzene ring. The signals as two closely separated doublets at 9.12 and 9.42 ppm were assigned to protons **g** and **h** due to β-pyrrole. Finally, at 10.34 ppm, in the most downfield region, resonances due to protons at meso positions were observed.

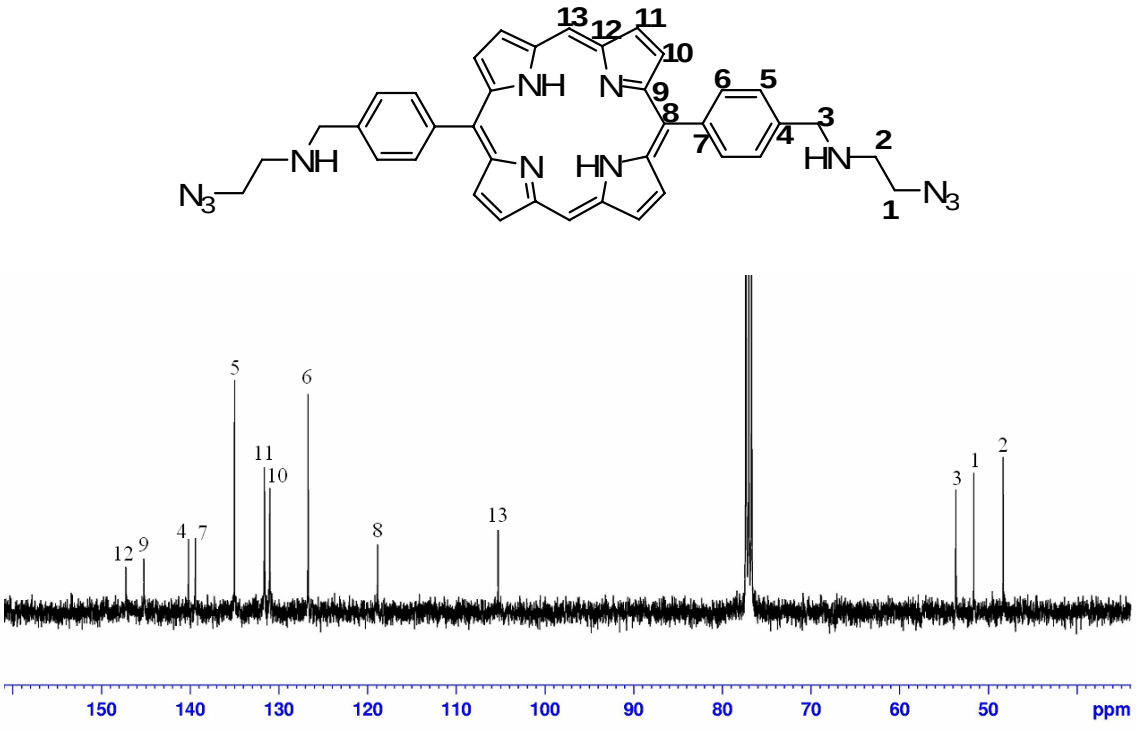

Figure 3.14. ^{13}C NMR spectrum of **19** in $CDCl_3$ at rt.

^{13}C NMR spectrum of **19**, reveals three signals in the upfield region due to C**2**, C**1**, and C**3** at 48.3, 51.7 and 53.7 ppm, which were assigned taking the inductive effect into account as explained for the previous spectra. In the further downfield region, two adjacent chemical shifts where observed, which belong to C**13** and C**8** at 105.3 and 118.9 ppm, respectively. The rest of the signals were assigned for the carbons of phenyl and porphyrin rings by taking into account the electronic effects of substituents.

(2-Azido-ethyl)-[4-(15-{4-[(2-azido-ethylamino)-methyl]-phenyl}-porphyrin-5-yl)-benzyl]-amine dihydrochloride (**20**) was prepared by protonation of **19**. Although the characteristic band of out-of-phase N=N=N stretching mode was observed at 2096 in the spectrum of free base, it was observed at 2116 in the spectrum of the acid form as more intense band. As in the case of monomer **14** and its acid dication **15**, there is a downward shift of the absorption of N-H stretching, that was observed at 3245 cm^{-1}, after acidification of the monomer. Additionally, the intensity of the band was also reduced by acidification.

The UV-Vis spectrum of 20 reveals the Soret band at 417.8 nm and two absorption peaks at 566.8 and 612.5 nm due to the Q band indicating the D_{4h} symmetry of porphyrin dication.

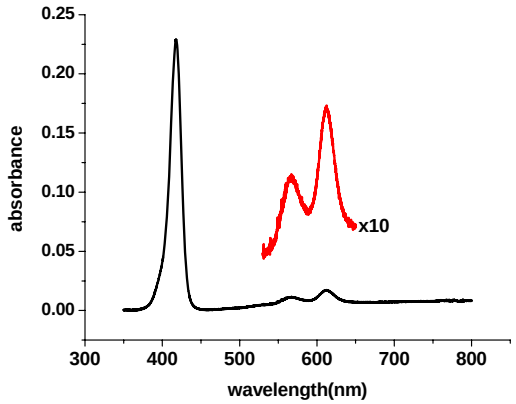

Figure 3.15. UV-Vis spectrum of **20** (3.7865 x 10^{-6} M, 2N HCl, rt)

	Wavelength (nm)	Absoptivity ($mol^{-1}.L.cm^{-1}$)
B(0,0)	417.8	6.049 x 10^4
Q(1,0)	566.8	3.045 x 10^3
Q(0,0)	612.5	4.577 x 10^3

Table 3.5. UV-Vis data of **20**

3.3.4.1. 5, 10, 15, 20-Tetrakis-(4-bromomethyl-phenyl)-porphyrin (21)

The precursor of monomer **22** with tetra-phenyl substituted at meso positions was synthesized according to the literature[24] by acid catalyzed condensation of pyrrole with α-bromo-p-tolualdehyde as shown in Scheme 3.7.

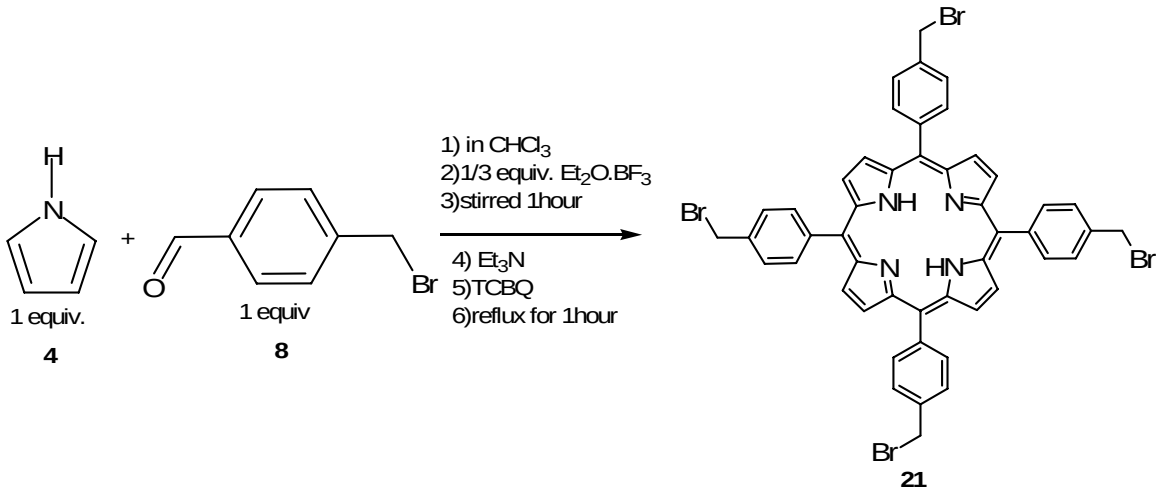

Scheme 3.7. Synthesis of **21**.

3.3.4.2. Prop-2-ynyl-{4-[10,15,20-tris-(4-prop-2-ynylaminomethyl-phenyl)-porphyrin-5-yl]-benzyl}-amine (22)

To synthesize monomer **22**, the precursor porphyrin **13** was treated with excess propargyl amine to prevent over-alkylation as shown in Scheme 8.

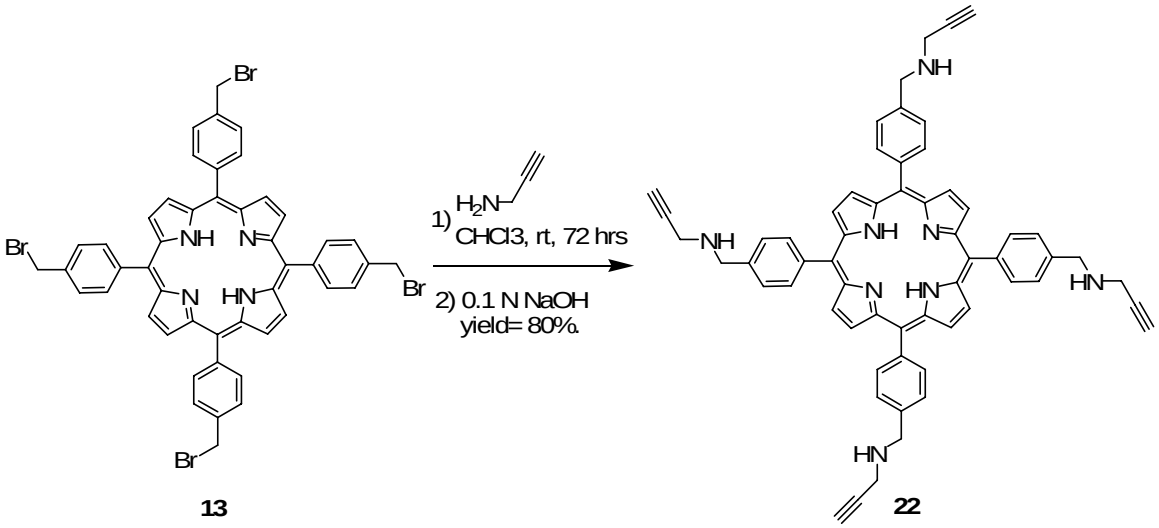

Scheme 3.8. Synthesis of **22**.

After the necessary work-up, porphyrin **22** was purified by column chromatography using methanol, DCM as an eluent subsequently, the resulting purple colored solid was converted to its hydrochloride salt by dissolving in 0.1 N aq. HCl. The

salt was recrystallised from water-acetone to obtain the protonated porphyrin **23** in 80% yields.

The porphyrin **22** was characterized by UV-Vis spectroscopy and the results are tabulated in Table 3.6.

	Wavelength, λ (nm)	Molar Absorptivity ($mol^{-1}.L.cm^{-1}$)
B(0,0)	413	$5.78x\ 10^5$
$Q_y(1,0)$	518	$1.5x10^4$
$Q_x(1,0)$	554	$8.3x10^3$
$Q_y(0,0)$	585	$5.7x10^3$
$Q_x(0,0)$	645	$4.9x10^3$

Table 3.6. UV-Vis data for **22.**

^{1}H NMR spectrum of **22**, reveals six different proton environments, which are consistent with the proposed structure. These resonances were assigned on the spectrum as shown in Figure 3.16.

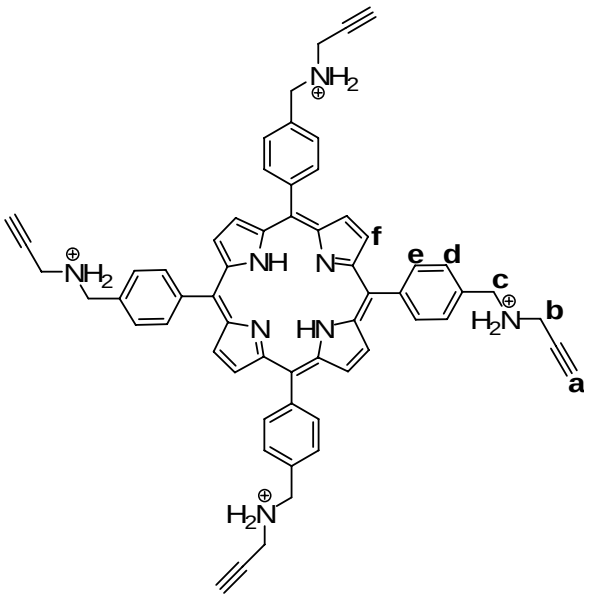

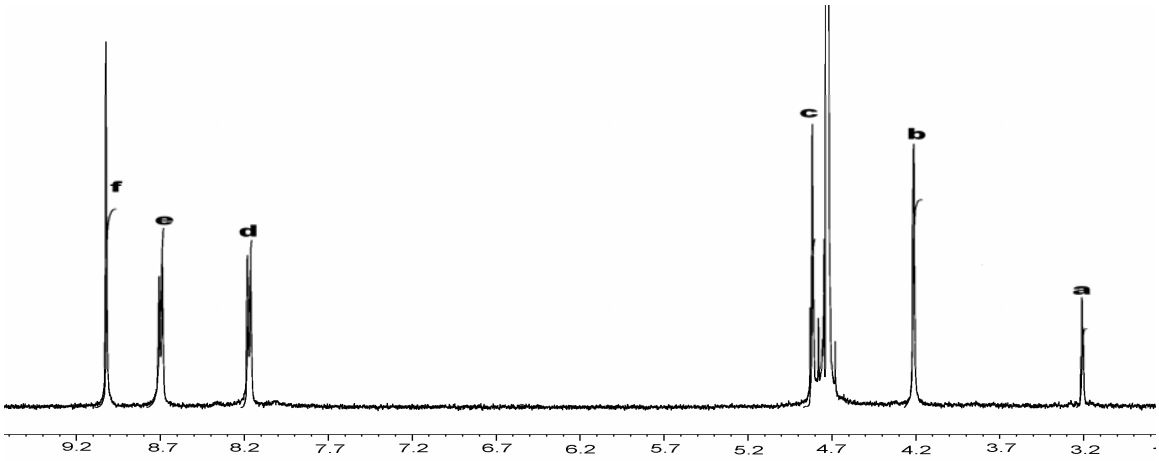

Figure 3.16. ^{1}H NMR spectrum of **22** in D_2O at rt.

The characterization of **22** was also carried out by ^{13}C NMR spectroscopy and the Figure 3.17 shows the ^{13}C NMR spectrum with assignments of resonances due to carbon of porphyrin **22**.

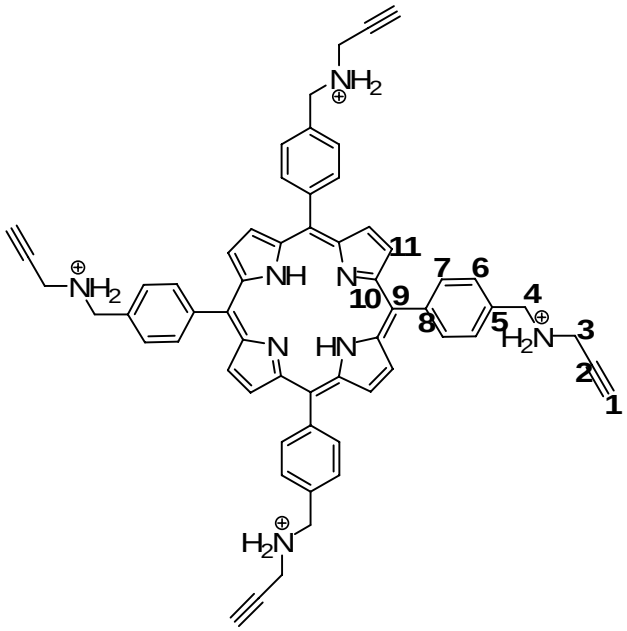

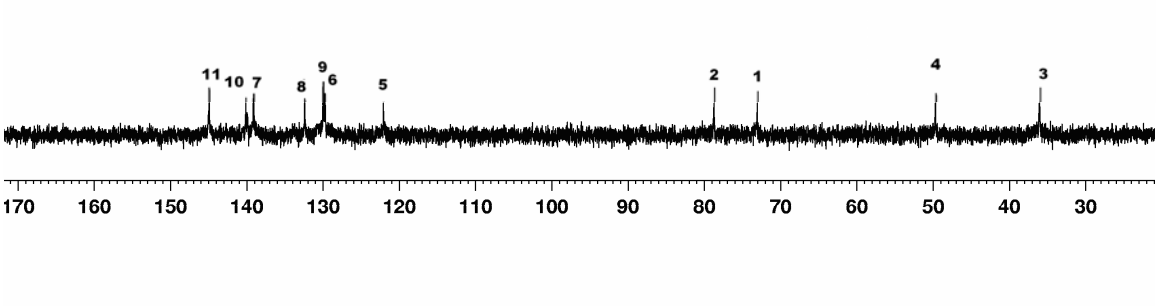

Figure 3.17. ^{13}C NMR spectrum of **22** in D_2O-DSS mixture at rt.

Moreover, the monomer **22** was characterized through elemental anlysis and mass spectroscopy apart from ^{1}H NMR, ^{13}C NMR and UV-Vis. The characterization data indicated that the target compound **22** was synthesized successfully.

3.4. Synthesis and Characterization of Rotaxanes

3.4.1. [3] rotaxane (25)

After the preparation of the monomers, first we wanted to synthesize [3] rotaxane to investigate the impact of CB[6] on the porphyrin core properties.

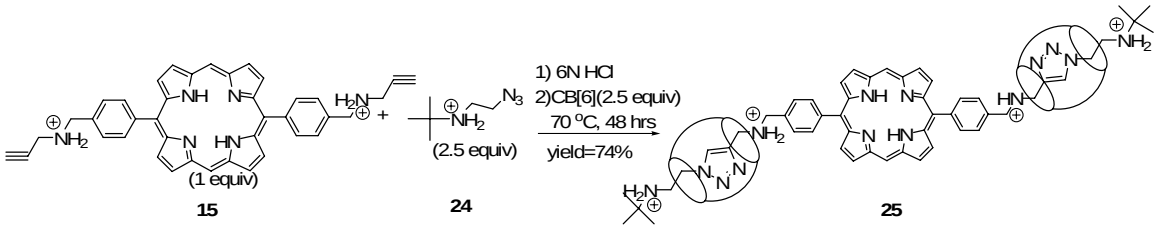

Scheme 3.9. Synthesis of **25**.

For the synthesis of [3] rotaxane **25**, one equivalent of monomer **15** was dissolved in 6 N HCl (aq) solution. And then the solution of 2.5 equivalents of (2-Azido-ethyl)-tert-butyl-amine hydrochloride **24**, which was synthesized according to the literature procedure, was added. After about 5 min, the solution of 2.5 equivalents CB[6] was added under stirring to the reaction mixture. The resulting green colored solution was heated to 70 ^{o}C for 48 hrs. After the reaction was complete, the solvent was removed under reduced pressure. The solid residue was washed with MeOH to remove excess

monomers. The resulting precipitates were dissolved in hot water and was filtered through 0.45 μm membrane to remove excess CB[6]. The filtrate was concentrated under reduced pressure and precipitated into ethanol/acetone mixture. Green colored powder was collected through filtration and dried under vacuum. The yield was 74%.

The infrared spectrum of **25** (Figure 3.18) showed no peak due to azide groups at about 2090 cm^{-1} indicating the monomers were used up to form triazole rings. However, the signals due to –C=N stretching of triazole, usually appears at approximately 1650 cm^{-1} was not seen clearly in the spectrum. It probably overlapps with the carbonyl peak of the CB[6] at 1700 cm^{-1} because of encapsulation of triazole by CB[6], which shields triazole ring and as a result high energy is required for the vibration.

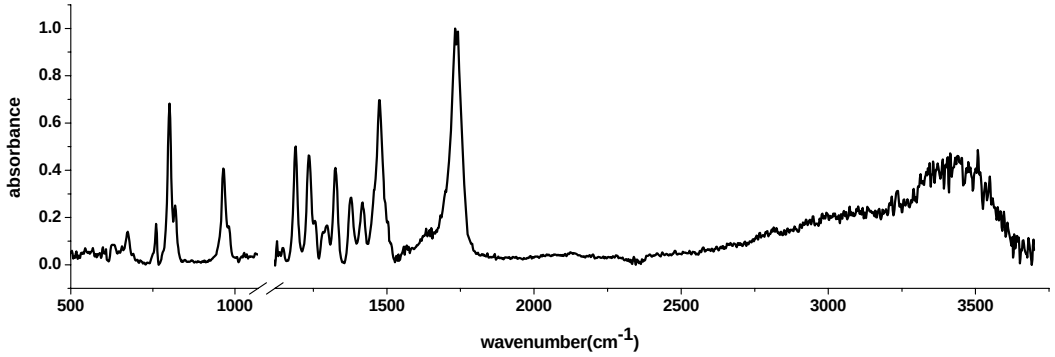

Figure 3.18. Infrared spectrum of **25**

Solution of compound **25** was prepared in H_2O and the UV spectrum shown in Figure 3.19 was taken. Wavelength and molar absorptivity are tabulated in Table 3.7. Although **25** is soluble in water in contrast to the porphyrin monomers, the solubility was very poor. The Soret band was observed at 402 nm while the Q band peaks were at 505, 541, 566 and 621 nm, which indicate the existence of a free base porphyrin core in **25**.

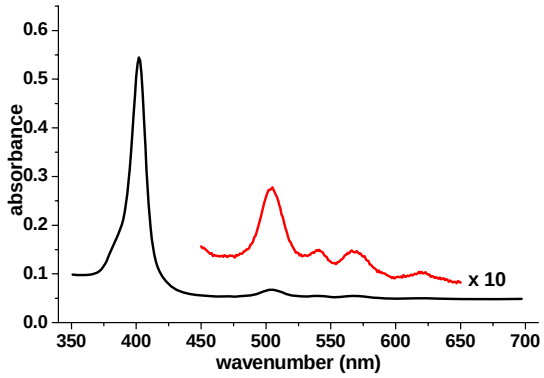

Figure 3.19. UV spectrum of **25** (1.048 x 10^{-6}, H_2O, rt).

	Wavelength, λ (nm)	Molar Absorptivity ($mol^{-1}.L.cm^{-1}$)
B(0,0)	402	5.20 x 10^5
$Q_y(1,0)$	505	6.47 x 10^4
$Q_x(1,0)$	541	5.24 x 10^4
$Q_y(0,0)$	566	5.23 x 10^4
$Q_x(0,0)$	621	4.78 x10^4

Table 3.7. UV-Vis data for **25**.

In addition, characterization was carried out by ^{1}H NMR. The ^{1}H NMR spectrum shows broad signals corresponding to [3] rotaxane. Even at low concentration broad peaks were observed. The reason can be attributed to the porphyrin-porphyrin interaction that causing aggregation, because only two meso positions of porphyrin were functionalized. However, [3] rotaxane is more soluble than the protonated monomer **16** in water, probably the rotaxane formation at two positions of porphyrin prevents the high degree of aggregation.

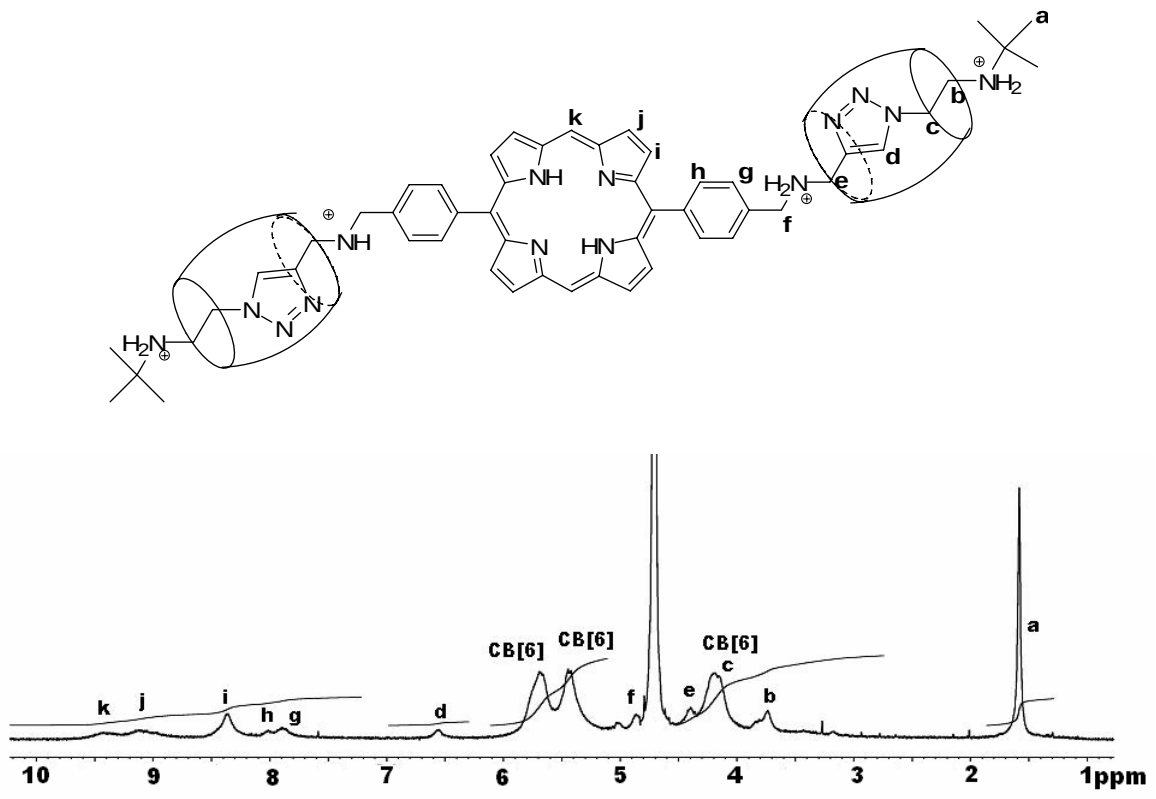

Figure 3.20. ^{1}H NMR spectrum of **25** in D_2O at rt.

In the most upfield region of the spectum at 1.6 ppm, there is a singlet resonance belonging to the hydrogens of stopper group tert-butyl. The integration proved the existence of 18 hydrogens as expected. The hydrogens of ethylene give signals at 3.8 ppm and 4.2 ppm that assigned as **b** and **c,** respectively. Since the triazole ring has deshielding effect, the hydrogens nearer to it, resonate downfield. Integration of both signals indicates that there are 4 hydrogens for each of them.

The methylene protons assigned as **e** and **f** produced singlets at 4.4 ppm and 4.85 ppm respectively. Since the deshielding effect of benzene ring is higher than that of triazole ring , methylene protons nearer to the benzene ring had signal in more downfield part. The existence of four hydrogens for each signal was proved by integration intensity as expected.

The resonances of CB[6] protons were observed at 4.25, 5.45 and 5.68 ppm. For the determination of [3] rotaxane the most important resonance, that belongs to the

triazole proton, was observed at 6.58 ppm as a singlet and the integration proved the existence of two protons. Therefore it was proven that at the both arm of the porphyrin monomer, triazole formation was succeeded through 1,3-dipolar cycloaddition catalyzed by CB[6].

The assignments of the other resonances due to the benzene and porphyrin ring protons were clearly shown in the ^{1}H NMR spectrum (Figure 3.20).

When the spectrum of [3]rotaxane was compared with that of **14**, it was observed that the resonances due to terminal alkyne proton disappeared, while triazole yielded a new singlet. It was also deduced that by rotaxanation the resonances due to benzene ring shifted to downfield region.

3.4.2. [5] rotaxane(26)

To synthesize [5]rotaxane, monomer **23**, was treated with four equivalents of (2-Azido-ethyl)-tert-butyl-amine hydrochloride **24** and four equivalents of CB[6] at rt as shown in the reaction Scheme 3.10. The reaction mixture was stirred at rt for 48 hrs. After the reaction was complete, the solvent was removed under reduced pressure and the green colored film was suspended in hot water to remove unreacted CB[6] by membrane filtration (0.45 μm pore size). The filtrate was concentrated and precipitated into ethanol-acetone mixture. [5] rotaxane was obtained in 85% yield.

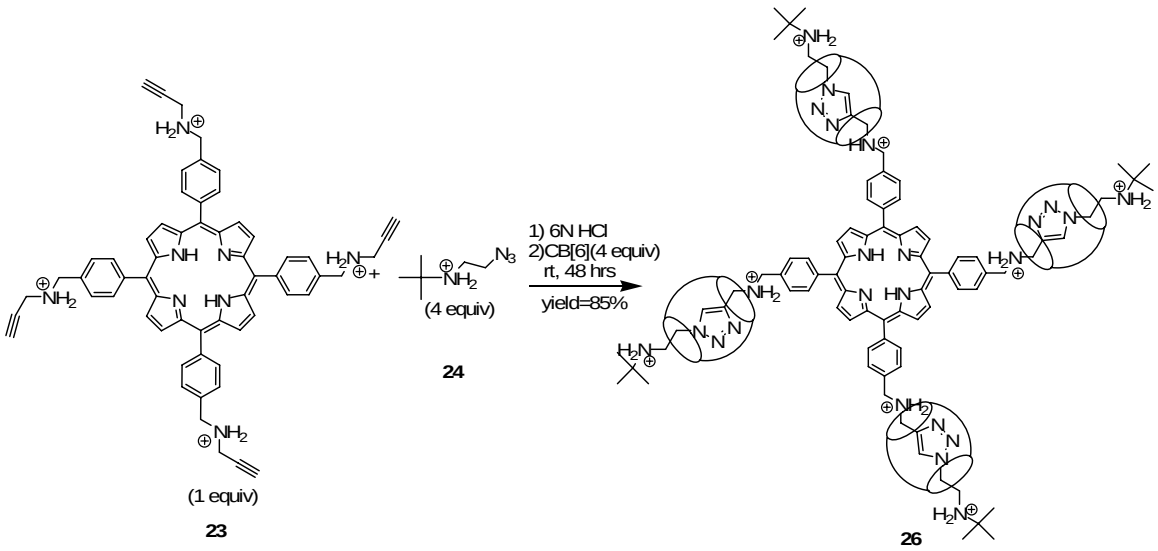

Scheme 3.10. Synthesis of **26**.

[5] rotaxane has a very good solubility in water, whereas [3]rotaxane has shown poor solubility in water. The UV-Vis spectrum of [5]rotaxane was taken in water. The Soret band was observed at 415 nm with four absorption peaks due to the Q band indicating that central nitrogens of the porphyrin core were not protonated (Table 3.8).

	Wavelength (nm)	Absorptivity ($mol^{-1}.L.cm^{-1}$)
B(0,0)	415	3.66×10^5
$Q_y(1,0)$	518	1.36×10^4
$Q_x(1,0)$	555	8.3×10^3
$Q_y(0,0)$	583	6.2×10^3
$Q_x(0,0)$	637	4.2×10^3

Table 3.8. UV-Vis data for **26** (5.0×10^{-6} M, H_2O, rt)

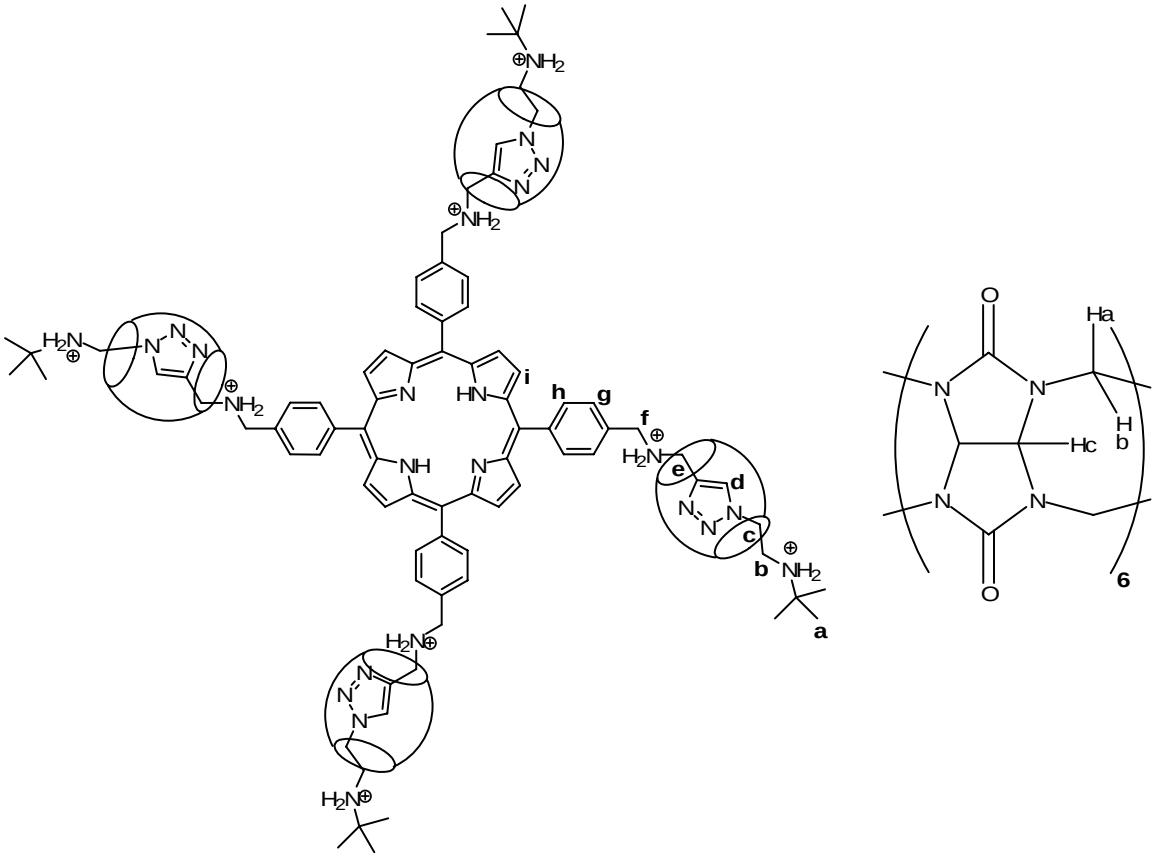

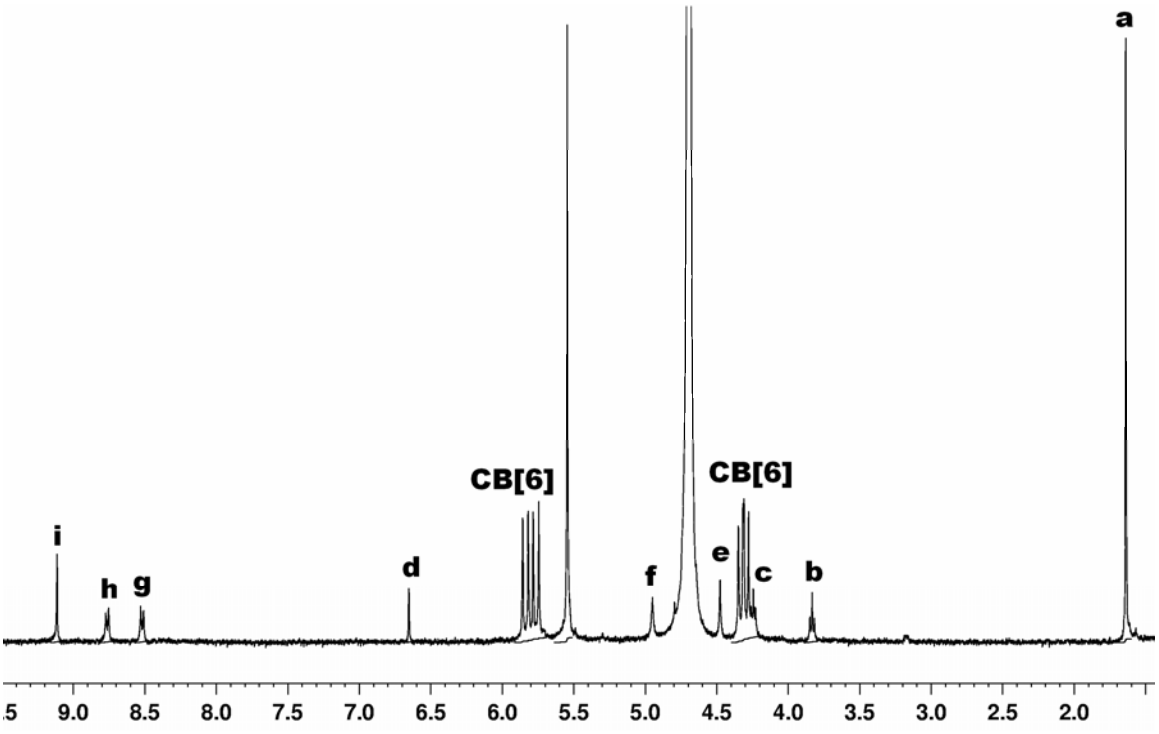

Figure 3.21. ^{1}H NMR spectrum of **26** in D_2O at rt.

To characterize [5]rotaxane, the ^{1}H NMR spectrum was recorded. As can be seen from the spectrum, the signals are sharp and well-resolved indicating that there is no porphyrin-porphyrin interaction as a result of aggregate formation. This probably can be attributed to steric hindrance since the porphyrin core is surrounded by four bulky groups, CB[6]. As in the previous cases, in upfield region of the spectrum, resonances due to aliphatic hydrogens took place. Tert-butyl hydrogens gave a singlet at 1.61 ppm while hydrogens of the ethyl group assigned as **b** and **c** coupled to each other to produce two adjacent triplets at 3.81 and 4.13 ppm respectively. As the last aliphatic hydrogens, methylene hydrogens named as **e** and **f** gave singlets at 4.39 and 4.86 ppm.

The ^{1}H NMR spectrum of free CB[6] shows signals at 4.43, 5.75 and 5.97 ppm due to H_a, a 12H-doublet, H_b a 12H doublet and H_c a 12H doublet respectively. However, in the spectrum of [5] rotaxane the signals due to H_a and H_b further splitted to give two doublets.

As expected, aromatic hydrogens resonated in the downfield region of the spectrum. As the most characteristic peak of the compound, a singlet at 6.62 ppm that belongs to triazole hydrogens was observed. The para substituted hydrogens coupled to each other to yield to adjacent doublets at 8.52 and 8.79 ppm with ^{3}J constant 9.9 and 10.1 Hz respectively. In the most downfield part of the spectrum, eight β hydrogens of porphyrin ring gave a singlet at 9.09 ppm.

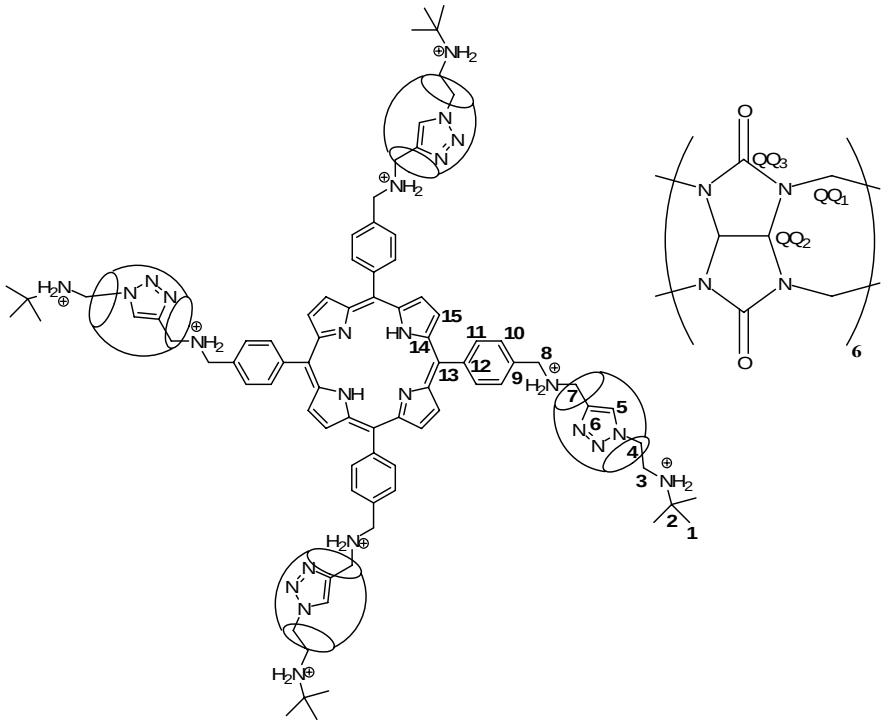

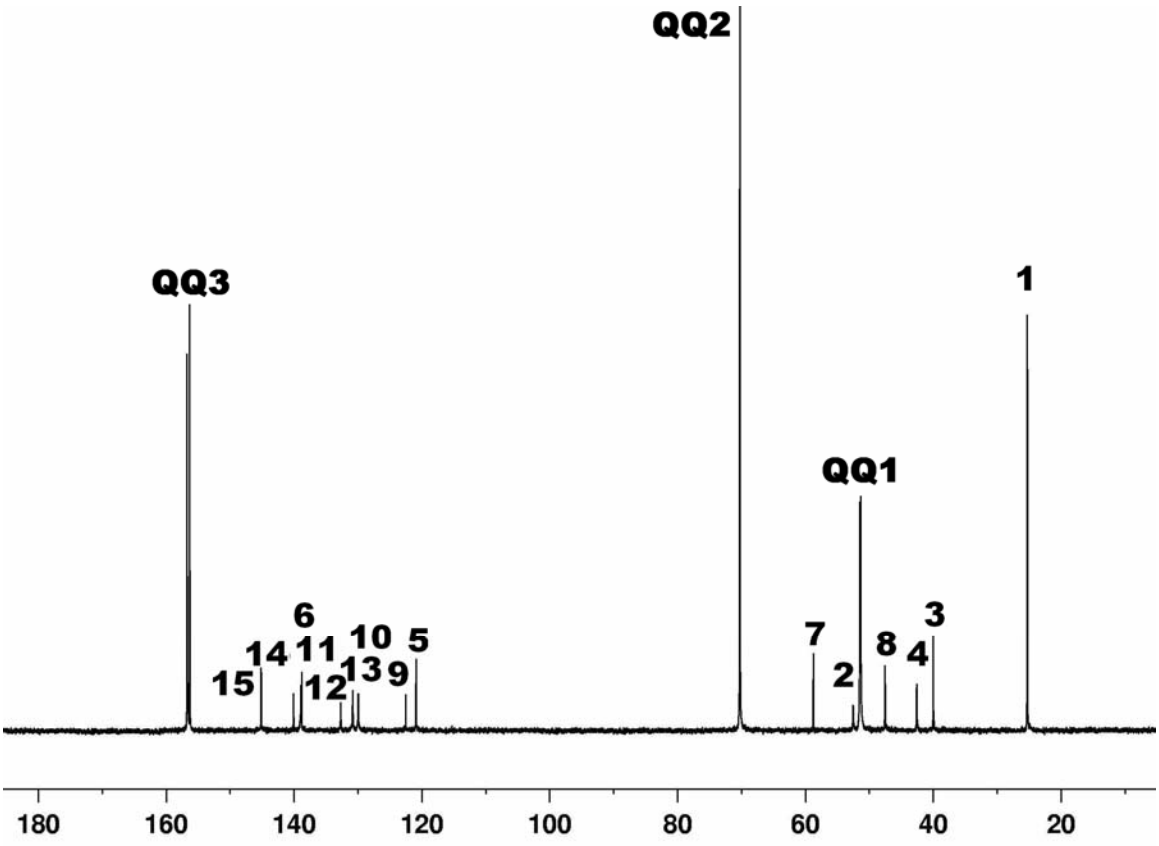

Figure 3.22. ^{13}C NMR spectrum of **26** in D_2O-DSS mixture at rt.

Characterization by ^{13}C NMR indicated that there are fifteen different carbon environments, apart from the resonances due to CB[6] carbons at 51.3, 51.5, 70.2, 156.3 and 156.7 ppm. Normally there are three different carbon environments for CB[6] resonating at 51, 71 and 158 ppm due to C1, C2, and C3 respectively. However, as can be seen from the spectrum of [5] rotaxane, there are two resonances due to C=O and methine carbon assigned as QQ3 and QQ1. This can be attributed to the complex formation of CB[6], in which it become unsymmetrical due to binding with different types of ammonium ions, whereas there is only one signal due to C2 which is not affected upon complexation. The resonances due to the other carbons were assigned as shown in Figure 3.22.

[5] Rotaxane was also characterized by elemental analysis and mass spectrometry. The results were reported in Experimental section.

3.5. Synthesis and Characterization of Polyrotaxanes

3.5.1. Polyrotaxane (27)

After the preparation of difunctional dialkyne **15** and diazido **20** attached to porphyrin core, we wanted to synthesize the target polyrotaxane **27**, which was expected to form in a polyaddition fashion via 1,3-dipolar cycloaddition catalyzed by macrocycle CB[6].

It should be mentioned here that the monomers **14** and **19** are well soluble in organic solvents such as $CHCl_3$ and MeOH before converting to their salts. However, after the protonation they become insoluble in organic solvents as expected but also in water, which was not expected. Therefore the polymerization reaction has to be carried out in strongly acidic conditions.

The insolubility of monomer **15** and **20** in water is probably due to π-π interaction of porphyrin cores. At low pH, nitrogens of porphyrin core and the nitrogens on the amines of monomers get protonated thus due to electrostatic repulsion between porphyrin cores, no aggregate forms.

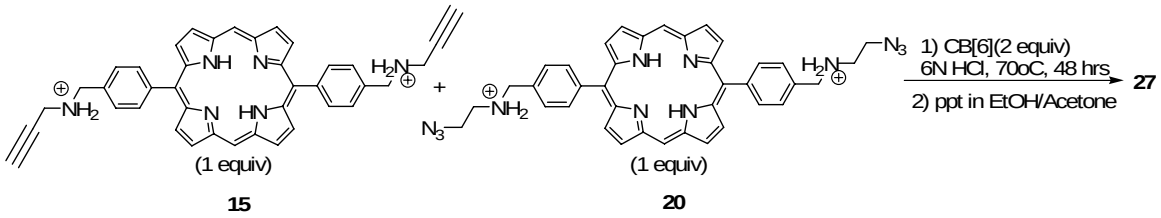

Scheme 3.11. Synthesis of **27**.

Polyrotaxane **27** was synthesized as shown in Scheme 3.11, by one equivalent of monomer **15**, one equivalent of monomer **20** and two equivalents of CB[6] in 6N HCl. The resulting green colored solution was stirred at 70 ^{o}C. After 48 hrs, the reaction mixture was concentrated to ½ to its initial volume and precipitated into EtOH/Acetone mixture. Polyrotaxane **27** was obtained.

It was expected that the polymerization would improve the solubility of monomers. But, unfortunately the resulting polymer is only soluble in acidified water. This hampered characterization of the polymer in more details.

First the characterization of **27** was realized through IR spectroscopy. To confirm that polymerization occurred, one equivalent of dialkyne monomer **15**, one equivalent of diazodo monomer **20** and two equivalents of CB[6] were mixed. After preparing a KBr pellet out of this mixture, its IR spectrum was recorded. As shown in Figure 3.23, the IR spectrum of this mixture (Figure 3.23b) was compared to the IR spectra of polyrotaxane **27** (Figure 3.23c) and CB[6] (Figure 3.23a). The characteristic peak due to the azide group at 2100 cm^{-1} almost completely disappeared in the spectrum of polyrotaxane which suggests, that azide was used in the triazole formation through 1,3-dipolar cycloaddition, as a result of polymerization.

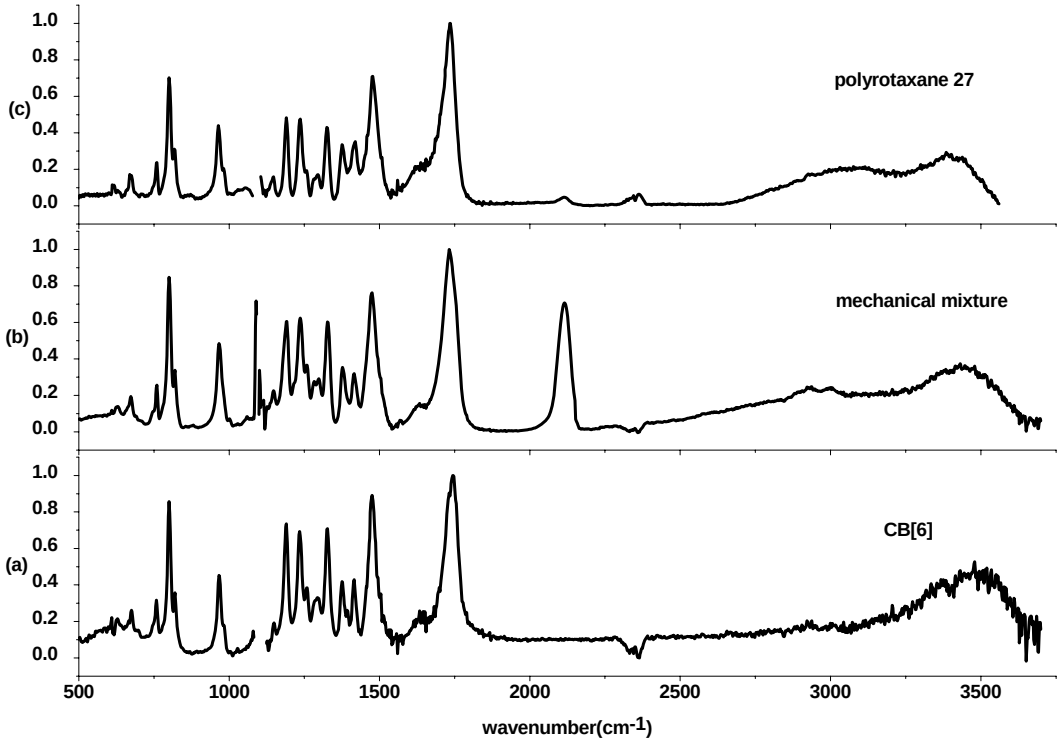

Figure 3.23. (a)Infrared spectrum of CB, (b) mechanical mixture of **15**, **20** and CB[6] and (c) polyrotaxane.

Polyrotaxane **27** was managed to dissolve in 2N HCl (aq) solution and its UV-Vis spectrum was recorded as shown in Figure 3.24. UV-Vis spectrum reveals Soret band at 420 nm and two absorption peaks at 567 and 614 nm due to the Q band by indicating that at this pH the central nitrogen of porphyrin was protonated and as a result its symmetry changed to D_{2h}.

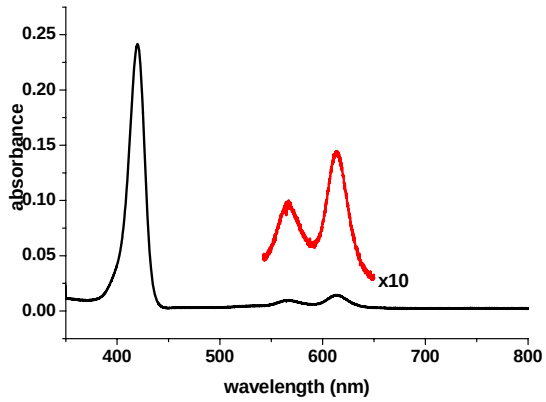

Figure 3.24. UV spectrum of **27** (2 N HCl, rt)

To characterize polyrotaxane, the ^{1}H NMR spectrum was recorded in dil. CD_3COOH. Due to solubility problems of the polyrotaxane, it cannot be purified properly. Therefore as can be seen there are some unidentified peaks in the ^{1}H NMR spectrum. As in the previous cases, resonances due to aliphatic hydrogens took place in upfield region of the spectrum. Two adjacent ethylene hydrogens assigned as **a** and **b** gave signals at 3.4 ppm and about 4 ppm, respectively. Since the signals were not well resolved the signals assigned as **d** and **e** due to the methylene protons were overlapped with the signals of CB[6] at around 4.2 ppm and 5.5 ppm respectively. As the most characteristic peak of the compound, a singlet at 6.6 ppm that belongs to encapsulated triazole hydrogens was observed. Additionally, another singlet at 7.9 ppm was observed with the same integration of the previous one. This signal may be attributed to the signals belonging to non-encapsulated triazole protons. The other hydrogens belonging to porphyrin and phenyl rings were assigned as in Figure 3.25.

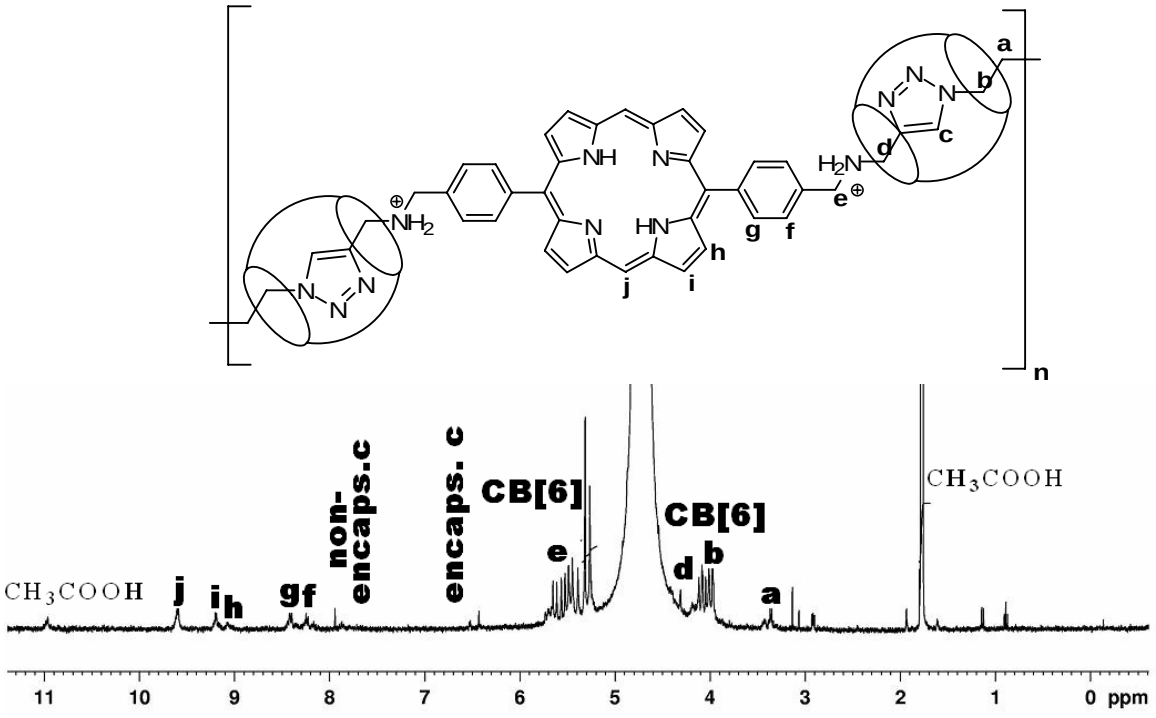

Figure 3.25. ^{1}H NMR Spectrum of **27** in D_2O-CH_3COOH mixture at rt**.**

3.5.2. Copolyrotaxane (28)

After having solubility problems with our polyrotaxane, we wanted to change one of the porphyrin cored monomers to a monomer with long aliphatic spacer since we expected improved solubility in the resulting polyrotaxane. Accordingly, we decided to use a diazide monomer **29**, since it was available in our lab.[100]

As in the polyrotaxane synthesis, one equivalent of **29** dissolved in water was mixed with one equivalent of **15** dissolved in 6N HCl. Then the solution of two equivalents CB[6] was added dropwise. The resultant mixture was heated at 70 ^{o}C for two days. After concentrating the reaction mixture to ½ its initial volume and precipitating into EtOH/Acetone mixture, **28** was obtained.

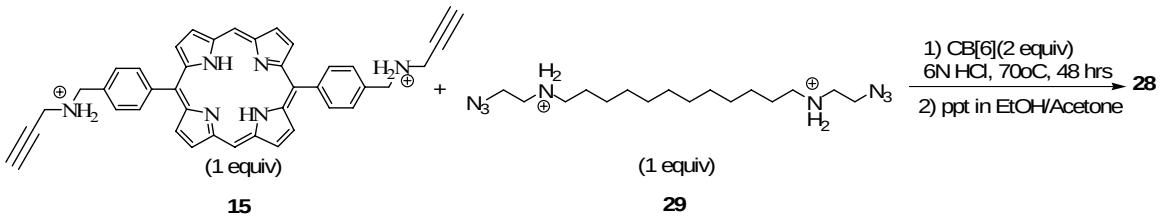

Scheme 3.12. Synthesis of **28**.

Characterization was done firstly by FT-IR spectroscopy. As in the case of **27**, the triazole ring stretching motion as the most important characteristic peak overlapped with the very strong carbonyl peak at about 1730 cm^{-1}. Therefore to confirm the copolyrotaxane formation, it was decided to compare IR spectra of CB[6] (Figure 3.26a), mechanical mixture (Figure 3.26b) prepared by mixing one equivalent of each monomer and CB[6] and copolyrotaxane **28** (Figure 3.26c). Since the most important evidence of formation of **28,** is to check the azide stretching band, sharp decrease in the intensity of characteristic azide peak at 2100 cm^{-1} proved the polymerization via 1,3-dipolar cycloaddition. The azide peak with very small intensity in copolyrotaxane spectrum possibly belongs to the end group of the polymer chain.

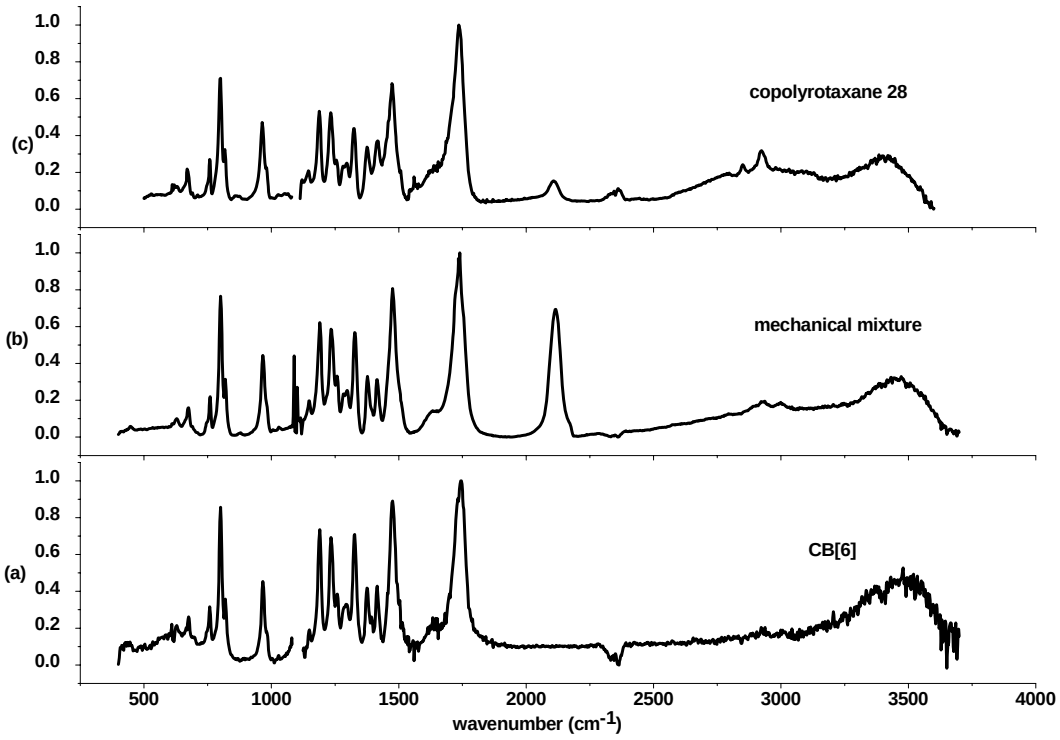

Figure 3.26. (a) Infrared spectrum of CB[6], (b) mechanical mixture of **15**, **29** and CB[6], (c) **28.**

The UV spectrum of the compound shown in Figure 3.27 was recorded in 2N HCl solution. The existence of the Soret band at 420 nm and the Q band with two peaks at 568 and 613 nm proved the protonation of porphyrin central nitrogens at 2N HCl.

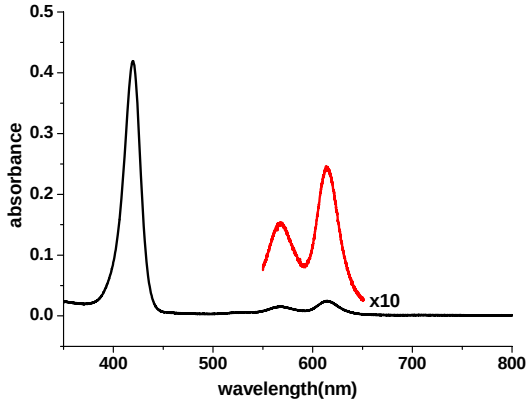

Figure 3.27. UV spectrum for **28** (2N HCl, rt).

To characterize copolyrotaxane, ^{1}H NMR spectrum was recorded. The copolymer has a better solubility than polyrotaxane in diluted deut. acetic acid. In upfield region of the spectrum, aliphatic hydrogens originated resonances. The methylene protons of long aliphatic chain assigned as **a** and **b** gave signals at 1.6 and 1.85 ppm, respectively. The methylene protons assigned as **c** and **d** gave signals at 3.15 and 3.65 respectively while other methylene protons assigned as **e, g** and **h** gave signals overlapped with the signals of CB[6] at around 4.3 ppm and 5.7 ppm respectively. As the most characteristic peak of the compound, a singlet at 6.6 ppm that belongs to encapsulated triazole hydrogens was observed. Additionally, another singlet at 8.1 ppm was observed with higher integration than the previous one. This signal may be attributed to the signals belonging to non-encapsulated triazole protons. The other hydrogens belonging to porphyrin and phenyl rings were assigned as in Figure 3.28.

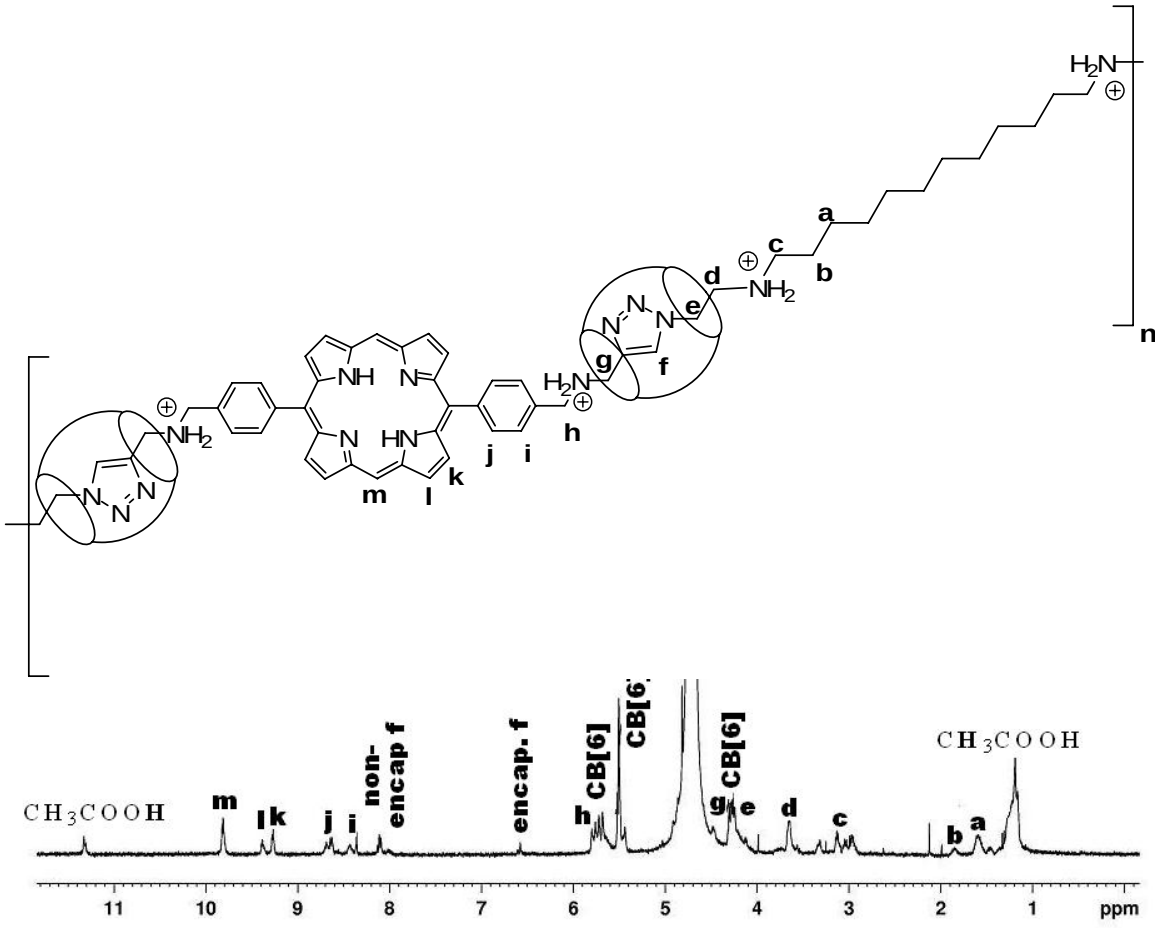

Figure 3.28. ^{1}H NMR Spectrum of **28** in D_2O-CD_3COOH mixture at rt**.**

CHAPTER 4. CONCLUSION

For the first time, we have synthesized and characterized [3]- and [5]-rotaxanes, polyrotaxane and copolyrotaxane containing a porphyrin ring as stopper group by the self-threading method. Although polyrotaxanes with porphyrin stopper groups had been synthesized earlier, their macrocycles were different than CB[6], which catalyzes 1,3-dipolar cycloadditions.

To synthesize rotaxanes and polyrotaxanes firstly porphyrin containing monomers have been synthesized and characterized. It was observed that the monomers were soluble in common organic solvents such as DCM. But it was necessary to protonate the amine part of the functional groups for the inclusion of both azide and alkyne functional groups interior of CB[6] to catalyze triazole formation. It was observed that at high pHs the monomers were soluble neither in organic solvents nor in water. The insolubility in water can be attributed to the formation of J-aggregation of monomers through edge-to-face interactions. To prevent aggregation and insolubility of monomers acidification was necessary. It was observed that by acidification of monomers, they became soluble as a result of deaggregation due to electronic repulsion between protonated porphyrin rings.

It is known that by encapsulation of porphyrin rings or their substituents with macrocycles such as cyclodextrin, the solubility of the porphyrin ring can be increased while aggregation formation is prevented. Therefore [3]-rotaxane was synthesized, in addition to the aim of modeling out of polyrotaxane. It was observed that there is almost no improvement in solubility of porphyrin. But the characterization of [3]rotaxane indicated that the synthesis has been successful.

Additionally, it was expected that the solubility can be improved by polymerization of monomers. But as in the case of model structure [3]rotaxane, the polyrotaxane was soluble in acidic water. As a result, although the characterization of polyrotaxane was difficult, it has been characterized. Therefore, the synthesis of first polyrotaxane containing porphyrin through self threading by 1,3-dipolar cycloaddition was successful.

Furthermore, to increase the solubility of polyrotaxane one of the monomers was replaced by a long aliphatic chain containing monomer that is well soluble in water. Unfortunately, it was observed that it is not enough to use long aliphatic chain monomer to improve the solubility. As in the previous cases, as a result of poor solubility the characterization was difficult. But the success of the copolyrotaxane synthesis has been also proved.

It is known that to improve the solubility substitution of all meso positions and substitution of phenyl with anionic or cationic species are two main methods. Therefore, monomer with four substituted porphyrin ring was synthesized and then [5]rotaxane was synthesized by using it. It was observed that both four substituted monomer and [5] rotaxane have been water soluble and well characterized.

As a conclusion, a novel polyrotaxane with trans substituted porphyrin ring has been synthesized via 1,3-dipolar cycloaddition catalyzed by CB[6], although it has low solubility in water.

5. REFRENCES

1. Lehn, J.-M. *Angew. Chem. Int. Ed. Engl.* **1992**, *29*, 1304
2. Lehn, J.-M.; Atwood, J. L.; Davies, J. E. D.; MacNicol, D. D. *Comprehensive Supramolecular Chemistry*, **1996**, Elsevier Science.
3. Steed, J. W.; Atwood, J. L. *Supramolecular Chemistry,* **2000**, John Wiley & Sons, Ltd.
4. Hollingsworth, M.D. *Science* **2002**, *295*, 2410.
5. Lehn, J.-M. *Science* **2002**, *295*, 2400.
6. Harrison, I. T.; Harrison, S. J. Am. Chem. Soc. 1967, 89, 5723.
7. Ooya, T.; Yui, N. *ACS Symp. Ser.* **2000,** *752,* 375.
8. Watanabe, J.; Ooya, T.; Park, K.D.; Kim, Y. H.; Yui, N. *J.Biomater. Sci., Polym. Ed.* **2000,** *11,* 1333.
9. Ooya, T.; Yui, N. *J. Controlled Release* **1999,** *58*, 251.
10. Ooya, T.; Yui, N.; Eguchi, M.; Ozaki, A. *Int. J. Pharm.***2002,** *242,*47.
11. Ooya, T.; Yui, N. *Macromol. Chem. Phys.* **1998,** *199,* 2311.
12. Ooya, T.; Yui, N. *Crit. Rev. Ther. Drug Carrier Syst.* **1999**,*16*, 289.
13. Fujita, H.; Ooya, T.; Yui, N. *Macromol. Chem. Phys.***1999,** *200*, 706.
14. Fujita, H.; Ooya, T.; Yui, N. *Macromolecules* **1999,** *32,*2534.
15. Ikeda, T.; Watabe N.; Ooya, T.; Yui, N. *Macromol. Chem. Phys.***2001**, *202,*1338.
16. Ikeda, T.; Ooya, T.; Yui, N. *Polym. J.* **1999**,*31,*658.
17. Ooya, T.; Yui, N. *ACS Symp. Ser.***2000,***752,*375.
18. Ooya, T.; Yui, N.; Tomita, H.; Lee, W. K.; Huh, K. M. *Macromol. Rapid Commun.* **2002,***23,*179.
19. Caciali, F.; Wilson, J. S.; Michels, J. J.;Daniel, C.; Silva, C.; Friend, R. H. *Nat. Mater.* **2002**, *1*, 160.
20. Gibson, H. W.; Bheda, M. C.; Engen, P. T. *Prog. Polym. Sci.* **1994,** *19*, 843.
21. Gibson, H.W.; Marand, H. *Adv. Mater.* **1993**, *5*, 11.
22. Gibson, H. W. In *Large Ring Molecules*, **1996**, J. Wiley and Sons, New York.
23. Philp, D.; Stoddart, J. F. *Angew. Chem. Int. Ed. Engl.* **1996**, *35*, 1154.
24. Amabalino, D. B.; Stoddart, J. F. *Chem. Rev.* **1995**, *95*, 2725.

25. Born, M.; Ritter, H. *Macromol. Chem. Rapid Commun.* **1991**, *12*, 471.
26. Schill, G.; Zollenkopf, H. *Nachr. Chem. Techn.* **1967**, *79*, 149.
27. Schill, G.; Luttringhaus, A. *Angew. Chem. Int. Ed. Engl.* **1964**, *3*, 546.
28. Tuncel, D. and Steinke, J. H. G. *Macromolecules,* **2004**, *37,* 289.
29. Ogata, N.; Sanuim, K.; Wada, J. *J. Polym. Sci., Polym. Lett. Ed.* **1975**, *14*, 459.
30. Ogino, H. *JACS* **1981**, *103*, 1303.
31. Ogino, H.; Ohata, K. *Inorg. Chem.* **1984**, *23*, 3312.
32. Manka, J. S.; Lawrence, D. S.*JACS*, **1990**, *112*, 2440.
33. Rao, T. V. S.; Lawrence, D. S. *JACS*, **1990**, *112*, 3614.
34. Dick, D.L.; Rao, T. V. S.; Sukumaran, D.; Lawrence, D. S. *JACS*, **1992**, *114*, 2664
35. Ishnin, R.; Kaifer, A.E. *JACS*, **1991**, *113*, 8188.
36. Wenz, G.; Bey, E.; Schmidt, L. *Angew. Chem. Int. Ed. Engl.* **1992**, *31*, 783.
37. Kunitake, M.; Kotoo, K.; Manabe, O.; Muramatsu, T.; Nakashima, N. *Chem. Lett*. **1993**,1033.
38. Harada, A.; Kamachi, M. *Macromolecules* **1990**, *23*, 2821.
39. Harada, A.; Li, J.; Kamachi, M. *Nature* **1992**, *356*, 325.
40. Harada, A.; Okada, M.; Li, J.; Kamachi, M. *Macromolecules* **1995**, *28*, 8406.
41. Harada, A.;Kamachi, M. *J. Chem. Soc. Chem. Commun.* **1990**, 1322.
42. Harada, A.; Li, J.; Suzuki, S.; Kamachi, M. *Macromolecules* **1993**, *26*, 5267.
43. Born, M.; Ritter, H. *Macromol. Chem. Rapid Commun.* **1991**, *12*, 471.
44. Izatt, R. M.; Pawlak, K.; Bradshaw, J. S. *Chem. Rev.* **1991**, *91*, 1721.
45. Agam, G.; Graiver, D.; Zilkha, A. *JACS* **1976**, *98*, 5206.
46. Agam, G.; Graiver, D.; Zilkha, A. *JACS* **1976**, *98*, 5214.
47. Gibson, H.; Marand, H. *Adv. Mater.* **1993**, *5*, 11.
48. Shen, Y. X.; Xie, D.; Gibson, H. W. *J. Am. Chem. Soc.* **1994**, *116*, 537
49. Marand, E.; Hu, Q.; Gibson, H. W.; Veytsman, B. *Macromolecules* **1996**, *29*, 2555.
50. Gibson, H. W.; Liu, S.; Lecavalier, P.; Wu, C.; Shen, Y. X. *J. Am. Chem. Soc.* **1995**,*117*, 852.
51. Gibson, H. W.; Liu, S.; Gong, C.; Ji, Q.; Joseph, E. *Macromolecules,* **1997**, *30*, 3711.
52. Gibson, H. W.; Liu, S. *Macromol. Symp.* **1996**, *102*, 55.

53. Gibson, H. W.; Engen, P.T.; Lee, S. H.; Liu, S.; Marand, H.; Bheda, M. C. *Polym. Prepr. Am.Chem. Soc. Div. Polym. Chem.* **1993**, *34(1)*, 64.

54. Amabilino, D. B.; Stoddart, J. F. *Pure Appl. Chem.* **1993**, *65*, 2351-2359.

55. Pasini, D.; Raymo, F. M.; Stoddart, J. F. *Gazz.Chim. Ital.* **1995**, *125*, 431-435.

56. Langford, S. J.; Stoddart, J. F. *Pure Appl. Chem.* **1996**, *68*, 1255-1260.

57. Amabilino, D. B.; Raymo, F. M.; Stoddart, J. F. *Comprehensive Supramolecular Chemistry*; Hosseini, M. W., Sauvage, J.-P., Eds.; Pergamon: Oxford, 1996; Vol. 9, pp 85-130.

58. Raymo, F. M.; Stoddart, J. F. *Pure Appl. Chem.* **1997**, *69*, 1987-1997.

59. Gillard, R. E.; Raymo, F. M.; Stoddart, J. F. *Chem. Eur. J.* **1997**, *3*, 1933-1940.

60. Raymo, F. M.; Stoddart, J. F. *Chemtracts* **1998**, *11*, 491-511.

61. Behrend, R.; Meyer, E.; Rusche, F. *Liebigs Ann. Chem.* **1905**, *339*, 1.

62. Mock, W.L.; Freeman, W. A.; Shih, N. Y. *JACS*, **1981**, *103*, 7367.

63. Kim, J.; Jung, I. S.; Kim, S.Y.; Lee, E.; Kang, J. K.; Sakamoto, S.; Yamaguchi, K.; Kim, K. *JACS*, **2000**, *122*, 540.

64. Mock, W.L.; Shih, N. Y. *J. Org. Chem.* **1983**, *48*, 3618.

65. Mock, W.L.; Shih, N. Y. *J. Org. Chem.* **1983**, *48*, 3619.

66. Kim, K.; Selvapalam, N.; Oh, D. H. *J. Incl. Phenom.*, **2004**, *50*, 31-36.

67. Mock, W. L.; Pierpont,J. *J. Chem. Soc., Chem. Commun.*, **1990**, *21*, 1509.

68. Jun, S.-I.; Lee, J.-W.; Sakamoto, S.; Yamaguchi K.; Kim, K. *Tetrahedron Lett.*, **2000**, *41*, 471.

69. Lee, W.; Kim, K. P. and Kim, K. *Chem. Commun.*, **2001**, 1042-1043.

70. Whang, D.; Jeon, Y.-M.; Heo, J.; Kim, K.; *JACS;* **1996**; *118*(45); 11333

71. Asakawa, M.; Ashton, P. R.; Brown, G. R.; Hayes, W.; Menzer, S.; Stoddart, J. F.; White, A. J. P.; Williams, D. J. *Adv. Mater*. **1996**, *8*, 37.

72. Jeon, Y.-M.; Whang, D.; Kim, J.; Kim, K. *Chem. Lett*. **1996**, 503.

73. Lee, E.; Kim, J.; Heo, J.; Whang, D. and Kim, K. *Angew. Chem. Int. Ed.*, **2001**, *40*, 399-402.

74. Whang, D.; Kim, K.; *J. Am. Chem. Soc.* **1997**, *119*(2), 451.

75. Whang, D.; Heo, J.; Kim, C.-A.; Kim, K. *Chem. Commun.* **1997**, 2361-2362.

76. Lee, E.; Heo, J.; Kim, K. *Angew. Chem. Int. Ed.* **2000**, *39*, 2699-2701.

77. (a) Meschke, C.; Buschmann, H.-J.; Schollmeyer, *Macromol. Rapid. Commun.* **1998**, *19*, 59-63.

(b) Buschmann, H. J.; Meschke, C.; Schollemyer, E. *Polymer*, **1999**, *40*, 94

78. Tuncel, D. and Steinke, J. H. G. *Chem. Commun.*, **2001**, 253–254

79. Tuncel, D. and Steinke, J. H. G., *Chem. Commun.*, **1999**, 1509.

80. Tuncel, D. and Steinke, J. H. G. *Chem. Commun.*, **2002**, 496–497.

81. Choi, S.; Lee, J. W.; Ko, Y. H.; Kim, K. *Macromolecules* **2002**, *35*, 3526-3531.

82. Tan, Y.; Choi, S.; Lee, J. W.; Ko, Y. H.; Kim, K. *Macromolecules* **2002**, *35*, 7161-7165.

83. Wasielewski, M. R. *Chem.Rev.***1992**, *92*, 435.

84. Harriman, A.; Sauvage, J.-P. *Chem. Soc. Rev.***1996**, *25*, 41.

85. Murakami, Y.; Kikuchi, J.; Hisaeda, Y.; Hayashida, O.*Chem. Rev.*, **1996**, *96*, 721.

86. Scolaro, L. M.; Romeo, A.; Pasternack, R.F. *J. Am. Chem. Soc.*, **2004**, *126*, 7178.

87. Schneider, H.J.; Wang, M. *J. Org. Chem.***1994**, *59*, 7464.

88. Schneider, H.J.; Wang, M. *J. Org. Chem.***1994**, *59*, 7473.

89. Kano, K.; Fukuda, K.; Wakami, H.; Nishiyabu, R.; Pasternack, R. F. *JACS*, **2000**, *122*, 7494.

90. Kano, K.; Nishiyabu, R.; Asada, T.; Kurodo, Y. *JACS*, **2002**, *124*, 9937.

91. Kano, K.; Kitagishi, H.; Tamura, S.; Yamada, A. *JACS*, **2004**, *126*, 15202.

92. Wang, X.; Pan, J.; Shuang, S. *Spectroc. Acta A*, **2001**, *57*, 2755.

93. Clarke, S. E.; Wamser, C. C.; Bell, H. E. *J. Phys. Chem. A.*, **2002**, *106*, 3235.

94. Treibs, A.; Ha¨berle, N. *Liebigs Ann. Chem.* **1968,** *718*, 183.

95. Lee, C. H.; Lindsey, J. S. *Tetrahedron* **1994**, *50*, 11427

96. Bruckner, C.; Karunaratne, V.; Rettig, S. J.; Dolphin, D.*Can. J. Chem.* **1996**, *74*, 2182.

97. Litter, B. J.; Miller, M. A.; Hung, C. H.; Wagner, R. W.; O` Shea, D. F.; Boyle, P. D.; Lindsey, J. S. *J. Org. Chem.* **1999**, *64*, 1391.

98. Ka, J. W.; Lee, C. H. *Tetrahedron Lett.*, **2000**, *41*, 4609.

99. Wen, L.; Li, M.; Schlenoff, J. B. *JACS*, **1997**,*119*, 7726.

100. Tiftik, H. B. *Senior Project*, **2004-2005**.